LBL-20645
UC-350

Lawrence Berkeley Laboratory
UNIVERSITY OF CALIFORNIA

APPLIED SCIENCE DIVISION

Factors Influencing Soil as a Source of Indoor Radon: Framework for Assessing Radon Source Potential

W.W. Nazaroff, B.A. Moed, R.G. Sextro,
K.L. Revzan, and A.V. Nero

July 1989

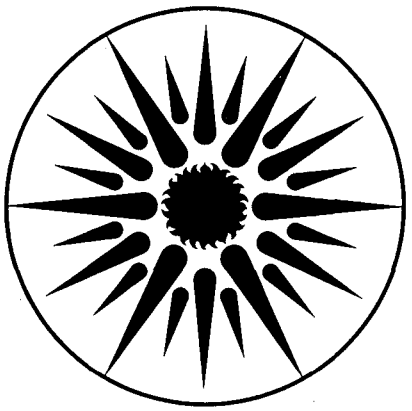

APPLIED SCIENCE DIVISION

Prepared for the U.S. Department of Energy under Contract Number DE-AC03-76SF00098.

DISCLAIMER

LBL-20645
EEB-Vent 85-19

FACTORS INFLUENCING SOIL AS A SOURCE OF INDOOR RADON: FRAMEWORK FOR ASSESSING RADON SOURCE POTENTIAL

W. W. Nazaroff*, B. A. Moed†, R. G. Sextro, K. L. Revzan, and A. V. Nero

* Department of Civil Engineering
University of California

and

Indoor Environment Program
Applied Science Division
Lawrence Berkeley Laboratory
1 Cyclotron Road
Berkeley, California 94720

July 1989

† Present address: Indoor Geo-Radon Services, P. O. Box 5985, Berkeley, CA 94705

This work was supported by the Assistant Secretary for Conservation and Renewable Energy, Office of Building and Community Systems, Building Systems Division, and by the Director, Office of Energy Research, Office of Health and Environmental Research, Human Health and Assessments Division and Pollutant Characterization and Safety Research Division of the U. S. Department of Energy under Contract No. DE-AC03-76SF00098. It was also supported by the U. S. Environmental Protection Agency (EPA) through Interagency Agreement DW89930801-01-0 with DOE.

TABLE OF CONTENTS

I. INTRODUCTION

Soil and rock are the source of most radon to which people are exposed. In fact, the only other sources of significance are building materials and even these generate radon because of radium that originated in the earth (or to a small degree from predecessor radioisotopes that originated in the earth themselves.) In discussing radon sources, then, it is common and convenient to distinguish not only among the materials that contain the radium that leads to indoor radon, but also among the agents and pathways by which radon enters. When we speak of soil as the source of indoor radon, we implicitly mean that portion of the total indoor radon concentration which originates in the earthen material near the structure and moves, via molecular diffusion and convection, directly through the building substructure and into the indoor air. That movement is generally restricted to distances of several meters or less, and must occur within several half-lives of radon, i.e., within a few weeks.

The other agents by which radon generated in the soil may enter indoor air are potable water, outdoor air and natural gas. For countries in which high indoor radon levels are common, including Canada, the United States and Sweden, there is substantial evidence that the source of most radon at levels of concern in indoor air is the underlying soil from which radon directly enters the building substructure by a combination of convective and diffusive transport. Such evidence may be grouped into four categories: (1) experimental efforts to account for indoor radon concentrations by balancing rates of entry and removal (George and Breslin, 1980; Nero and Nazaroff; 1984; Nazaroff et al., 1985); (2) remedial measures taken to reduce high indoor radon concentrations (AECB, 1980; Ericson and Schmied, 1984; Nitschke et al., 1984; Turk et al., 1987; Ericson and Schmied, 1987; Cliff et al., 1987; Scott, 1988); (3) theoretical and numerical studies of radon migration from soil into buildings (Bruno, 1983; DSMA Atcon, 1983; Nero and Nazaroff, 1984; Nazaroff, 1988); and (4) experimental studies of pressure fields and tracer gas

migration in the soil adjacent to houses (Nazaroff et al., 1987a; Sextro et al., 1987; Hodgson et al., 1988).

An understanding of the sources and transport processes accounting for radon in indoor air is of considerable importance. Radon levels may be unacceptably high in a substantial proportion of the housing stock in developed countries. In the United States, for example, data on the distribution of indoor radon concentrations suggest that four million single-family dwellings have radon concentrations exceeding the 4 pCi/l (150 Bq m^{-3}) guideline recently established by the Environmental Protection Agency (Nero et al., 1986). Furthermore, of the two major factors that determine indoor concentrations—the radon entry rate and the ventilation rate—the entry rate appears to be more variable and hence the more important factor in determining which houses have high levels. Thus, identifying houses with high levels, designing optimal control measures, and predicting the impact of changes in building construction practice on indoor radon concentrations—all depend upon knowledge of radon sources.

This report is concerned extensively with the transport mechanisms by which radon migrates in soil air and through building substructures. The discussion necessitates a summary of some important characteristics of soil: grain size, permeability, porosity, moisture content, and the diffusivity of gaseous species through soil pores. The mechanisms of radon generation in soil and emanation into soil pore space are described. Then some relevant features of building construction and operation that relate to radon entry are discussed. Of particular importance are substructure design, the location and size of substructure penetrations, and operations, such as the use of a fireplace or a mechanical exhaust ventilation, that may lead to a lowering of the air pressure in the structure relative to that outdoors. The physics of radon migration in soil are discussed, including the governing equations describing radon migration in soil that account for production, diffusion, convection, and radioactive decay. Mechanisms that generate pressure gradients in the soil and lead to convective transport of radon are examined. The relationship

between the air-exchange rate of a building and the indoor radon concentration is considered. Understanding this relationship is necessary to properly interpret the results of field measurements and to accurately predict the effect of changes in building operation on the indoor concentration. Recently developed mathematical models that account for radon migration and entry are examined. Sources of data on soil characteristics and other important parameters affecting radon entry, such as climate, are reviewed. The report contains a discussion of the use of these data, in conjunction with the basic production and transport equations, for the assessment of the radon source potential of geographic areas. Recently devised techniques for measuring the radon source potential of a plot of land in advance of construction are described briefly.

The focus of the present discussion is on the most abundant radon isotope, ^{222}Rn, and on the building practices used for single-family dwellings in the United States. Thoron (^{220}Rn), the other radon isotope of some importance, is discussed to a lesser degree. Although on average it is generated at the same rate in soil as ^{222}Rn, its much shorter half-life leads to a much shorter migration range and generally lower concentrations indoors. The discussion is, for the most part, sufficiently general that the extension to other building types follows once the key building characteristics are identified. Control techniques for preventing the direct entry of radon from soil have been treated by others (e.g., Scott, 1988) and are not considered here.

Another important point must be made concerning the scope of this report. For circumstances of principal concern, it is considered here that radon is generated throughout the soil in the vicinity of the building. Some of the discussion in this report does not apply to cases in which this paradigm does not hold, an example being radon generation within and migration from fractured, near-surface bedrock into a building. It is known that ordinary soil can be the source of high indoor radon concentrations, particularly if the soil has high radium content and/or permeability. The extent to which the indoor radon problem in the United States is accounted for by such circumstances is not known. Radon

migration through fractured rock and soil has been investigated by Schery and coworkers (Schery et al., 1982; Schery and Siegel, 1986; Schery et al., 1988).

A schematic representation of the key elements of soil as a source of indoor radon is presented in Figure 1. It is useful to distinguish two main concepts. "Radon availability" identifies the factors that influence the concentration of radon in soil air in the absence of structures. "Radon migration" groups the factors that determine the movement of radon from the soil air into buildings. This element depends on both soil and building-related factors. Both concepts contribute to the process by which soil serves as a source of indoor radon. They combine in a manner that is roughly multiplicative: soil is a small source of indoor radon if either the rate of generation of radon in the soil pores or the rate of migration of pore air from the soil into the building is small.

In Figure 1, the boxes represent the major states of radon from its generation in soil to its entry into a building; labels on horizontal arrows indicate a characteristic of the soil that is a measure of how readily radon moves from one state to the next; labels on vertical arrows indicate parameters and processes that significantly influence the rate of transition from one state to another. Labels on diagonal arrows indicate paths by which radon generated in soil may fail to enter a building. Among many features of this representation, one may note that moisture plays a role at several steps in the process.

II. PHYSICAL CHARACTERISTICS OF SOIL

Soil, as defined by the U. S. Soil Conservation Service (SCS), is "the collection of natural bodies occupying portions of the earth's surface that supports plants and that has properties due to the integrated effect of climate and living matter, acting upon parent material, as conditioned by relief, over periods of time" (USDA, 1962). Soils are formed from rock, the parent material, by a suite of processes, including mechanical weathering, chemical weathering, biological reactions associated with plants and microorganisms, and eluviation and illuviation (Paton, 1978). The product of these and other processes is the soil profile, composed of a succession of roughly horizontal layers, or horizons, that reflects the combined effects of local genetic factors.

The physical characteristics of a soil play key roles in determining the radon concentration in nearby buildings. These characteristics are determined, ultimately, by geologic processes by which the soils were created and transported. Many of these characteristics have been widely investigated for other purposes by civil engineers (Scott, 1963; Terzaghi and Peck, 1967) agronomists (Baver, 1940), petroleum engineers (Muskat, 1946; Scheidegger, 1960; Collins, 1961), and ground water hydrodynamicists (Freeze and Cherry, 1979). It is instructive to briefly review the information from these fields that is relevant to indoor radon. Important factors relating to radon production in soil are outside the scope of these fields and are treated in Section III.

A. Grain-Size Distribution, Porosity and Moisture Content

Soils comprise two major volume fractions. The solid fraction consists mainly of mineral grains of a wide range of sizes, and also includes a small amount of organic matter. The void fraction consists of liquid (usually water) and gas. The gas is generally similar in composition to air. The void fraction is also known as the soil porosity, and the volume fraction of water is often called the moisture content. A soil is saturated when the moisture content equals the porosity.

Soils are classified according to the size distribution of the solid grains, with the major divisions being clay, silt and sand. Characteristic particle sizes for each class are given in Table 1. Soils are generally mixtures of these three components. As indicated in Figure 2, the relative proportions of these components determine the basic soil texture classification. Grains larger than sand and up to 15 cm in diameter are classified as gravel. In contrast to the larger particles, which are formed by mechanical weathering, clays are formed by chemical processes. Because of their small size and active surfaces, they may interact in a complex manner with other grains and with water. Consequently, they exhibit macroscopic properties, particularly sorption of radioisotopes and interaction with water, that are quite different from those of silts and sands.

Apart from this distinction in the formation process between clays and other soil types, the physical characteristics of soil pertaining to fluid flow vary widely with grain size distribution. However, attempts to predict these characteristics for a particular soil on the basis of grain size distribution have not been successful over the entire range of grain sizes. Reasonably good results have been obtained for coarse- and medium-textured soils, while poorer results have been obtained for fine-textured soils. Discussions of such efforts may be found in the literature (Muskat, 1946; Scheidegger, 1960; Collins, 1961; ACS, 1969; Garcia-Bengochea et al., 1979; Pall and Mohsenin, 1980). Here, we present some representative data and simple analytical results as a basis for making numerical estimates of radon migration rates through soil.

As can be seen in Table 1, soil porosities are commonly in the range 0.4-0.6. By comparison, uniformly sized spheres have a porosity between 0.26 (close packing) and 0.48 (open packing). Because of the greater tendency for small platelike particles to "bridge," clays tend to have higher porosities than sands. Poorly sorted soils, that is, having a wide range of grain sizes, may have porosities of 0.3 or less.

The pore space within soils may be thought of, paradoxically, as both continuous and discrete: large pores are connected by narrower channels. The pore space has two

major components: the "textural" pore space, always present, which results from the random packing of the soil particles; and "structural" pore space, present only in well-aggregated soils, which exists between the soil aggregates. Structural pores, when present, are generally larger than the textural pores. Structural porosity is therefore an important factor in determining a soil's permeability. Transient aggregates may form due to cracking upon drying in soils containing a high percentage of clay-sized particles. Long-lived aggregates, which withstand wetting cycles, tend to form in soils containing much colloidal and organic material (Childs, 1969).

The moisture content of a soil not only depends on the grain-size distribution, but may be highly variable over time. A variety of physical effects controls the migration of liquid water in the soil pores. These forces form the basis for distinguishing among the components of the liquid phase (Baver, 1940). For our purposes, a classification system with three categories is most useful. The "hygroscopic" component of soil water is adsorbed on the grain surfaces by local electrostatic forces. This component is the most tightly bound and may be retained for relatively long periods even when the soil is otherwise dry. It is particularly important in clays due to the small grain size, the polar nature of water molecules and the crystalline structure of the clay particles. The "capillary" component of soil water is held in small pores and in a film around the particles by surface tension. The most variable component is termed "gravitational" water—that contained in the large pores, which is free to move under the influence of gravity.

Some understanding of the magnitude of these components for different soil types may be gained from the parameters "field capacity" and "wilting point" (Marshall and Holmes, 1979). The field capacity refers to the volume fraction of water in soil after it has been thoroughly wetted, then drained for about two days. The wilting point refers to the moisture content at which test plants growing on the soil wilt and do not recover if their leaves are kept in a humid atmosphere overnight. These can be expressed in terms of the saturation percent or volume percent, determined with respect to the pore volume or total

volume, respectively. As with porosity, both parameters increase with decreasing particle size. Typical values for the field capacity and for the wilting point are presented in Table 1.

Moisture content is a very important factor for radon emanation and migration in soil. For a well-drained soil, the void volume contains water in the smaller pores and air in the larger pores. As discussed in a later section the capillary water increases the radon emanation coefficient by absorbing the recoil energy of the newly formed atom. However, this water does not increase the resistance of the soil to air flow to a great degree since it is the larger pores that make the dominant contribution.

B. Permeability

One of the most important physical characteristic of soil pertinent to indoor radon is its permeability, i.e., how readily a fluid—in this case air—may flow through it. Permeability relates the apparent velocity of fluid flow through the soil pores to the pressure gradient. This relationship, described by Darcy's law, is discussed in detail in a later section. Here, our attention is focused on the range of values of soil permeability and the factors that may affect it.

The concept "intrinsic permeability" has been introduced to distinguish the characteristics of the medium from those of the fluid, both of which influence the rate of fluid flow. The intrinsic permeability is determined by the structure of the medium only, and is defined as the volume of a fluid of unit viscosity passing through a unit cross section of the medium in unit time under the action of a unit pressure gradient (Muskat, 1946, p. 71; see also Section V.B). The units of intrinsic permeability are length squared. We will use the terms "air permeability" and "water permeability" to refer to the permeability of soils to these fluids, in units of m^2. We note that the terminology and units associated with permeability vary from one field of study to another. In some cases, "Darcy" is used as a permeability unit, where 1 Darcy = 9.9×10^{-9} cm^2. In hydrology, it is customary to divide the intrinsic permeability by the viscosity of water and multiply by the density of water and

by gravitational acceleration to obtain the "hydraulic conductivity," which then has units of a velocity. At 20°C, a hydraulic conductivity of 0.01 m s^{-1} corresponds to a water permeability of 1.0×10^{-9} m^2.

The importance of soil permeability in the study of indoor radon arises from the very broad range of values it assumes: as shown in Figure 3, the permeability of common soils in the absence of structural pores may span about 10 orders of magnitude. We shall see that at the lower end of this range, molecular diffusion is the dominant process by which radon migrates through soil near buildings. At the upper end of this range, convective flow is the dominant radon migration mechanism. Since the convective flow rate increases with increasing permeability, and since the radon entry rate increases with convective flow of soil air into the substructure, the potential for radon entry is expected to increase monotonically with permeability for large grained soils. The actual entry rates are influenced by the characteristics of the building shell and the building operation.

Conceptually, permeability is based on the macroscopic properties of soil, i.e., the bulk volume flux of a fluid for a given pressure differential. This bulk property clearly depends on the microscopic characteristics of the soil: the size, shape, number and orientation of pores, in particular, and the moisture content. Larger-grained soils generally have higher permeabilities: their pores are larger and consequently the frictional resistance to fluid flow at the surface of the grains is of lesser importance than it is in fine-grained soils. Beyond this qualitative understanding, there has been considerable research toward establishing quantitative relationships among physical parameters of a porous medium and its permeability. The approaches have included empirical correlations, simplified physical modeling and statistical theories. Probably the most widely accepted approach to linking geometric properties of a porous medium with its permeability was first developed by Kozeny (Scheidegger, 1960). His approach was to solve the Navier-Stokes equation, which describes the momentum balance in a fluid, for an assemblage of channels of various

cross-sections, but of constant length. When the resulting flow is compared with Darcy's law, the following expression for permeability is obtained:

$$k = \frac{c\varepsilon^3}{TS^2} \tag{1}$$

where c is a constant that depends on the pore shape and, theoretically, varies between 0.5 and 0.67; ε is the porosity; T is the tortuosity, an empirical factor greater than or equal to 1.0 that accounts for the fact that the flow channels are not straight; and S is the specific surface area. For uniform, spherical particles,

$$S = \frac{6\,(1-\varepsilon)}{d} \tag{2}$$

where d is the particle diameter.

For uniformly sized particles, we see that the permeability varies approximately as the square of the particle diameter. In Table 2 we present representative permeabilities for the three main soil types based on these equations. In comparing these results with Figure 3, we see that the representative permeabilities show the same general dependence on particle size as indicated by the characteristic data.

Most of the literature on empirical investigations of variations in permeability with grain-size and air- or water-filled porosity reports saturated water permeability or, equivalently, hydraulic conductivity (e.g., Fraser, 1935; Baver, 1938; Burdine, 1953; Mason et al., 1957; Bedinger, 1961; Garcia-Bengochea et al., 1979). Relationships among several factors—hydraulic conductivity at 100% saturation, soil texture, air-filled porosity, and total porosity—were investigated for 8600 soil cores from 1000 sites in seven states by Mason et al. (1957). Bulk density was measured to indicate total porosity. The air-filled porosity at 60 cm of water tension was measured to indicate the percentage of large pores at moisture contents slightly greater than field capacity. (Tension is defined as the suction

applied to a column of soil, in this case due to gravity acting on a 60-cm column of water, i.e., approximately 6000 Pa.) This tension can drain only pores larger than 15 μm, and yields a moisture content of about 14% in coarse-textured soils and 35% in medium-textured soils (Marshall and Holmes, 1979, p. 195). The soils were classified texturally, taxonomically, and by depth within the soil profile. Analysis of variance was performed between hydraulic conductivity and percentage of large pores, and between permeability and bulk density, within and between sites, for cores grouped by texture and by Great Group. ("Great Group" is a general soil taxonomic category, discussed further in Section VII.A.1.d.) Among the 1000 sites, the percentage of large pores, or air-filled porosity, was better correlated with hydraulic conductivity than was bulk density, or total porosity. Correlation coefficients ranged from 0.46 to 0.85, indicating that between 21 and 72% of the variation in log k_w was accounted for by the percentage of large pores, where k_w represents the geometric mean hydraulic conductive under saturated conditions. Figure 4 is a plot of the geometric mean of k_w vs. the average percentage of large pores for soils from two horizons, grouped by texture. Horizon S is shallower than horizon D, so that the degree of compaction is lower, and therefore the total porosity is higher. This plot suggests that the percentage of large pores, or the air-filled porosity at a tension of 60 cm water, is an excellent indicator of hydraulic conductivity. Texture was not as reliable an indicator of water permeability, at least for the broad textural classes used here (five classes as compared with the twelve classes shown in Figure 2).

The Kozeny theory applies only to a soil completely saturated with the fluid of interest. For the case at hand, this means a soil with a small moisture content. In general, the permeability of soil is dependent on the degree of saturation of the fluid, especially within the large pores. Recognition of this dependence has led to the use of the term "relative permeability," which is defined as the ratio of the effective permeability at a given saturation to the permeability when the saturation is 100 percent for the fluid of interest (Corey, 1957). Studying variations in relative permeability with percent saturation

improves our understanding of the influence of moisture content on the air permeability of soils.

Figure 5 shows the relative permeability for air (k_{ra}) and water (k_{rw}) as functions of water saturation for a loamy sand (Corey, 1957). An important point is illustrated here: for this soil, the value of the air permeability remains roughly constant, and equal to that for the soil when dry, until water fills a large fraction, about 42%, of the pore space. For the surface and subsurface samples studied, the percent saturation at field capacity was 43% and 47%, respectively, suggesting that the air permeability, for sandy soils, is not strongly affected by changes in moisture content below the field capacity. As moisture content increases above field capacity, the large pores begin to fill with water, and the reduction in air permeability is large. Other studies have shown that the air permeability at field capacity ranges from 0.6 to 0.8 of that of the dry medium (Botset, 1940; Osaba et al., 1951).

The influence of moisture content below field capacity on the air permeability is greater for clayey soils than for sandy soils for two reasons: the mean pore size is smaller than in sands, so that at field capacity there is a greater tendency for pore blockage in clayey soils; and clayey, or cohesive, soils develop aggregates between which most of the fluid flow occurs (Mitchell et al., 1965; Barden and Pavlakis, 1971; Garcia-Bengochea et al., 1979). The formation of aggregates is, as mentioned above, strongly influenced by moisture content. The generation of structural pores, associated with the formation of aggregates, leads to an increase in permeability because these pores are relatively large.

A further important consideration is the possibility of chemical interactions between soil grains and water. Such interactions tend to retard the flow of water through the soil. Consequently, the apparent intrinsic permeability for water flow through soil may be lower than that for air flow through soil. Since most measurements of the permeability of soil have used water as the fluid, there may be a systematic underestimation in applying these data to the analysis of radon migration in soil. This effect may be great for soils with large clay contents, since the soil structure may change with moisture content.

In addition to the complicating effect of soil moisture, theoretical analyses, such as that due to Kozeny, invariably reflect analyses on a porous medium that is an idealization from even the most regular soil. Undisturbed soils exhibit many complicating features. All soils consist of a distribution of particle sizes, and both the breadth of the distribution and its shape may affect permeability in a way that is not adequately described by the specific surface area. Another factor that may be of particular importance in considering soil as a source of indoor radon is anisotropy in soil permeability. For example, because sedimentary beds are deposited in layers with particles settling under the combined forces of gravity and fluid drag, one might generally expect the permeability of an undisturbed sedimentary soil to be greater in the horizontal than in the vertical direction. One might further expect this effect to be enhanced for platelike clay minerals, as compared with more equidimensional sand grains. Directional permeability measurements have been made on samples of water-bearing consolidated soils consisting of sand, silt and clay. The results showed higher horizontal permeabilities by factors of 1.4 to 7 depending on the site (Rice et al., 1969). Similar measurements were made on settled sand and limestone samples. Where there were differences, the horizontal permeability was higher, but typically by only 20%. Differences between horizontal and vertical permeabilities of less than an order of magnitude may not be significant, given the range of permeability values. However, differences of a factor of 1000 have been measured (Bowles, 1979). The significance for radon entry is this: a higher permeability in the horizontal than in the vertical direction may lead to a larger volume of soil providing radon for the structure.

Structural pore space, when present, strongly influences the permeability of soil, and may impart to soils which are texturally clays and clay loams permeabilities similar to those of coarse sands (Topp et al., 1980). The presence of biopores—penetrations in the soil due to animal or plant activity—may also increase the permeability of fine- and medium-textured soils to values similar to those associated with coarse-textured soils (McKeague et al., 1982).

Whatever complications exist in assessing the behavior of undisturbed soils from theoretical analyses are amplified in investigating radon entry into buildings. Here the nearby soils have often been disturbed and redistributed during construction and the roots of landscaping vegetation may increase the local permeability. Nevertheless these effects may be of secondary importance relative to the very large effect of particle size on permeability. Consequently, simple on-site measurements or relevant data from published sources on soil grain-size distribution or permeability may be of considerable use in strategies and techniques for identifying buildings with high concentrations.

C. Diffusivity

In addition to migration with bulk movement of the fluid in the soil pores, species may migrate through the pores by random molecular motion. As is discussed in Section V.A, this tendency of a substance to migrate down its concentration gradient is described by Fick's law, which relates a concentration gradient to a flux. The coefficient relating these parameters is termed the molecular diffusivity, or diffusion coefficient. In a porous medium, it is a property of the fluid(s) in the pores, the pore structure, and the diffusing species.

For migration through the pores of a granular material, there are as many as four ways in which Fick's law may be written, depending upon whether one uses bulk or pore volume to determine concentration and bulk or pore area to determine flux density; different diffusion coefficients result and the symbols and terminology have not become standardized in the literature. The "bulk" diffusion coefficient, herein denoted D, relates the gradient of the interstitial concentration of the diffusing species to the flux density across a *geometric* or *superficial* area. The "effective" or "interstitial" diffusion coefficient, denoted D_e, relates the gradient of the interstitial concentration to the flux density across the *pore* area. (Note that this is the equivalent to the coefficient that relates the gradient of the

bulk concentration to the flux density across the geometric area. The fourth possible formulation has, fortunately, not been used.) These coefficients are related by the porosity:

$$D = D_e \varepsilon \tag{3}$$

The diffusion of radon through soil pores has been investigated for several purposes. Globally, the movement of radon from soil into the atmosphere appears to be primarily due to molecular diffusion (Wilkening et al., 1972). Since radon is not emitted from oceans, it has been used as an atmospheric tracer for continental air masses (Pearson and Jones, 1965). Another interest in which radon diffusivity in soil arises is uranium exploration: by mapping soil gas concentrations of radon near the surface, one may be able to identify subsurface deposits of soils enriched in uranium (Fleischer and Mogro-Campero, 1980). Diffusion of radon through soil has recently been widely investigated in connection with the use of earthen covers to retard the release of radon into the atmosphere from uranium mill tailings piles (Silker and Kalkwarf, 1983; Strong et al., 1981). Radon diffusion in soil has also been studied in connection with earthquake prediction (King, 1984/85).

The results of several measurements of the radon diffusion coefficient through soil are summarized in Table 3. The upper bound is given by the diffusion coefficient of radon in open air (denoted D_o), 1.2×10^{-5} $m^2 s^{-1}$ (Hirst and Harrison, 1939). Typically, the effective diffusion coefficient of radon in soil of low moisture content is 10^{-6} $m^2 s^{-1}$.

As in the case of permeability, there have been numerous attempts to relate the diffusivity ratio D/D_o to the physical parameters, particularly ε, of the porous medium. From work on CO_2 migration in soils, Buckingham (1904) proposed the correlation

$$\frac{D}{D_o} = \varepsilon^2 \tag{4}$$

Later Penman (1940), studying a wide range of porous materials, obtained the correlation

$$\frac{D}{D_o} = 0.66\,\varepsilon \qquad 0.0 < \varepsilon < 0.66 \tag{5}$$

Currie (1960) discusses other correlations and reports on experiments showing that such correlations must account for the shape of the grains. He concluded that a correlation of the form

$$\frac{D}{D_o} = \gamma\,\varepsilon^{\mu} \tag{6}$$

where γ and μ are properties of the material, fit data from a wide range of media.

Water plays an important role in influencing the radon diffusion coefficient in soil. In a saturated soil, the radon diffusion coefficient may be reduced to 2×10^{-10} $m^2\,s^{-1}$ (Tanner, 1964). This value is so much lower than that in air that, for practical purposes, we can view the effect of water on the radon diffusion coefficient in soil as blocking a fraction of the available pore space. The results of one study of the radon diffusion coefficient as a function of the fraction of pore space filled with water are presented in Figure 6. For low moisture contents, water is predominantly on grain surfaces and in small pores. Since transport through the larger pores dominates, the diffusion coefficient is a weak function of moisture content. As the soil nears saturation, the larger pores become occluded and the rate of reduction in diffusion coefficient with increasing moisture content grows.

Currie (1961) investigated the relationship between moisture content of porous materials and the bulk diffusivity of hydrogen. He classified materials according to whether or not the grains had an internal pore structure: sand, for example, constituted a solid particle system whereas a soil containing much clay was considered a "crumbly"

particle system. He found that the behavior of these two types differed, particularly in the region near completely dry. In this region, the diffusivity depended very slightly on moisture in the crumbly particle systems but strongly on moisture in the solid particle system. He interpreted these data as indicating that the moisture in the crumbly particle system was taken up in the internal pores of the particles and, hence, had little influence on diffusive migration through the sample which was dominantly through the larger pores. Once the internal pores were saturated, the solid and crumbly particle systems behaved similarly, with the dependence of diffusivity on moisture well-represented by

$$\frac{D_w}{D} = \left[\frac{\varepsilon_a}{\varepsilon}\right]^{\sigma} \tag{7}$$

with σ approximately equal to 4. In this equation D_w is the bulk diffusion coefficient of the wet soil, ε_a is the air-filled porosity (air volume divided by total volume), and ε is the total porosity excluding the internal pores of the crumbs.

The diffusion coefficient for the other isotopes of radon has been observed to be comparable to that for radon-222.

III. RADON PRODUCTION IN SOIL

The discussion in this section focuses on the characteristics of soil that influence the rate of radon emanation into the pore air of the soil. We consider two parameters: the radium content and the emanation coefficient.

A. Radium Content

The radium content of the soil is typically given as an activity concentration per unit mass. The radium content in these terms is equivalent to the total production rate of radon in the soil, with 1 Bq kg^{-1} of radium yielding a radon production rate of 1 atom kg^{-1} s^{-1}, or 0.00756 Bq kg^{-1} h^{-1}.

Table 4 and Figure 7 present data on ^{226}Ra and ^{232}Th concentrations in surface soils. The data in Figure 7 are based on aerial measurements of ^{214}Bi gamma emissions (Revzan et al., 1988a; Revzan, 1988). Each point in the figure indicates the surficial ^{226}Ra content averaged over a 20 × 20 km area. For these 22,000 points, the arithmetic mean radium content is 27 Bq kg^{-1} with a standard deviation of 12 Bq kg^{-1}. See Section VII.A.2 for a discussion of the use of these data for geographical assessment of the radon source potential.

The data in Table 4 result from measurements of gamma activity of soil samples collected primarily along U.S. interstate highways (Myrick et al., 1983). The ^{226}Ra content was determined primarily from ^{214}Bi emissions from samples that had been sealed and stored long enough for ^{214}Bi to come to equilibrium with its radium precursor. Data on ^{232}Th, the primordial precursor of ^{220}Rn, reflect gamma emissions from a combination of its decay products. The longest-lived species in the chain from ^{232}Th to ^{220}Rn is ^{228}Ra with a half life of 5.7 years, very short in terms of geologic time scales. Hence, the ^{232}Th content of a soil is a good indicator of its rate of production of ^{220}Rn.

The radium content of soils tends to reflect the radium content of the rocks from which the soil formed. Table 5 summarizes the ^{226}Ra and ^{224}Ra content of rocks. These

data are a compilation of over 2500 laboratory-based γ-spectrometric analyses reported in English-language publications (Wollenberg and Smith, 1984). The radium concentrations within each rock class except the intermediate extrusives were found to be distributed lognormally. Radium contents tended to decrease with silica contents in extrusive and intrusive igneous rocks, with the exception of alkali feldspathoidal rocks, which are rare. The extremely high ^{226}Ra contents listed in the ranges within the chemical sedimentary and shale classes are undoubtedly due to phosphates and black shales, respectively. The mean values for rocks excluding alkali rocks in Table 5 tend to support the data for soils given in Table 4; the ranges suggest that the range of Ra concentrations, even in soils distant from U mining and milling sites, is probably larger than indicated in Table 4.

In combination, these studies suggest that surface soils in the United States typically contain 10-100 Bq kg^{-1} of both ^{226}Ra and ^{224}Ra.

Values much higher than the range given by these studies have been found in soils near uranium mining areas and mill tailings piles. For example, Powers et al. (1980) found a range of 15-1700 Bq kg^{-1} of ^{226}Ra for 28 samples collected near uranium mining and milling areas in Wyoming, New Mexico and South Dakota. In Jaduguda, Bihar, India, an area with known deposits of uraniferous materials, ^{226}Ra concentrations of 40-200 Bq kg^{-1} were reported (Iyengar and Markose, 1982). Sixty-three samples from Canada collected near the surface of two mill-tailings piles contained a mean ^{226}Ra concentration of 1760 Bq kg^{-1} (Kalin and Sharma, 1981).

B. Emanation Coefficient

Only a fraction of the radon generated in soil ever leaves the solid grains and enters the pore volume of the soil. The fraction of radon generated in soil that escapes the grains is known as the "emanation coefficient" or, alternatively, "emanating fraction" or "emanating power."

Experimental measurements of the emanation coefficient of rocks and soils have been made by many investigators. These data, summarized in Table 6, indicate an approximate range of 0.05-0.7 for soil. We have some understanding of the basic physical processes leading to radon emanation from soil (see Figure 8); however, measured emanation coefficients are considerably higher than predicted by simple physical models.

Conservation of linear momentum dictates that upon being created by the alpha decay of radium, ^{222}Rn and ^{220}Rn atoms possess kinetic energies of 86 and 103 keV, respectively (Bossus, 1984). The newly formed atom travels from its site of generation until its energy is transferred to the host material. The distance travelled depends on the density and composition of the material. The range of ^{222}Rn is 0.02-0.07 μm for common minerals, 0.1 μm for water, and 63 μm in air; the range of ^{220}Rn in air is 83 μm (Tanner, 1980).

The emanation coefficient is considered to have three components: direct recoil, indirect recoil, and diffusion. These components arise from the locations of the end points of the path of the recoiling radon atom. The direct recoil fraction refers to radon atoms that terminate their recoil in the fluid-filled pore space. Atoms that leave the grain in which they were created, traverse a pore, and penetrate another grain form the basis for the indirect-recoil fraction. They must then migrate out of the pocket created by their passage to enter a pore. The diffusion fraction refers to radon atoms that begin and end their recoil within a single grain, then migrate to the pore through molecular diffusion.

Analysis of the emanation process for uniformly distributed radium in undamaged soil grains leads to much lower emanation coefficients than are generally observed. Consider first the maximum recoil fraction. Only radium atoms within the recoil range of the surface generate radon atoms that have any possibility of escaping the grain. Andrews and Wood (1972) and Bossus (1984) computed the escape probability for radon atoms generated within the recoil range of the surface of a spherical particle and obtained 23.5 and 25% respectively. If we then consider a spherical particle, with diameter 20 μm

(corresponding to a medium-coarse silt), having a radon recoil range of 0.035 μm, this model predicts that only 0.25% of the radon atoms generated in the grain leave it during recoil. An analysis of the diffusion of radon in intact grains suggests that the diffusion fraction is entirely negligible: diffusion coefficients for argon in rock-forming minerals were measured to be 10^{-31} to 10^{-69} m^2 s^{-1} (Tanner, 1964); corresponding radon diffusion lengths are 10^{-13} to 10^{-32} m.

Two hypotheses have been advanced to account for the large discrepancy between measured and theoretical emanation coefficients (Tanner 1964; Tanner, 1980). The first is that radium is not distributed uniformly but rather is concentrated in secondary crusts or films on the surfaces of the grains. The second hypothesis suggests that chemical corrosion and, particularly, radiation damage due to the decay of its precursors, damages the crystalline structure in the vicinity of the radium atoms, facilitating the leaching of the mineral in the damaged zone and thereby increasing the emanation coefficient. These hypotheses are not mutually exclusive, and both are substantiated by experimental data.

The first hypothesis is supported by the results of two studies. In one, the ^{226}Ra and ^{224}Ra concentrations of two soil samples were measured as a function of grain size and found to decrease nearly monotonically as grain size increased (Megumi and Mamuro, 1974). This trend would be expected if a portion of the radium content of each grain were contained in a surface layer. The second study measured ^{238}U and ^{232}Th series concentrations in 70 soil samples and found them to vary linearly with the fraction of the soil mass having particle diameter less than 20 μm (Jasinska et al., 1982). Tanner (1980) has suggested that uranium and thorium are not compatible with the crystalline structure of major minerals and, hence, are commonly found in accessory minerals, adsorbed on the surface of clay particles, or are present in other coatings.

Data supporting the second hypothesis comes from a study by Barretto (1973) of the effect of annealing rocks, sands and minerals. Invariably for the six samples studied the radon emanation coefficient dropped as the annealing temperature was increased. For

heating to 1000 °C, the average ± one standard deviation of the emanation coefficient of the annealed sample, divided by its original emanation coefficient was 0.23 ± 0.23.

Additional pertinent evidence is contained in the results of a study of radon emanation from the island of Hawaii (Wilkening, 1974). The ^{222}Rn emanation coefficient was found to be very much smaller for samples from lava fields (average 0.02) than for samples from either thin organic soils (0.55) or deep agricultural soils (0.70). Being of recent origin, and formed by the rapid cooling of a molten solid, lavas would be expected to have relatively uniform distribution of ^{226}Ra and minimal radiation damage. Consequently, their much lower emanation coefficient is not surprising.

Moisture content has been demonstrated in several studies to have a large effect on the emanation coefficient (Thamer et al., 1981; Strong and Levins, 1982; Ingersoll, 1983; Stranden et al., 1984). Data showing this effect for uranium ore tailings are presented in Figure 9. The explanation for this phenomenon appears to lie in the markedly lower recoil range for radon in water than in air. A radon atom entering a pore that is partially filled with water has a very high probability of terminating its recoil in the water. From there, it is readily transferred to the air in the pore. At equilibrium, the partitioning between air and water is described by Henry's law (Boyle, 1911). Mass transfer from water to air is rapid: an aqueous diffusion coefficient of order 10^{-9} m^2 s^{-1} (Bird et al., 1960) and a water layer thickness of order 10 μm suggests a characteristic time for transport to the air of 0.1 s; thus equilibrium is achieved rapidly.

The characteristic pore dimension of a soil is related to its grain-size distribution. For a soil having a narrow distribution of grain sizes, the characteristic pore size is the same order as the characteristic grain size. Hence, even for clayey soils, for which the characteristic grain size is of order 1 μm, the pore dimensions are much larger than the radon recoil range in water. Consequently, one would expect the dependence of emanation coefficient on moisture content in most soils to show the general trend indicated in Figure 9. As a soil is dried from saturation, the emanation coefficient drops slowly at first as the

gravitational water is removed. Once the large pores are drained and capillary water begins to be affected, the emanation coefficient drops substantially. Finally, when only adsorbed water remains, there is little effect of further drying of the soil. This layer is too thin to be very effective in stopping the recoiling radon atoms.

In combination with the discussion in previous sections, this suggests that radon release from soil, combining emanation and migration, is a maximum when the soil is moist. Having the soil grains covered and the small pores filled with water results in a high radon emanation coefficient, but—as most movement takes place through the larger pores—only reduces the radon migration rate to a small degree. This level of moisture, corresponding approximately to the range between the wilting point and the field capacity, is the most common state of natural soils. When the soil is dry, the rate of radon migration is slightly enhanced, but the emanation coefficient may be substantially reduced. When the soil is wet, the emanation coefficient is slightly higher, but the diffusivity and permeability are greatly reduced.

To account for the moisture dependence of the emanation coefficient of radon from 17 samples of crushed ore, Thamer et al. (1981) proposed the following model. The ore was assumed to consist of radioactively inert rock grains held together by a porous cementing material. The pores were treated as cylinders with diameters varying according to a measured pore-size distribution. The radium in the sample was assumed to be uniformly distributed within an annular region of constant thickness around each pore. Finally, moisture was assumed to occur in layers of equal thickness on the inner surface of the radium-bearing annulus.

Two parameters were allowed to vary to fit the data: the inert rock fraction determined the magnitude of the dry emanation coefficient and the thickness of the radium-bearing annular regions determined the ratio of saturated to dry emanation. With this model, the researchers were successful in matching the dependence of the emanation

coefficient on moisture in most cases. Their model yielded values of 0.78 ± 0.11 for the inert rock fraction and 0.025 ± 0.011 μm for the thickness of the radium-bearing regions.

Temperature has also been found to be a factor in determining the radon emanation coefficient, although over the range of temperatures common for surface soils this effect is of minor importance. Stranden et al. (1984) found that the radon exhalation rate for a soil sample increased by 55% when the temperature was increased from 5 to 50°C. They suggested that the increase with temperature may be due to a reduction in physical adsorption. Barretto (1973) found a much smaller temperature dependence for the emanation coefficient of a granite sample: 0.106 at 265°C to 0.081 at -20°C. He found though that when the sample was cooled to -80°C, the emanation coefficient decreased markedly to 0.028. On the other hand, Tanner (1985) found the rate of emanation of radon from a natural, uranium mineralized, very permeable sandstone core to decrease with increasing temperature over the range of 24 to 100°C. The results were reversible, indicating that the observed effect was probably not due to changes in moisture content.

Radon condenses at temperatures much lower than those found in the environment. For a pure sample at standard pressure, the boiling point and melting point are -62°C and -71°C, respectively (Gray and Ramsay, 1909). At very low partial pressures, i.e. under all environmental conditions, radon condenses on surfaces at approximately -150°C (Rutherford and Soddy, 1903). Common experimental techniques for concentrating radon from an air stream involve collecting the radon on activated charcoal cooled to the temperature of solid CO_2 (-78.5°C) (Lucas, 1957), or on glass wool cooled to the temperature of liquid N_2 (-196°C) (Ingersoll et al., 1983).

IV. BUILDING CHARACTERISTICS

Three aspects of building design and operation play key roles in influencing radon entry from soil. One is the design and operation of the ventilation system which may affect the pressures that drive bulk air flow through the soil. A second is the design and operation of the building's thermal conditioning system, which again may affect the indoor-outdoor pressure differences. The third factor is the design and construction of the building substructure which controls the degree of movement between the air in the soil and the air in the building.

In addition to these factors, the very presence of a house may influence the spatial distribution of soil moisture and, thereby, the emanation and migration of radon. Except for one anecdotal report (Nazaroff and Doyle, 1985), such effects have not been documented; however, they seem reasonable to expect based on common experience. For example, a house serves as an umbrella to precipitation such that the soil underlying it tends to be drier than the surrounding uncovered soil. As we have seen, the moisture content of soil is an important factor influencing the radon emanation coefficient, effective diffusion coefficient, and soil permeability.

A comprehensive treatment of building practices that influence radon entry is beyond the scope of this report. Even within a single country, relevant construction practices vary widely, depending principally on the purpose of the building, the climate, and the structural and drainage characteristics of the local soil. In the United States, construction practices are governed for the most part by municipal codes, rather than by federal or state guidelines. The discussion in this report covers only some of the key features of building practice pertaining to radon entry, and focuses on single-family residential structures which have been the most extensively studied. Some further discussion may be found in Scott (1988).

A. Ventilation

Ventilation refers to the total supply rate of outdoor air into a building, whether intentional or not. It serves the purpose of controlling odors, maintaining a proper balance of metabolic gases, and diluting pollutants generated by indoor sources. The most important aspect of ventilation for radon entry from soil is its relationship to the pressure difference between the base of the outside walls and the building's substructure openings. This relationship is discussed explicitly in Section VI.B. Here, our objective is to provide a brief introduction to building ventilation.

The ventilation rate has three components. Infiltration refers to the uncontrolled leakage of air into the building through cracks and holes in the building shell. Natural ventilation is the flow of air into the building through open doors and windows. Mechanical ventilation is the provision of air by means of fans.

In most single-family dwellings in the United States, at times when the outdoor air must be heated or cooled for thermal comfort, infiltration is the predominant component of ventilation. The forces that drive infiltration arise from wind and buoyancy; these are discussed quantitatively in Section VI.A. Models have been developed that predict infiltration on the basis of the wind speed (including corrections for local shielding), temperature difference, and leakiness of the structure (Liddament and Allen, 1983). Data on infiltration rates in U.S. housing are presented in Nazaroff et al. (1987b).

At times when the outdoor air temperature is in the approximate range of 15-25°C, depending on the habits of the building occupants, the rate of natural ventilation may become very large, and the indoor-outdoor pressure difference very small. Concentrations of radon and its progeny inside a residence with open doors and windows are typically close to the outdoor levels.

A major difficulty with the use of infiltration as the principal means of ventilating a building is the lack of control. A building with a relatively large leakage area may be

uncomfortably drafty when weather conditions are severe. But during mild weather, the infiltration rate of a "tight" building may be so low that moisture, odor, or other indoor air quality problems result. Consequently, there is considerable interest in the use of mechanical ventilation systems in residential buildings.

A balanced mechanical ventilation system is designed to operate with equal amounts of supply and exhaust air, often passed through a heat-recovery device to reduce energy costs (Fisk and Turiel, 1983). In this case, its effect on the pressure distribution across the base of the building walls is probably negligible. Alternatively, in an unbalanced system, either exhaust or supply ventilation is provided in excess. For example, in a supply-only system, the pressure inside the building is increased, and air flows out either through designed penetrations or through leaks in the building shell. This approach should in principle have the beneficial side effect of reducing radon entry by lowering, or even reversing, the pressure gradient in the surrounding soil. Caution must be exercised to avoid material damage in cold climates due to the freezing condensation of moisture in exfiltrating air.

Mechanical systems provide the ventilation in most commercial buildings, although small ones may be ventilated like residences. Common commercial design specifies a higher rate of fresh-air supply than exhaust, so that the building is operated at a pressure slightly higher than ambient.

The use of exhaust fans for local (or general) ventilation may have the undesirable side effect of increasing radon entry rates. Recent modeling of this situation suggests that exhaust ventilation may be a suitable, but not optimal, method of providing air exchange for crawl-space houses and for basement houses surrounded by low permeability ($<10^{-12}$ m^2) soil (Mowris and Fisk, 1988). Exhaust ventilation is not recommended for basement houses with highly permeable soil unless measures are taken to impede soil gas entry.

B. Heating and Air-Conditioning System

The thermal conditioning system of a building may influence the rate of radon entry by altering the pressure differences that induce air flow across a building's substructure. The operation of such systems also may alter radon exposures by changing the distribution of radon concentrations within a building. As is generally true for building design and operation, the characteristics of heating and air-conditioning systems vary widely across the building stock. The discussion in this section is intended to illustrate the manners in which heating and air-conditioning systems may affect radon entry and distribution.

An assessment of the effect of thermal conditioning systems may be divided into two components. One component—how the system influences the indoor-outdoor temperature difference—is largely independent of the details of the system. As discussed in Section VI.A.2, a positive indoor-outdoor temperature difference leads to net inward pressure across the lower part of a building (and net outward pressure across the upper part). Thus, an inadvertent effect of operating a heating system is to increase the rate of entry of radon from soil. (However, because the air-exchange rate of the building may also increase, the effect on indoor concentrations is complex, as discussed in Section VI.B.) Conversely, one expects that reducing indoor temperatures by operating an air-conditioning system concomitantly reduces radon entry rates, and indoor concentrations.

The second component—how the system directly influences air movement within a building and, therefore, pressure differences across the building shell—is strongly dependent on the nature of the system. At one extreme, electric resistance baseboard heating has no direct influence on air movement from one zone to another in a building, and so its contribution via this component to radon entry and distribution is negligible. At the other extreme, consider a gas-fired forced-air furnace located in the basement of a residence. Often, the air needed for combustion is taken from the basement, rather than from outdoor air. The discharge of this gas through the flue reduces the air pressure in the

basement. A typical gas-fired residential furnace, with an output rating of 100,000 BTU h^{-1} (106 MJ h^{-1}) and an efficiency of 70%, would discharge about 40 m^3 h^{-1} of air when operating. Furnace duty cycles during the heating season are commonly less than 50%, so an average exhaust flow of less than 20 m^3 h^{-1} would be expected from a gas-fired furnace. Still, this may represent a significant fraction of the air flowing through a basement: at 0.2 air changes per hour, 50 m^3 h^{-1} is the total air flow rate through a 250 m^3 basement.

The operation of the air distribution system is potentially more significant. During furnace operation, a large flow rate of air—typically 10 house volumes per hour—is recirculated through the house and the furnace heat exchanger. For an unconditioned basement, the system is designed to take air from the living area, pass it through the furnace, then return it to the living area. However, given prevailing installation practices, leaks in the air ducts are almost inevitable. These leaks produce two consequences that are significant with respect to indoor radon: (1) they promote air mixing between the basement—which generally has a higher radon concentration—and the living area; and (2) they alter the pressure between the basement and the living area, thereby influencing radon entry into the basement. For example, if the leaks are principally on the return-air side of the furnace, the air pressure in the living area will be increased; the air pressure in the basement will be decreased; and the rate of radon entry from soil into the basement will be increased. Evidence for these and other effects of gas furnace operation on radon entry and distribution is reviewed by Grimsrud and Odenwalder (1988).

Other activities, whether or not associated with a building's thermal conditioning, also may influence radon entry by altering the indoor-outdoor pressure differences. For example, fireplace operation can, because of the large rate of air flow out of the chimney, lower the pressure in a house and significantly increase the air-exchange rate (Modera and Sonderegger, 1980). In the only case studied, a concomitant increase in the rate of radon entry was observed that nearly compensated for the increased ventilation rate (Nazaroff et al., 1985). The use of exhaust fans or a clothes dryer could also increase the rate of radon

entry by increasing the inward pressure gradient across the building shell. The effect of operating such devices is significant only if the exhaust flow rate is at least a significant fraction of the baseline ventilation rate of the building.

C. Substructure

Single-family dwellings in the United States are most commonly built with the lowest floor made either of poured concrete and in direct contact with the underlying soil, or of wood and suspended above the soil. In the former case, the floor may lie below the soil grade; we designate this a basement substructure. Alternatively, the floor may be built to the same level as the soil surface, a substructure type often called "slab-on-grade." The substructure for a house having a suspended wood floor is known as a crawl space.

Each type has unique characteristics that influence radon entry, with the greatest differences occurring between crawl-space substructures and the others. Among the three types, radon entry into basements has received most of the research and remedial attention (George and Breslin, 1980; AECB, 1980; Hernandez and Ring, 1982; Hernandez et al., 1984; Nazaroff et al., 1985; Holub et al., 1985), but entry into slab-on-grade (Scott and Findlay, 1983) and crawl space houses (Nazaroff and Doyle, 1985) has been studied as well.

The influence of the building substructure on radon entry can be separated into three factors: the degree of coupling between indoor air and soil air; the size and location of openings and penetrations through the substructure; and the nature of the soil-substructure interface. The first two of these are discussed below; the third is considered in Section VI.D.

1. Degree of Coupling Between Indoor Air and Soil Pore Air

The interior of a slab-on-grade or a basement house is potentially well-coupled to the nearby soil. Recommended construction practice calls for the concrete slab to be underlaid by a layer of gravel or crushed stone that in turn lies upon the subsoil (Crane,

1947). An intermediate plastic membrane may be present, depending on the normal moisture conditions of the surrounding soil. Any penetrations through the concrete and plastic sheeting, if present, constitute a link between the underlying soil and the indoor air that is distributed by means of the gravel layer to the entire area beneath the floor. If the pressure inside the house is reduced with respect to the pressure at the base of the outside walls, that pressure differential is effectively applied across the underlying soil. If the soil is sufficiently permeable, a large radon entry rate can result.

A house with a crawl-space substructure may be well-coupled to the underlying soil or not, depending on whether the crawl-space is vented. The venting generally required to prevent moisture damage, e.g. 0.67 m^2 of vent area per 100 m^2 of floor area (Uniform Building Code, 1982), is sufficient in principle to uncouple the indoor air from the soil: essentially all air flowing through the floor of the living space enters the crawl space through the vents, rather than through the soil. Consequently, very high radon entry rates due to soil gas influx, as sometimes found in houses with a basement, are not expected in houses having a vented crawl space.

On the other hand, if the crawl space is unvented and the underlying soil exposed, then the house is well-coupled to the soil, and the radon entry rate may be large. One study conducted in Illinois found that in 9 of 22 such houses indoor radon concentrations exceeded 180 Bq m^{-3} and in 6 of these the concentration was greater than 370 Bq m^{-3} (Rundo et al., 1979).

2. *Substructure Penetrations*

Penetrations in the building shell that are most important for radon entry are those through the floor and, in the case of a house with a basement, those through the wall below soil grade. Common routes of entry and means of sealing them are discussed thoroughly in Scott (1988). We note here only a few points in this regard.

Penetrations in the floor of a slab-on-grade or basement house are commonly found at the floor-wall joint, around service entrances (particularly for water supply pipes and the sanitary sewer lines), and in association with floor drains or perimeter drainage systems. The size of these penetrations is almost invariably great enough so that the principal resistance to air flow through the soil and building substructure is in the soil. Hence, for radon entry into concrete-floored houses, the absolute size of penetrations, unless unusually small, is relatively unimportant. The relative sizes among penetrations and their position may be important. By influencing the length of the path which air must traverse through soil before entering the substructure, these latter factors play a role in determining the volume of soil that may contribute its radon to the indoor air.

In a crawl-space house, penetrations may be found along the foundation sill plate, and around plumbing and sewer pipes, electrical wiring, and heating and air conditioning ducts where they pass through the floor. As suggested by the previous discussion, if the crawl space is vented, these penetrations probably have little effect on radon migration through the nearby soil. Their total size does however influence radon entry by affecting the proportion of radon entering the crawl space from the soil that enters the house, rather than exiting to the outside air.

V. RADON MIGRATION IN SOIL

In this section, we develop a mathematical formulation describing the radon concentration in the pore air of a differential volume of soil. The equation accounts for the migration of radon by molecular diffusion and forced convection and the production and removal of radon by radioactive decay. In addition to the variables described in earlier sections, application of this equation to the problem of radon entry into buildings requires specifying the pressures at the surface of the soil and inside the building and the building geometry. Analytic solutions to this equation do not exist, except for the simplest geometries. Consequently, a complete treatment requires the use of a numerical model, an undertaking that has only recently been started (DSMA, 1983; Scott, 1983; Eaton and Scott, 1984; DSMA, 1985; Mowris, 1986; Loureiro, 1987; Mowris and Fisk, 1988). Dimensional analysis permits one to identify circumstances under which one or more of the terms of the governing equation become negligible and, consequently, may be ignored, thereby simplifying the detailed quantitative analysis.

We begin with discussions of Fick's law and Darcy's law which, respectively, underlie the description of migration due to molecular diffusion and forced convection. A general differential transport equation is then presented. By the use of scaling arguments, conditions are identified under which the problem of analyzing radon migration in soil near a building may be simplified.

Note that this analysis is predicated on the assumption that the dominant component of radon entry can be understood by considering steady-state, pressure-driven flow across building substructures. Evidence clearly supports the conclusion that elevated indoor radon concentrations *can* be accounted for by this framework (Nazaroff, 1988; Nazaroff and Sextro, 1989). It is not yet clear, though, that this paradigm is the appropriate model for most buildings with elevated indoor concentrations. It is possible, for example, that radon entry is largely caused by transient flow resulting from the compressibility of air and induced by fluctuations in barometric pressure, wind, and temperature differences. It is

also possible that soil heterogeneity, particularly in the interface region near the building substructure, is a critical factor determining whether or not indoor concentrations are elevated. Nevertheless, we proceed with the analysis of the simpler case, based on the premise that our conceptual representation of the physical world should be the simplest possible that is consistent with empirical evidence. The present analysis would serve as a foundation for future work, even if changes in the representation become necessary to explain new evidence.

A. Diffusive Migration—Fick's Law

To begin, we consider a gas made up of two species, A and B. The molar flux of A relative to stationary coordinates may be expressed as (Bird et al., 1960)

$$N_A = x_A (N_A + N_B) - c D_0 \nabla x_A , \qquad (8)$$

where N_A and N_B are the fluxes of A and B, respectively with respect to fixed coordinates (mol m^{-2} s^{-1}), x_A is the molar fraction of A in the mixture, c is the molar concentration of the gas (mol m^{-3}), D_0 is the diffusion coefficient (m^2 s^{-1}) (see Section II.C), and ∇ is the three-dimensional gradient operator. The first term on the right hand side represents the flux density of A due to convection, while the second term gives the diffusional flux density relative to the molar average velocity. This expression embodies Fick's first law which states that the diffusional flux density is proportional to the concentration gradient. Fick's law is based on experimental observations and is consistent with the postulates of kinetic theory for an ideal gas. Other physical conditions that may lead to a diffusive flux are neglected in this expression, in particular temperature gradients, pressure gradients, and external forces (e.g., due to an imposed electric field). They are usually unimportant relative to the concentration gradient.

For the case of radon in air, we can make major simplifications in equation (8). First, since the mole fraction of radon in air is always extremely small (40,000 Bq m^{-3}, a

typical concentration in soil air, is equivalent to a mole fraction of ^{222}Rn of 7.6×10^{-16} at 20 °C), the molecular diffusion of radon may be neglected as a source of convection of the mixture. That is, we may neglect the term $x_A N_A$ as small compared with N_A. A further simplification results from approximating the molar concentration of air as a constant. Hence

$$N_{Rn} = x_{Rn} N - D_o \nabla c_{Rn} \tag{9}$$

where **N** is now the molar flux density of air relative to stationary coordinates and $c_{Rn} = cx_{Rn}$, is the molar concentration of radon. It is convenient to multiply this equation by Avogadro's number and the decay constant of radon so that

$$J_{Rn} = I_{Rn} V - D_o \nabla I_{Rn} , \tag{10}$$

where I_{Rn} is the activity concentration of radon (Bq m^{-3}), J_{Rn} is the activity flux density (Bq m^{-2} s^{-1}), and $V = N/c$ is the net air velocity (m s^{-1}). The discussion in this section focuses on the implications of the diffusive flux ($-D_o \nabla I_{Rn}$). The convective flux ($I_{Rn} V$) is discussed in the following section.

Before proceeding, it is worthwhile to note a potentially important assumption implicit in equations (8) - (10). We have treated radon in air as an effectively binary mixture. This means that we neglect any migration of radon that may result from the diffusion of another species in air (except as that diffusion causes convection of the mixture). Whether multicomponent diffusion effects are important for radon migration in soil is not known. A case that may prove to be significant is radon migration due to the diffusion of water vapor. Further discussion of multicomponent diffusion may be found in Bird et al. (1960).

Thus far in this section, we have assumed the radon to be migrating in open air. Considering the diffusion of radon in soil, we need to adjust our description to account for

two effects of the solid matrix: the area through which radon may diffuse is reduced and the average path length that radon must traverse to reach one point from another is increased. These factors are embodied in the replacement of the binary diffusion coefficient, D_0, with an effective diffusion coefficient, D_e, so that

$$\mathbf{J}^{d}_{Rn} = -D_e \nabla I_{Rn}. \tag{11}$$

In this equation, $\mathbf{J}^{d}_{Rn}$ represents the diffusive flux density of radon activity per unit of pore area of the soil. The relationships among D_e, D (the bulk diffusion coefficient), and D_0 were discussed in Section II.C.

Two implicit approximations remain in the description of diffusive flux given in equation (11). It is worthwhile to examine them briefly before continuing. First, we have assumed that, as in open air, all the kinetic interactions of the radon atoms occur with gas molecules. This is a reasonable approximation so long as the pores are large relative to the mean free path of the radon atoms, which is comparable with that for the major constituents of air, 0.065 μm at 25°C. Pore dimensions are of the same order as grain size, hence for all soils larger than clays, this assumption is good. For smaller pores, the molecular transport process is termed Knudsen diffusion. The flux density remains proportional to the concentration gradient; however, the diffusivity is proportional to the pore radius and thus is a strong function of position within the pores (Youngquist, 1969).

The second approximation is that all radon in the soil exists in one of two states: within the air contained in the soil or within the solid soil grains. This approximation embodies at least three simplifications. First, we are treating the pore size distribution as unimodal, or, in the parlance of Currie (1961) we are treating the soil as solid grained, rather than crumbly. Alternatively, we are assuming that the characteristic time for migration out of the small pores of a grain into the major pores of the soil matrix is small relative to the migration time through the major pores. The second simplification neglects

the fraction of radon that is present in soil water. At 20°C, the coefficient of solubility, defined as the ratio of concentrations at equilibrium, for radon between water and air is 0.25 (Boyle, 1911). If the moisture saturation is 50% and the temperature is 20°C, the amount of radon in the gas phase of the pores is 4 times as large as that in the water phase. This effect will be considered explicitly below. Finally, we neglect any possible adsorption of radon on the surfaces of the soil grains. As radon is an inert gas, and since its condensation temperature is much lower than environmental temperatures, this would seem to be a good assumption. Experimental evidence of the effect of adsorption on radon release from geologic materials has been reviewed by Tanner (1980). He concluded that the studies were insufficient to determine whether this is an important factor.

For a dry, solid-grained soil through which radon migrates only by diffusion, the following equation describes the activity concentration in the pores.

$$\frac{\partial I_{Rn}}{\partial t} = D_e \nabla^2 I_{Rn} - \lambda_{Rn} I_{Rn} + G \tag{12}$$

where λ_{Rn} is the decay constant of radon (2.1×10^{-6} s^{-1} for ^{222}Rn and 0.0125 s^{-1} for ^{220}Rn), and G is the volumetric radon generation rate in the soil pores (Bq m^{-3} s^{-1}). We have assumed that the diffusion coefficient is constant. The generation rate may be determined from parameters already introduced:

$$G = f \rho_s A_{Ra} \lambda_{Rn} \frac{1-\varepsilon}{\varepsilon} \tag{13}$$

where f is the emanation coefficient, ρ_s is the density of the soil grains (commonly 2.65×10^3 kg m^{-3} and rarely not in the range $(2.6\text{-}2.8) \times 10^3$ (Scott, 1963)), A_{Ra} is the radium activity concentration in the soil (Bq kg^{-1}), and ε is the porosity.

Considering the case of uncovered soil of infinite depth and extent, and assuming the radon concentration to be zero at the soil surface, the steady-state solution to the one-

dimensional form of equation (12) yields the radon activity concentration in the soil pores at a depth z below the surface:

$$I_{Rn}(z) = I_\infty (1 - e^{-z/\vartheta}) \tag{14}$$

where $I_\infty = G/\lambda_{Rn}$ is the activity concentration of radon in the pores at large depths and $\vartheta = (D_e/\lambda_{Rn})^{1/2}$ is known as the diffusion length. For ^{222}Rn, a typical value of ϑ is 1 meter or less.

The flux density of radon from uncovered soil due entirely to diffusion is given by multiplying equation (11) by ε so that the flux is determined per unit geometric area. Substituting equation (14), we obtain the result

$$J_{Rn}^d = \varepsilon \lambda_{Rn} \vartheta I_\infty = (D_e \lambda_{Rn})^{1/2} \rho_s f A_{Ra} (1-\varepsilon) \tag{15}$$

Taking as typical values for ^{222}Rn, $D_e = 2 \times 10^{-6}$ m^2 s^{-1}, $\rho_s = 2.65 \times 10^3$ kg m^{-3}, f = 0.2, A_{Ra} = 30 Bq kg^{-1}, and ε = 0.5, we obtain J_{Rn}^d = 0.016 Bq m^{-2} s^{-1}. By comparison, Wilkening et al. (1972) estimated the mean world-wide flux of ^{222}Rn to be approximately 0.015 Bq m^{-2} s^{-1}.

Because of its much larger decay constant, the activity flux of ^{220}Rn should generally be larger than that of ^{222}Rn, although the molar flux should be substantially less. Flux of ^{220}Rn from dry, uncovered soil measured at six sites in New Mexico was found to be 1.6 ± 0.3 Bq m^{-2} s^{-1} (Crozier, 1969), 100 times larger than the typical value for ^{222}Rn cited above, but, in molar terms, 60 times less.

The diffusion of radon from soil through concrete slabs and into houses has been analyzed theoretically (Culot et al., 1976; Collé et al., 1981; Landman, 1982; Landman and Cohen, 1983). The results show that a structurally intact slab is an effective barrier against radon entry: a reduction in flux to approximately 5% or less of the value for uncovered soil is expected for a typical case (Collé et al., 1981; Nero and Nazaroff, 1984). Experimental

measurements of flux through concrete slabs confirm that the diffusion of radon through concrete is much less than needed to account for radon in houses (George and Breslin, 1980). If the slab is cracked, the diffusional flux may be greatly increased. Landman (1982) determined that 25% of the flux from uncovered soil would penetrate the slab if a 1 cm gap existed for every 1 m of slab. Even for relatively large penetrations, however, the resulting diffusive flux is still very much smaller than the observed entry rates in some houses.

In addition to affecting the emanation coefficient and the diffusion coefficient, the presence of water in the soil pores alters the diffusive transport equation. If we assume that radon is partitioned between water and air according to Henry's law, and that diffusion of radon within the water can be neglected, then the transport equation can be written

$$\frac{1}{\varepsilon}\frac{\partial(I_a\varepsilon_a + I_w\varepsilon_w)}{\partial t} = D_e' \nabla^2 I_a - \frac{1}{\varepsilon}\lambda_{Rn}(I_a\varepsilon_a + I_w\varepsilon_w) + G' \qquad (16)$$

where I_a is the radon concentration in the air volume, I_w is the radon concentration in the water volume, and ε_a and ε_w are the air and water porosities, respectively, so that $\varepsilon_a + \varepsilon_w = \varepsilon$. The radon concentrations in the two phases are related by $I_w = \kappa I_a$, where κ is the coefficient of solubility of radon in water. The solution to the steady-state problem for a semi-infinite soil is analogous to equations (14-15) with modified diffusion length, infinite depth concentration, and surface flux.

$$\vartheta = \left[\frac{\varepsilon}{\varepsilon_a + \kappa\varepsilon_w}\right]^{1/2}\left[\frac{D_e'}{\lambda_{Rn}}\right]^{1/2}$$

$$I_\infty = \frac{G'\,\varepsilon}{\lambda_{Rn}(\varepsilon_a + \kappa\varepsilon_w)}$$

$$J^d_{Rn} = (D_e' \lambda_{Rn})^{1/2} \rho_s f' A_{Ra} (1-\varepsilon) \left[\frac{\varepsilon_a^2}{(\varepsilon_a + \kappa\varepsilon_w)\, \varepsilon} \right]^{1/2} \tag{17}$$

For $\varepsilon_a = \varepsilon_w = 0.25$ and $\kappa = 0.25$, and assuming that moisture has no effect on D_e and f, ϑ is increased by 26%, I_∞ is increased by 60% and J^d_{Rn} is decreased by 37%. Of course, in general, the change in moisture has a substantial effect on both D_e and f. For example, the results presented in Figures 6 and 9 indicate that for the respective samples, the effective diffusion coefficient is decreased by a factor of 5, and the emanation coefficient is increased by a factor of 4, for the wet case relative to the dry case.

B. Convective Transport—Darcy's Law

In the middle of the 19th century, H. Darcy conducted experiments on the flow of water through sand columns. His results showed that for a given column the volumetric flow rate, Q, was proportional to the difference of the fluid heads at the inlet and outlet of the column, Δh, and to its cross-sectional area, A, and inversely proportional to the length of the column, L:

$$Q = \frac{c_1 \Delta h\, A}{L} \tag{18}$$

where c_1 is a constant dependent on the sand. Muskat (1946) argued theoretically that the relationship

$$v = \frac{Q}{A} = \frac{c_2 d^2}{\mu} \frac{\Delta P}{\Delta L} \tag{19}$$

should hold under restricted conditions. In this expression, c_2 is a constant, d is a length scale related to the soil grain size or pore diameter, μ is the viscosity of the fluid, and $\Delta P/\Delta L$ represents the pressure drop per column length. The derivation of this equation follows from dimensional analysis and the postulate that, for sufficiently low Reynolds

numbers ($Re = dv\rho/\mu$), the flow though a porous material should be analogous to viscous flow through a pipe, as described by Poiseuille's law (Bird et al., 1960). In deriving equation (19) and throughout the discussion that follows, the effects of gravity are neglected.

Equation (19) can be converted to differential form by allowing ΔL to become infinitesimal. Then, if the soil permeability is constant and isotropic, Darcy's law may be written

$$\mathbf{v} = -\frac{k}{\mu}\nabla P \tag{20}$$

where $\mathbf{v}$ is the superficial velocity vector, i.e., the flow per unit geometric area defined over a region large relative to individual pores but small relative to the overall dimensions of the soil; k is the intrinsic permeability as discussed in Section II.B; and ∇P is the gradient of the dynamic pressure. This expression appears to be valid even if the permeability is not constant.

If the soil permeability is not isotropic, the permeability coefficient is replaced with a 3×3 permeability matrix, $\mathbf{K}$, and Darcy's law becomes (Scheidegger, 1960; Scott, 1963; Rice et al., 1969)

$$\mathbf{v} = -\frac{1}{\mu}\mathbf{K} \cdot \nabla P \tag{21}$$

Given the superficial air velocity through soil, the radon activity flux per unit pore area due to convective flow is expressed by

$$J_{Rn}^{c} = \frac{I_{Rn}\,\mathbf{v}}{\varepsilon} \tag{22}$$

Darcy's law has been observed to break down as Reynolds number increases. In contrast to viscous flow in pipes, for which Poiseuille's law remains valid for $Re < 2000$,

experimental evidence has shown deviations from Darcy's law for Reynolds numbers in the range of 0.1-75 (Scheidegger, 1960). In the case of pipe flow, the deviations are associated with the onset of turbulence. Deviations from Darcy's law with increasing Reynolds number are sometimes attributed to turbulence (Burmister, 1954). It is more likely, however, that the flow remains laminar and that this effect is due to the emerging importance of the inertial term in the Navier-Stokes equation as the Reynolds number increases through order 1 (Scheidegger, 1960; Bird et al., 1960; Schlichting, 1979; Whitaker, 1984).

Under most circumstances, for the problem of radon entry into buildings, Darcy's law would be expected to hold in the soil. For a typical dynamic pressure gradient of 5 Pa m^{-1}, the Reynolds number is less than one for all soils having a permeability less than approximately 10^{-9} m^2, i.e., for all soils finer than gravel.

A second assumption in the development of Darcy's law is, as in the case of applying Fick's law to porous media, that the pores are large relative to the mean free path of the gas. Corrections are possible if this assumption is not true (Scheidegger, 1960); however, determining the fluid velocity analytically becomes more difficult. It seems probable that this refinement is not of great importance in the problem at hand as the pores of soils through which convective flow is likely to be important are generally large relative to the mean free path.

If we assume that Darcy's law holds, we may combine equation (20) or (21) with a continuity equation and an equation of state to obtain a governing equation for the dynamic pressure in the soil. By solving the governing equation for a specified geometry subject to appropriate boundary conditions on the dynamic pressure and/or the velocity, we may determine the convective velocity field in the soil, or, alternatively, the volume flow rate, e.g., into a building substructure. The velocity field is needed as input to analysis of the full transport equation, as discussed in the next section. The volume flow rate into the

building, combined with an estimate of the radon concentration in the entering air, can be used to compute the radon entry rate attributable to convective flow.

For the remainder of the discussion in this section, we assume Darcy's law accurately describes air flow through soil, and that the soil is homogeneous and isotropic with respect to the permeability. It can be shown that, under these constraints, and for the problem of radon migration in soil, air in the soil may be treated as incompressible and, in steady state, the dynamic pressure satisfies the Laplace equation:

$$\nabla^2 P = 0 \tag{23}$$

This is a classic equation in applied physics which arises in connection with problems other than fluid flow in porous media, including electrical potential in the vicinity of charged bodies (Lorrain and Corson, 1970), fluid flow at high Reynolds number outside the boundary layer (Schlichting, 1979), and heat conduction in solids (Carslaw and Jaeger, 1959). Consequently, there is a considerable literature on methods of solving Laplace's equation. Analytical solution methods include conformal mapping and separation of variables through a coordinate transformation (Morse and Feshbach, 1953). The latter approach can be valuable for radon entry if the building being investigated has, or can be approximated as having, certain symmetry (Nazaroff et al., 1985; Nazaroff et al., 1987a; Nazaroff, 1988). A graphical technique called flow-net sketching is useful if the problem can be treated as two-dimensional and the pressure at the surface of the soil assumed to be constant (Scott, 1963; Terzaghi and Peck, 1967). It yields the fluid streamlines and isopotential lines and can be used to estimate the velocity field and the total flow rate. Similar results with similar constraints can be obtained from an experimental technique using the electrical analog to the fluid flow problem (Scott, 1963). The most powerful and flexible technique is numerical modeling using a finite-difference (Loureiro, 1987) or a

finite-element method (Desai and Abel, 1972). It is also the most costly to develop and implement.

Several workers have reported on investigations of aspects of convective radon migration in soil for applications other than radon entry into buildings (Kraner et al., 1964; Andrews and Wood, 1972; Clements and Wilkening, 1974; Israelsson, 1980; Bates and Edwards, 1981; Schery et al., 1982; Rogers et al., 1983; Schery et al., 1984). Of particular interest are the results of the studies in New Mexico of radon exhalation from uncovered soil. Clements and Wilkening (1974) found that barometric pressure changes of 1000-2000 Pa over a period of 1-2 days produced convective velocities of order 10^{-6} m s^{-1} at the surface of a soil with permeability of 10^{-12} m^2. The radon flux from the surface was thereby changed by 20-60% compared to the rate associated with molecular diffusion alone. We shall see that this is a small effect for a large change in dynamic pressure relative to the effects of pressure differences on radon entry into buildings.

In a later study in gravelly sandy loam in the same area, Schery et al. (1984) concluded that among the possible environmental influences leading to temporal variation in radon exhalation, atmospheric pressure changes and rainfall were the most important. Effects due to temperature and wind were either comparatively small or undetectable. The time-averaged radon flux from the uncovered soil surface was close to that expected for pure molecular diffusion. Based on an observed inconsistency between the near-surface radon concentration profile and the measured flux density, the investigators suggested that a contribution to the exhalation rate may have resulted from direct flow through inhomogeneities.

These studies suggest that molecular diffusion dominates convection as a process by which radon enters the atmosphere from uncovered soil. As is discussed in more detail in subsequent sections, the reverse is often true for buildings. There are two major differences between these cases. First, a building's substructure shell is an effective barrier to molecular diffusion, thereby reducing its importance. Second, the geometry of a

building and its operation lead to sustained pressure differences which may induce small yet persistent air flows into a building through the soil. Such sustained flows generally do not exist for horizontal surfaces of uncovered soil.

C. General Transport Equation

Following the discussion of the previous two sections, we may combine the effects of diffusion and convection into a general transport equation for radon migration in soil. For soil with negligible moisture content, the result is

$$\frac{\partial I_{Rn}}{\partial t} = \frac{1}{\varepsilon} \nabla \cdot D \, \nabla I_{Rn} - \frac{1}{\varepsilon} \nabla \cdot I_{Rn} \, v + f \, \rho_s \, \frac{1-\varepsilon}{\varepsilon} A_{Ra} \, \lambda_{Rn} - I_{Rn} \, \lambda_{Rn} \qquad (24)$$

If the moisture content of the soil is large enough for a significant fraction of the radon in the pores to be dissolved in the liquid, the transport equation is written

$$\frac{1}{\varepsilon} \frac{\partial (I_a \varepsilon_a + I_w \varepsilon_w)}{\partial t} = \frac{1}{\varepsilon_a} \nabla \cdot D' \, \nabla I_a - \frac{1}{\varepsilon_a} \nabla \cdot I_a \, v' + f' \, \rho_s \, \frac{1-\varepsilon}{\varepsilon} A_{Ra} \, \lambda_{Rn} - \frac{1}{\varepsilon} \lambda_{Rn} \, (I_a \varepsilon_a + I_w \varepsilon_w) \qquad (25)$$

where the primes indicate new values accounting for the moisture content and where we have neglected any moisture migration and any migration of radon within the water.

As previously noted, these equations have not been solved analytically, except for the simplest geometry (Clements and Wilkening, 1974; Schery et al., 1984). Consequently, to make much progress, we are left with two approaches: approximate analysis and numerical modeling. In the remainder of this subsection, we discuss aspects of approximate analysis. In Section VI.C, recent research on modeling radon entry into buildings, a task which is still in its early stages of development, is briefly discussed.

The most significant simplification possible in this problem is to be able to neglect one of the migration processes—molecular diffusion or convection—as negligible

compared with the other. To compare the relative importance of the two processes, we make some simplifying assumptions to equation (24), then make the equation dimensionless. The simplifying assumptions are that (1) the superficial velocity is described by Darcy's law; (2) the soil is isotropic and homogeneous with respect to the diffusion coefficient, permeability, porosity, emanation coefficient, radium content and bulk density; and (3) for the range of pressures of interest, air may be treated as incompressible. Then we may write

$$\frac{\partial I_{Rn}}{\partial t} = D_e \nabla^2 I_{Rn} + \frac{k}{\varepsilon\mu} \nabla P \cdot \nabla I_{Rn} + G - \lambda_{Rn} I_{Rn} \tag{26}$$

where G is defined by equation (13).

To make the equation dimensionless (following Bird et al., 1960, pp. 107-111), we multiply and divide each variable by a unique combination of a characteristic time λ_{Rn}^{-1}, length L, and pressure difference ΔP_o, as needed to make each dimensionless. Having done so, we may write equation (26) as

$$\frac{1}{N_\tau} \frac{\partial I_{Rn}^*}{\partial t^*} = \frac{1}{Pe_p} \nabla^{*2} I_{Rn}^* + \nabla^* P^* \cdot \nabla^* I_{Rn}^* + \frac{1}{N_\tau} (G^* - I^*) \tag{27}$$

where the asterisks denote dimensionless quantities. This equation has two dimensionless groups

$$Pe_p = k \varepsilon \Delta P_o (\mu D_e)^{-1} \tag{27a}$$

$$N_\tau = \Delta P_o k (\mu \varepsilon L^2 \lambda_{Rn})^{-1} \tag{27b}$$

The dimensionless groups are important variables: Pe_p, effectively a Péclet number for mass transfer in a porous medium, characterizes the relative importance of convective

transport with respect to diffusive migration, and N_τ characterizes the relative importance of radioactive decay with respect to convective flow as a means of removing radon from the soil pores.

Based on the values of these groups we may simplify the problem as follows. First, if $Pe_p >> 1$, diffusion may be neglected compared with convective flow as a transport process, and the governing equation in dimensional form becomes

$$\frac{\partial I_{Rn}}{\partial t} = \frac{k}{\varepsilon\mu} \nabla P \cdot \nabla I_{Rn} + G - \lambda_{Rn} I_{Rn} \tag{28}$$

If $Pe_p >> 1$ and $N_\tau >> 1$, the problem may be treated in steady state and radioactive decay neglected. The resulting equation is analogous to the convective heat transfer problem with internal sources in which conduction and viscous dissipation may be neglected (Carslaw and Jaeger, 1959).

If $Pe_p << 1$, convective transport may be neglected. The concentration is governed by the diffusion equation (equation 12). Finally, if $Pe_p << 1$ and $N_\tau >> Pe_p$, the problem reduces to Poisson's equation:

$$\nabla^2 I_{Rn} + \frac{G}{D_e} = 0 \tag{29}$$

Soil permeability is the most important parameter in determining which, if any, of these conditions is satisfied. Choosing typical values of $\Delta P_o = 3$ Pa, $\varepsilon = 0.5$, $\mu = 17 \times 10^{-6}$ kg m^{-1} s^{-1}, and $D_e = 2 \times 10^{-6}$ m^2 s^{-1}, then $Pe_p = 1$ if $k = 2.3 \times 10^{-11}$ m^2. Assuming these typical values apply, then for soils with much larger permeabilities, i.e., coarse sands and gravels, migration by molecular diffusion can be neglected. For soils with much smaller permeabilities, i.e., silts and clays not having significant structural permeability, convective transport can be neglected. If we further take L = 3 m as the scale of soil length through which transport must be considered (this length corresponds to half the

characteristic dimension of a house and, in most cases, enough radon is produced by the soil within this distance of a building to sustain high indoor concentrations), then the permeability at which $N_\tau = 1$ is 5×10^{-11} m^2.

VI. RADON ENTRY INTO BUILDINGS

A. Pressure-Generating Mechanisms

1. Wind

Consider the wind blowing directly on the side of a house. In the simplest model, if we neglect the shear stress between the wind and the ground, the change in momentum from the free-stream velocity must equal the increase in pressure at the wall where the velocity falls to zero. Hence

$$\Delta P_o = \frac{1}{2} \rho v^2 \tag{30}$$

where ρ is the air density, v is the velocity, and ΔP_o is the pressure at the wall minus the free-stream pressure. This equation may readily be derived from the one-dimensional, steady-state form of the Navier-Stokes equation, assuming the Reynolds number is much greater than one, a condition that for the case at hand is always satisfied.

Actual wind-induced pressures across the walls of a house are moderated from this simple calculation by several factors. Winds generally strike a house obliquely, reducing pressures. The typical height of a house is small enough that the effect of the ground on reducing wind speed is significant. Furthermore, houses are often shielded by other structures and vegetation. In accounting for these effects, wind engineers write equation (30) as

$$\Delta P = C_d (\frac{1}{2} \rho v^2) \tag{31}$$

where C_d is called the drag or pressure coefficient. It is determined empirically, often from wind-tunnel studies. It is found to be relatively independent of wind speed, but greatly dependent on small details of shape, orientation and shielding (Sachs, 1972). In one

study, ground-level data for an impermeable cube in a boundary-layer velocity profile indicated an average drag coefficient of 0.56 on the windward side, -0.49 on the side walls and -0.15 on the leeward side (Simiu and Scanlan, 1978).

These data apply only at the base of the walls, whereas for the problem of radon entry, we are interested in the pressures at the ground surface at distances up to several meters from the walls. A wind tunnel investigation of this matter was recently conducted (DSMA, 1985). The results, reproduced in Figure 10, show drag coefficients on the windward side of 0.2-0.5 extending distances comparable with the house dimensions.

Taking 0.4 and 3 m s^{-1} as representative values of the windward drag coefficient and wind speed, respectively, and assuming the pressure inside the house is the same as the free stream conditions, we obtain a pressure difference across the soil and substructure on the windward side of approximately 2 Pa. Note that the pressure difference varies as the square of the wind speed so that considerably larger pressure differences are possible.

Pressures induced by winds can fluctuate rapidly and so it is important to consider how rapidly pressure fluctuations at the surface of the soil are transmitted through it. This question has been addressed theoretically by Fukuda (1955), who obtained the following governing equation for the pressure fluctuations, φ, assuming them to be much smaller than the atmospheric pressure, P_a.

$$\frac{\partial \varphi}{\partial t} = \frac{k}{\varepsilon \mu} P_a \nabla^2 \varphi \qquad (32)$$

where the symbols are as previously defined. This is simply the diffusion equation with the term $D_p = kP_a (\mu\varepsilon)^{-1}$ being a "diffusion coefficient" for pressure disturbances. If, for simplicity, we consider a one-dimensional case, then the characteristic time for a pressure disturbance to propagate through a distance L_p is given by

$$\tau_p = \frac{L_p^2}{D_p} \tag{33}$$

Values of τ_p for L_p = 1 m and 5 m for different soil types are given in Table 7. For sandy and gravelly soils, propagation times are minutes or less, whereas for clayey soils, pressure disturbances can take many days to propagate.

Van der Hoven (1957) analyzed the spectral distribution of the wind speed at 100-m at Brookhaven, New York. As shown in Figure 11, reproduced from his results, the wind energy distribution is roughly bimodal with the low-frequency mode having a peak corresponding to a period of 4 days and the high-frequency mode having a peak at a frequency of about 1 minute. There is a large spectral gap for periods from about 10 minutes to 2 hours which is believed to be generally present. From these data we can conclude that for soils with sufficiently high permeabilities for pressure-driven flow to be important, a large fraction of the wind power is sufficiently sustained so that the pressure disturbance is completely propagated through the soil and a steady-state pressure distribution may be assumed. However, a significant portion of the wind energy occurs with fluctuations at sufficiently high frequency so that the steady-state pressure assumption is not strictly valid.

2. *Temperature Differences*

A pressure differential that varies with height exists across any vertical wall separating air masses of different temperatures. Otherwise known as the "stack effect," this pressure difference arises because air is a compressible fluid, whose density varies with temperature, and which is acted upon by gravity.

Consider a wall of height H separating air masses of temperature T_i and T_o. If we assume that the ideal gas law applies and that the temperature on either side of the wall is

constant, then the conditions of fluid statics require that the pressure vary with height on either side of the wall according to

$$P = P_0 e^{-mgz/RT} \tag{34}$$

where P_0 is the pressure at reference height z=0; m is the molar weight of air (0.029 kg mol^{-1}); g is the acceleration of gravity (9.8 m s^{-2}); R is the universal gas constant (8.31 J mol^{-1} K^{-1}); and T is the temperature (K). If we now define z_0 as the height at which the pressures on either side of the wall are equal, then we find that the pressure difference across the walls is

$$\Delta P(z) \approx \alpha \left[\frac{1}{T_i} - \frac{1}{T_o}\right](z-z_0) \tag{35}$$

where $\alpha = 3454$ Pa m^{-1} K. In deriving equation (35) we have made the approximation $e^{-x} \approx 1-x$, valid for $x<<1$. As with wind-induced pressure differences, a positive ΔP implies a net inward pressure.

A representative situation has $T_i = 293$ K, $T_o = 273$ K, and $z_0 = 3$ m, so that $\Delta P(0) = 2.6$ Pa. Since $|T_o - T_i| << T_o$ or T_i for any situation involving an occupied building, the pressure difference due to the stack effect is approximately proportional to the temperature difference.

3. *Other Processes*

Several other processes can, in principle, lead to convective flow of soil air into or through building substructures. Here we will consider two factors: barometric pressure changes and precipitation. These processes are complex and relatively little work pertaining to them has been reported. Consequently, our discussion will be brief and qualitative.

Compared with the pressure changes associated with winds and temperature differences, the magnitude of barometric pressure changes are large, with excursions from the long-term average routinely exceeding 100 Pa. However, these pressure changes can only be effective in inducing the flow of soil air into a building if they lead to a sustained difference in pressure between the indoor air and the pore air of the nearby soil. An inverse correlation between indoor radon concentration and the rate of change of barometric pressure was observed in the basement of a house in Princeton, New Jersey during the late spring (Hernandez et al., 1984). The authors inferred that the short-term variation in radon entry rate exceeded an order of magnitude for rates of change in pressure from -76 to 45 Pa h^{-1} (-0.75 to 0.44 mbar h^{-1}) . In another study, no correlation between radon entry rate into a house with a basement and rate of barometric pressure change was apparent (Nazaroff et al., 1985).

Although there has been no experimental verification, one might expect to find the influence of barometric pressure changes to be substantial for a house with a basement in relatively permeable soil at a time when the surface of the soil was frozen. Under such circumstances, barometric pressure changes could lead to a flow of soil gas that is "funneled" through the basement as a result of the reduced permeability at the surface of the surrounding soil. A similar situation might exist for buildings with any type of substructure immediately following a heavy rain. Still another case where radon entry rate may be strongly correlated with barometric pressure changes is one in which landscaping has resulted in a low permeability cap over a relatively highly permeable soil.

One expects that the effect of barometric pressure changes on radon entry rate would also depend on the depth of the soil to an impermeable zone. If the air reservoir in the soil were restricted to a small depth below the foundation with a low permeability layer (e.g., clay or water table) below, barometric pressure changes should be relatively ineffective in inducing flow.

Through a piston-like displacement of soil air, a heavy rainfall could potentially lead to a short-term increase in radon entry rate independent of the barometric pressure. At such a time, the permeability of the wet soil surrounding the house is considerably smaller than that of the dry soil beneath it; hence, radon-bearing soil gas could be forced through penetrations in the substructure. Evidence that such an effect might occur is shown in Figure 12. During the two-day period of March 29-30, 1983, coincident with a heavy rainfall, radon concentrations indoors and in the crawl space rose to their highest values for the entire five-week monitoring period. The investigators could not rule out the possibility that the increased concentrations were due to a reduction in permeability of the surrounding soil combined with the concurrent drop in barometric pressure (Nazaroff and Doyle, 1985).

4. Experimentally Observed Dynamic Pressure Differences

Experimental data have been collected on outdoor-indoor pressure differences that could cause a sustained flow of air through soil and into building substructures. The size of these pressure differences is consistent with expectations based on the previous discussion.

Intensive monitoring of a single-family residence near Chicago was conducted during February-May 1982 (Nazaroff et al., 1985). Dynamic pressure differences were measured between a reference point in the basement of the house and four outdoor points located just above ground level, one at the center of each wall. Averaging over the four outdoor points, the mean outdoor-indoor pressure difference over the fifteen week period was 2.3 Pa, with weekly average values ranging from 0.6 to 4.3 Pa. As expected, the pressure difference was strongly correlated with indoor-outdoor temperature difference.

Revzan (1989) presented the results of a nine-month (October 1986 through July 1987) radon monitoring study in two New Jersey homes. On a three-day average basis, the pressure difference between outdoor air and the basement at one house was in the range 1-8 Pa, with the mean value in the range 3-4 Pa. At the second house, the pressure

difference was measured across a basement wall, 15 cm above the slab floor. In this case, the three-day-average pressure difference varied between near zero and 6.5 Pa, with an approximate mean of 3 Pa. In both cases, net inward pressure was strongly correlated with the mean indoor-outdoor temperature difference.

Hubbard et al. (1988) reported on outdoor-basement pressure differences measured during the winter in a house in New Jersey. For a ten-day period with electric heat, the mean pressure difference was 2.2 Pa; with a gas-fired furnace providing heat for a seven-day period, the mean pressure difference was 3.4 Pa.

Holub et al. (1985) reported measurements of indoor-outdoor pressure differences across the wall of a basement in Colorado during winter. They observed a mean inward pressure of 0.5 and 0.9 Pa during two periods, of three and ten days duration, respectively. The indoor-outdoor temperature difference during this period was not reported.

B. Relationship Between Indoor Radon Concentration and Ventilation Rate

1. Analysis

Because both the radon entry rate from soil and the air-exchange rate of a building vary with the pressure difference across the building shell, the variation of indoor radon concentration with air-exchange rate is more complex than suggested by a simple mass-balance model (e.g., Bruno, 1983). An understanding of this relationship is essential for the proper interpretation of indoor concentration measurements, as well as for predicting the change in indoor radon concentration for a specified change in the air-exchange rate. The present state of knowledge is not sufficient to address all of the possible situations. Consequently, the discussion in this section is illustrative rather than comprehensive.

It is convenient to divide the radon entry modes into two categories. We will designate as "passive" those modes that act independently of the dynamic pressure difference across the building shell. Specific examples of passive entry are molecular

diffusion from building materials and release associated with household water use. By contrast, modes that are limited by the rate of pressure-driven flow through the building substructure are designated as "active" entry mechanisms. High rates of radon entry from soil into residential basements are largely due to active modes. The total radon entry rate, S_v, may be written as the sum of contributions from these two modes:

$$S_v = S_p + S_a(\Delta P_f) \tag{36}$$

where S_p and S_a represent the radon entry rates by passive and active modes, respectively, and ΔP_f denotes the effective dynamic outdoor-indoor pressure-difference across the lower part of the building structure.

It is likewise useful to distinguish two ventilation modes. In "balanced" systems the air-exchange rate is effectively independent of the dynamic pressure difference across the building shell. A mechanical ventilation system that provides equal supply and exhaust flows is balanced. Mechanical ventilation that provides only supply or exhaust, and infiltration, are considered "unbalanced" ventilation modes: the air-exchange rate varies directly with the pressure difference across the building shell. The total ventilation rate, λ_v, is the sum of the rates due to these two modes:

$$\lambda_v = \lambda_{v,b} + \lambda_{v,u}(\Delta P) \tag{37}$$

where $\lambda_{v,b}$ and $\lambda_{v,u}$ represent the ventilation rates associated with balanced and unbalanced modes, respectively, and ΔP is a characteristic pressure difference, such as the mean of the absolute value, across the building envelope.

The unbalanced ventilation component is related to the average dynamic pressure difference across the building shell by a power-law relationship (Sherman, 1980):

$$\lambda_{v,u} = \frac{E}{V} (\Delta P)^n \qquad 0.5 < n < 1.0 \tag{38}$$

where E is the permeability coefficient of the building envelope (with dimensions L^{3+n} T^{2n-1} M^{-n}) and V is the interior volume. E is equal to the product $A_o(2/\rho)^n$, where A_o is the effective leakage area of the envelope (Sherman, 1980).

The characteristic dynamic pressure difference can be estimated as the sum of three components—those due to temperature differences, wind, and unbalanced mechanical ventilation. (Flow from a chimney would be considered in the last of these categories.)

$$\Delta P = (\rho/2)\, f_s^2\, |T_o - T_i| + (\rho/2)\, f_w^2\, v^2 + |\Delta P_{mv,u}| \tag{39}$$

where ρ is the air density, and f_s and f_w are stack and wind parameters (Sherman, 1980).

The value of the exponent in equation (38) is determined by the relative importance of two energy-loss mechanisms as air flows through the penetrations in the building shell. For penetrations that have relatively large width and short length, energy loss is largely due to the inertia of the air at the outlet of the crack. If this is the dominant situation for the structure, the value of the exponent approaches 0.5 for reasons that are analogous to the square-root dependence of the pressure difference with wind speed (see equation 30). The other limiting case is fully developed laminar flow in the cracks. This requires that the cracks be long, narrow and that the flow have small Reynolds number. In this case, viscous dissipation is the dominant energy loss mechanism. This flow regime is analogous to the flow through soil described by Darcy's law (equation 20); the exponent in equation (38) approaches 1.0 in the limit in which this mode dominates. Measurements of n yield values in the range 0.5-0.75 (Blomsterberg et al., 1979; Modera et al., 1983). The value n=0.5 has been adopted in a commonly used infiltration model (Sherman, 1980).

The variation of the active component of the radon entry rate with pressure difference depends on both the mode of entry and on the details of the building-soil air coupling. To be specific, we consider the common example of a house with a basement which has a perimeter penetration such as a crack at the floor-wall joint or a drain tile connected through an untrapped pipe to a basement sump. For small source rates, the concentration of radon in the entering soil gas is independent of the flow rate and, consequently, independent of pressure difference. In this case, assuming that the effective dynamic pressure difference at the base of one or more of the walls is inward (i.e., ΔP_f is positive), $S_a \propto (\Delta P_f)$. On the other hand, if the source rate is large, the soil gas is depleted, and the influence of the dynamic pressure difference on radon entry is diminished. A theoretical analysis of this situation has shown that $S_a \propto (\Delta P_f)^{0.66}$ in this case, again assuming $\Delta P_f > 0$ (Nazaroff, 1988). If ΔP_f is negative, i.e. the pressure across the building substructure is outward, we expect $S_a \approx 0$. These conditions are summarized by

$$S_a = \begin{cases} 0 & \Delta P_f < 0 \\ \beta(\Delta P_f)^m & \Delta P_f > 0 \quad 0.66 < m < 1.0 \end{cases} \tag{40}$$

where the coefficient β depends on the radium content and emanation coefficient of the soil, on the permeability of the soil, and on the coupling between the building interior and the soil air.

In analogy with equation (39), ΔP_f can be expressed as the sum of three components (Mowris, 1986):

$$\Delta P_f = \rho g(z-z_o)\frac{T_o-T_i}{T_o} + c_f \rho \frac{v^2}{2} + \Delta P_{mv,u} \tag{41}$$

where the thermal effect is an approximation of equation (35) and c_f is an average pressure coefficient for the lower part of the structure (cf. equation 31).

We may now write a general expression for the indoor radon concentration for this case. We may write the steady-state mass-balance equation for radon in indoor air (Bruno, 1983) as

$$I - I_o = \frac{S_v}{\lambda_v} \tag{42}$$

where we have assumed $\lambda_v >> \lambda_{Rn}$. Substituting equations (36), (40) and (41) for S_v and equations (37)-(39) for λ_v, and assuming that $\Delta P_f < 0$, we obtain

$$I - I_o = \frac{S_p + \beta \left(\rho g (z-z_0) \frac{T_o-T_i}{T_o} + c_f \rho \frac{v^2}{2} + \Delta P_{mv,u}\right)^m}{\lambda_{v,b} + \frac{E}{V}\left(\rho \frac{f_s^2}{2} |T_o-T_i| + \rho f_w^2 \frac{v^2}{2} + |\Delta P_{mv,u}|\right)^n} \tag{43}$$

It is instructive to consider two limiting cases. In Case a, we assume that the active entry rate is zero. In this case, $I-I_o = S_p/\lambda_v$, and we recover the result for the simple mass-balance case. In Case b, we assume first that $S_p=0$ and $\lambda_{v,b}=0$. We also assume that the ratios $\Delta T : v^2 : \Delta P_{mv,u}$ remain constant. The latter assumption would hold, for example, if one of the three terms greatly dominated the other two for both ΔP and ΔP_f. In this case, $I - I_o \approx (\Delta P)^{m-n}$. And, since $\lambda_v \propto (\Delta P)^n$, we obtain the result

$$I - I_o \propto \lambda_v^{[(m-n)/n]} \tag{44}$$

These results are presented in Figure 13. Surprisingly, for much of Case b, the indoor radon concentration is expected to increase with ventilation rate. Note, however, that many assumptions went into this analysis. For example, we implicitly assumed that a single dynamic pressure difference ΔP_f could be used to represent the entire base of the building. While this is reasonable for the thermal and unbalanced mechanical ventilation components, wind pressures are highly directional. A more thorough analysis would treat

the walls separately. In addition, the assumption that the dynamic pressure differences due to thermal effects, wind and unbalanced ventilation remain in constant proportion limits the applicability of this result. Mowris (1986), in analyzing the effect of adding exhaust ventilation to houses, found consistent reduction of indoor radon concentration. In any case, it is clear that the relationship between indoor radon concentration and air-exchange rate is a complex one that varies considerably with the particular circumstances of a house. One cannot reliably assume, as has often been done (e.g., Cohen, 1980; Hurwitz, 1983), that the indoor radon concentration is inversely proportional to the air-exchange rate for a given house.

2. *Experimental Results*

The relationship between indoor radon concentration and air-exchange rate in a single house has been examined in detail in two studies. In the first, the ventilation rate in a house with a very low infiltration rate ($<0.1\ h^{-1}$) was varied by means of a balanced mechanical ventilation system (Nazaroff et al., 1981). As expected, the radon concentration varied as predicted by equation (42).

In the second study, indoor radon concentration and air-exchange rate were monitored continuously in a house with a basement over a five-month period (Nazaroff et al., 1985). In this case, the changes in air-exchange rate were due to a combination of changing weather conditions, the intermittent use of a fireplace and exhaust fans, and the opening of doors and windows. A confounding feature of this experiment in the present context was the bimodal nature of the radon entry rate. It appeared that major pathways for radon entry could be either opened or closed, perhaps due to changing moisture levels in the nearby soil.

The variation of radon concentration with air-exchange rate from this study is presented in Figure 14. In the case of high entry rate (open triangles), the variation is similar to the prediction of equation (44) with n=0.75 (cf. Figure 13b). For the low entry

rate case, the behavior is more complex, perhaps indicating that neither passive nor active entry modes are dominant.

The curves plotted in Figure 14 reflect the predictions of two simple models. The dashed line corresponds to equation (42) with $I>>I_0$. The solid line reflects a two-component entry model that is much simpler than equation (43). In particular, the active entry component is assumed to be proportional to the infiltration rate. This would be expected if the exponent in equation (38) was n=1, and if the source rate was small. D'Ottavio and Dietz (1986) showed, by extending the formulation of this model to incorporate radon entering from outdoor air and the variability of radon concentration in soil air, that a better fit to a portion of the data could be obtained.

C. Modeling Radon Entry

The complexities associated with the production and migration of radon in soil and its entry into buildings, point to the need for detailed mathematical models to develop a satisfactory understanding of the effects of the many factors involved. During this decade, the development of such models has been undertaken. In this section, the central features of these efforts are described and the direction of continuing efforts is mentioned.

Overall, the modeling efforts have been based on three distinct approaches. The choice that distinguishes these approaches is between simplicity and power. Conceptually, the least complex approach is parametric modeling, but it also the least suitable for generalizing results from one case to a broader class of buildings. At the other end of the spectrum are finite-element or finite-difference models: these powerful tools require substantial effort to implement, validate, and use.

The first detailed mathematical modeling of radon migration and entry into buildings was undertaken by Scott and coworkers (DSMA, 1983; Scott, 1983; Eaton and Scott, 1984; DSMA, 1985). In this work, a finite-element approach was used, with the soil comprising 1780 variable-sized elements. The model was restricted to examining uniform

and isotropic soils, houses with basements, radon transport due to convective flow, and dynamic pressure gradients arising from temperature differences and wind. Nevertheless, some interesting and useful results have been obtained: for one case, an increase in permeability from 10^{-11} to 10^{-10} m^2 led to an increase in radon entry rate by a factor of 4.5 (DSMA, 1983); variations in wind speed and direction can lead to substantial changes in radon entry rate in the absence of other factors (DSMA, 1985); for a typical Canadian house with surrounding soil having a radium content of 59 Bq kg^{-1} and permeability of 5×10^{-11} m^2, the average radon entry rate and radon concentration would be 4×10^7 Bq h^{-1}, and approximately 200 Bq m^{-3}, respectively (DSMA, 1985).

A second example in the class of finite-element/finite-difference models was reported by Loureiro (1987). This model simulates radon migration by both diffusion and convection in the vicinity of a basement having a floor-wall gap. An aggregate layer adjacent to the basement may be specified to have distinct characteristics from the remainder of the soil. The results indicate that, for a outdoor-indoor pressure difference of 5 Pa, convective flow dominates diffusion as a radon migration process for soil permeabilities in excess of 10^{-12} m^2. As expected, for larger permeabilities, the indoor radon concentration was found to be increase strongly with increasing permeability and with increasing pressure difference. Most of the simulations carried out by Loureiro were for conditions in which the indoor radon concentration was lower than the range of interest, i.e. order 1 Bq m^{-3}. However, this work forms a solid foundation for further analysis.

Recently, more advanced analysis based on finite-difference modeling has been initiated at Lawrence Berkeley Laboratory. The present approach is based on a model developed for simulation of simultaneous transport of water, vapor, air, and heat in porous and fractured media (Pruess, 1987). The use of such a model permits examination of the potential significance of complex phenomena, such as transient flow and the effect of thermal gradients in the soil.

A simpler modeling approach based on deterministic analysis also has been developed in the past few years (Mowris, 1986; Mowris and Fisk, 1988; Nazaroff, 1988). The work by Mowris and Fisk emphasized calculation of the flow rate of air through soil and into building substructures for given processes that induce pressure differences (as described here in Section VI.A.) The radon concentration in the soil gas was assumed to remain constant at its value at infinite depth (I_∞, see equation (14).) The model was used to evaluate the effect of mechanical exhaust ventilation on indoor radon concentrations for houses with either a basement or a crawl-space. It was concluded that exhaust ventilation was appropriate (but not optimal) for houses with vented crawl spaces, or—if surrounded by impermeable soil ($k \leq 10^{-12}$ m^2)—with a basement. But, if the soil permeability is higher, exhaust ventilation could lead to an increase in radon concentration in a house with a basement.

The recent modeling work of Nazaroff (1988) was based on a Lagrangian frame of reference in which molecular diffusion of radon through the soil pores was neglected. A house with a basement and a perimeter leakage path at the level of the floor was represented by a buried cylindrical cavity with a horizontal axis in a uniform soil. The air flow field in the soil for a prescribed surface-cavity pressure difference was obtained from an analytical solution to the Laplace equation. The radon concentration entering the cavity was obtained by numerically integrating the exponential ingrowth equation (analogous to equation (14), with $\lambda_{Rn}t$ replacing z/ϑ) along fluid streamlines from the soil surface to the surface of the cavity. The results show that soil having ordinary ^{226}Ra content and moderately high permeability (10^{-10} m^2) can be responsible for indoor radon concentrations of order 500 Bq m^{-3}.

The third approach, parametric modeling, has been utilized recently by Revzan et al. (1988b) and Revzan (1989). In this approach, a simplified physical representation of a building and the surrounding soil is used to derive equations describing the indoor radon concentration as a function of controlling variables. Coefficients in these equations are

retained as unknown variables, whose values are determined by statistical analysis of extensive experimental data sets collected at specific sites. For the few sites studied, much of the variability in 3-day-average indoor concentrations could be explained by the fitted models. Because of difficulties in generalizing the results, the principal value in this approach may be to provide information on radon entry dynamics, rather than to serve as a predictive tool. However, the conceptual approach may logically lead to the development of lumped-parameter models—analogous to the representation of electrical circuits by resistors, capacitors, inductors, etc.—that are useful predictive tools.*

D. Influence of the Building-Soil Interface and Soil Inhomogeneity

It is clear that transport across the interface between the building and the soil must be dominated by pressure-driven flow. Molecular diffusion through a concrete slab, for example, is much too slow to permit large radon entry rates (Bruno, 1983; Nero and Nazaroff, 1984). Furthermore, if molecular diffusion were the dominant transport mechanism for entry, then the radon entry rate would only vary slowly and moderately in time; instead, rapid and dramatic changes in the radon entry rate are observed. Also, the effectiveness of control measures that prevent the bulk flow of soil gas through building substructures demonstrates that pressure-driven flow dominates as a radon entry mechanism. However, it is not known, in general, whether pressure-driven flow dominates molecular diffusion as a radon migration process in the bulk soil.

In fact, there are three major paradigms for radon migration that can lead to high rates of entry from the soil. In the first, which has received the most attention, a building substructure is coupled to a uniformly permeable soil. In response to indoor/outdoor pressure differences, air flows through the soil and into the building substructure carrying with it a high concentration of radon generated by the soil grains. Theoretical analysis of

---

* The idea of using a lumped-parameter model to represent radon entry into buildings was suggested by A. J. Gadgil.

this system indicates that with ordinary radium content (40 Bq kg^{-1}) and moderately high permeability (10^{-10} m^2), the indoor radon concentration can be as high as 660 Bq m^{-3} (Nazaroff, 1988). With elevated radium content in the soil, the indoor radon concentration would be much higher.

The second paradigm has a house set in a soil in which the permeability of the undisturbed soil varies with position. Radon migrates from low permeability regions to high permeability zones by diffusion, then is swept by convective flow into the building. Examples of this case include (1) soils with gravelly seams (as reported in Nazaroff et al., 1987a); (2) low permeability soils with large structural openings, such as a cracked clay; and (3) a soil with high permeability and low permeability layers (as reported by Kunz et al., 1988).

In the third paradigm, radon migrates by diffusion to a high permeability zone at the soil-building interface, then is swept into the building by convective flow through this high permeability zone. One example of this case would be the presence of a highly permeable backfill layer adjacent to a basement wall in an otherwise low-permeability soil. A second example would be the presence of a thin (as small as order 1 mm) gap between a basement wall and the soil that leads to an entry path near the level of the floor.

The second and third paradigms share an important feature: molecular diffusion from a low permeability zone to a region of higher permeability is an essential aspect of the overall transport process. As a result, under these paradigms the radon entry rate is higher, possibly very much higher, than would be the case if radon migration were solely due to pressure-driven flow. These two paradigms are logically distinguished by the fact that for paradigm 2 the inhomogeneity is a property of the undisturbed soil, whereas for paradigm 3 the presence of the building-soil interface creates the high-flow pathway.

Why is the distinction among these three paradigms important? The premise of this report is that soil characteristics will be useful in identifying areas where elevated indoor radon concentrations are likely. However, the relative importance among parameters

depends critically upon the radon entry paradigm. In each case, the emanating radium content of the soil is important. However, the important transport-related parameters are distinct for each paradigm. In the first case, the permeability of the soil is the only important factor. For the second paradigm, there are three potentially important transport-related factors: the permeability of the high-permeability zone, the radon diffusivity in the low permeability zone, and the geometric relationships among the building substructure, the high-permeability zone, and the low-permeability zone. For the third case, the important factors are the radon diffusivity in the undisturbed soil and the permeability characteristics of the interfacial region between the soil and the building substructure; the permeability of the undisturbed soil is unimportant in this case. Thus, if the first paradigm represents the majority of cases having elevated concentrations, then soil permeability is a crucial parameter. On the other hand, if the third paradigm is the dominant one in that portion of the building stock with an indoor radon problem, then the details of the building-soil interface are very important, and the soil permeability is an unimportant parameter.

Therefore, this issue has important implications, not only for identifying regions in which elevated indoor concentrations are probable, but also in designing effective control measures to be applied in remedial action and in the new-building stock.

One further note concerning the distinction among these paradigms. The radon entry rate is limited by the volume of soil that can contribute its radon to indoor air on a sustained basis. For the third paradigm, this volume of soil is that located within a diffusion length (i.e. about one meter) of the building substructure. For the other two paradigms, the volume of soil is essentially unlimited; however, the highest potential entry rates are associated with the second paradigm.

VII. GEOGRAPHIC AND SITE CHARACTERIZATION OF RADON SOURCE POTENTIAL

The importance of soil as a source of indoor radon, combined with the increasing evidence of unacceptably high radon concentrations in a significant fraction of houses, has raised the question of whether one might predict where high indoor radon levels are likely, either on a geographic scale or on the scale of a single lot. At the geographic scale, if a method to achieve this goal were developed and validated, the cost of identifying those houses with elevated levels could be considerably reduced. At the scale of a building site, such a method could be used to determine whether construction practices in an area need to be modified to prevent elevated indoor concentrations in advance of construction. The case indicating such an effort could succeed is strengthened by the direct observation that there is a substantial variance in the mean indoor radon concentration among different areas (Nero et al., 1986).

One of the key factors governing the radon source potential of soil is its surficial radium content. Kothari and Han (1984) have shown a correlation for nine U.S. communities between the geometric mean indoor radon concentration and the geometric mean equivalent uranium (eU) concentration of the soil, as determined from National Airborne Radiometric Reconnaissance (NARR) data. (The NARR data base is described in Section VII.A.3.) Figure 15, based on their results, shows that the order-of-magnitude range in eU is associated with roughly a factor of five range in indoor radon concentrations. Revzan et al. (1988a) have analyzed the aerial radiometric data from the NARR program for the United States, and produced the map illustrated in Figure 7 showing average surficial radium-226 concentrations. Several areas known to have a high incidence of elevated indoor radon concentrations also have been found to have noticeably high soil radium concentrations compared with their surroundings. Moed et al. (1984) have confirmed that the variations in the aerial eU data correspond to differences in field

measurements of radium content and radon flux, and to laboratory measurements of radon emanation and radium content.

Previous sections of this report have discussed the soil physics involved in both radon availability and migration, and have identified the key factors that describe these processes. This section first examines the sources of data that are available that might be used directly or indirectly to estimate the radon source potential of geographical areas. Second, a framework is discussed that would utilize the availability and migration concepts with these data bases for assessing the radon risk of land on a geographic scale. The final topic of this section is an examination of the prospect for assessing radon source potential at the scale of a plot of land.

A. Geographic Data and Data Bases

Based on the discussion in this paper, the potential for high radon entry rates from soil depends on several factors that can be grouped into three categories: soil structural factors, including air permeability; soil radiological factors, including radium content; and climatological factors. Sources of information on these parameters in the United States are discussed in this section.

1. Soil Structural Factors

a. Water permeability: Modern detailed soil surveys published for counties by the U.S. Department of Agriculture's Soil Conservation Service (SCS) contain estimates of the saturated water permeabilities of mapped soils. If a reliable correlation were to be established between water and air permeabilities, these reports would constitute an extensive database for geographic radon assessments. Laboratory studies (Al-Jibury, 1961; Reeve, 1953 and 1965) and field studies (Weeks, 1978) of such relationships are therefore of interest.

Al-Jibury (1961) measured the saturated water permeability and the air permeability as a function of moisture tension (a parameter that is monotonically related to air-filled porosity) of disturbed and undisturbed samples of soils of varying textures. Figure 16 shows plots of air permeabilities at 100 cm or more of water tension vs. saturated water permeabilities (see also Section II.B). Data for undisturbed cores of soil are shown in Figure 16a, while data for systematically-packed, disturbed samples of soil are shown in Figure 16b. The bisectors are drawn to indicate deviations in the data from a one-to-one relationship between air and water permeability. The air-filled porosities corresponding to 100 cm water tension equal those at field capacity (Marshall and Holmes, 1979, p. 40). At this tension, most of the large textural pores were air-filled for all soils studied, yet cracks, or structural pores had not yet developed in the cohesive, or clayey soils. These results suggest that saturated water permeabilities as contained in the Soil Conservation Service's detailed soil survey reports should be roughly equivalent to the air permeabilities of soils at field capacity.

Reeve has measured the air and water permeability of disturbed, air-dried soil samples and used the ratio of air to water permeability as an indicator of soil structural stability (Reeve, 1953; Reeve, 1965). He has reported ratios ranging from 2.5 to 50,000 (Reeve, 1965). The highest ratios were measured on soils with high clay contents and unusually high exchangeable sodium concentrations; both of these conditions lead to strong structural changes when the samples are wetted. Furthermore, his use of systematically packed, air-dried samples maximizes the ratio and bears little resemblance to typical field conditions, since there is little hygroscopic and no capillary or gravitational water in the pore space when the air permeability measurement is made. His data for sandy loams and silt (clay contents < 15%) with low to moderate exchangeable sodium concentrations indicate ratios of 6 or less (Reeve, 1953). We would not expect convective transport of radon to be significant in the fine-grained soils that yielded very high ratios of air to water permeability when Reeve's method was employed.

Measured rates of change in air pressure at depth within the unsaturated zone during a change in barometric pressure at the land surface have been used, along with air-filled porosity data, to compute vertical air permeabilities and to estimate saturated water permeabilities (Weeks, 1978). The computed saturated water permeabilities were compared with recharge data at two geologically distinct sites. This study found that air permeability values so determined successfully estimated the hydraulic conductivities for the layered materials in the unsaturated zone when the following conditions were met: (1) the moisture contents within the unsaturated zone were less than or equal to field capacity; (2) the permeabilities were great enough so that the Klinkenberg effect (Klinkenberg, 1941), which becomes important as the mean free path of the gas molecules approaches the diameter of the pores, is negligible (see also Sections V.A and V.B); and (3) the structure of the materials is unaffected by wetting.

It therefore appears that for medium- and coarse-textured soils, i.e., those in which convective flow of soil gas is most likely, the SCS estimates of saturated water permeability should indicate, approximately, the permeability to air when moisture content is at or below field capacity. Table 8 contains the definitions of the classes of water permeability used by the SCS, and the equivalent intrinsic permeability and hydraulic conductivity.

b. Classification of Grain-Size Distribution: Grain-size may be a rough indicator of soil permeability. The SCS uses two classifications of grain-size distributions: texture and particle-size. The texture of a soil refers to the relative proportions within a mass of soil of three grain-size groups with grain diameters below 2 mm. The relative proportions of clay (<2 μm), silt (2 - 50 μm), and sand (50 - 2000 μm) determine the basic soil texture, as illustrated in Figure 2. This triangular chart is used by the Soil Conservation Service to assign basic soil textures. Adjectives may be prefixed to the basic soil texture class to describe the presence of fragments larger than 2 mm. For example, gravelly, cobbly, and

stony are adjectives used, respectively, when rock fragments between the following sizes are present: 0.2 and 7.6 cm, 7.6 and 25.4 cm, and greater than 25.4 cm.

Particle-size classifies the grain-size distribution of the whole soil, in contrast to texture, which only classifies the fine (<2 mm) earth. Particle-size classes are a compromise between historic engineering (see Figure 3) and pedologic (see Figure 2) classification schemes. Rock fragments, as used in definitions of particle-size classes, refer to all grains larger than 2 mm. Table 9 lists the names of the particle-size classes and their definitions. Particle-size classes are incorporated into the names of soil families, a soil taxonomic category (see Section VII.A.1.d below). In addition to the eleven classes defined in Table 9, forty additional "strongly contrasting" particle-size classes (e.g., sandy-skeletal over loamy) are used in family names of U.S. soils, for the purpose of identifying "changes in pore-size distribution that seriously affect the movement and retention of water" (USDA, 1975, p. 386).

It is therefore clear that particle-size classes, as incorporated into soil taxonomy as currently employed, were defined to estimate the saturated water permeabilities of soils. Work began on the current taxonomic system in 1951; therefore only the soil surveys published since then may be expected to include particle-size classifications for the mapped soils. Since soil texture is defined on the basis of grain-size distribution of only the fine fraction, and permeability of soils is controlled by the large pores, its value as an indicator of permeability is less certain. Figure 4 displays the mean saturated water permeabilities for 8600 soil samples grouped by texture. In general, the means decrease with grain-size, but in the absence of a measure of dispersion for each textural class, we hesitate to make generalizations. Because soil texture has been included in all soil survey reports regardless of date, we have reviewed correlations between texture and ^{238}U and ^{226}Ra concentrations, radon emanation coefficient and soil permeability. Concentrations of U and Ra increase with decreasing grain-size (Megumi and Mamuro, 1977; Jasinska et al., 1982); emanation coefficient increases with specific surface area, which has an inverse correlation with grain-

size (Bossus, 1984); and the saturated water permeability decreases as grain-size decreases (Mason et al., 1957; Al-Jibury, 1961).

c. Soil Drainage: Soil drainage, as a process, refers to the rate and extent of the removal of water from the soil, in relation to additions, particularly by runoff and by flow through the soil to the deep subsurface. General classes of soil drainage, which are included in all modern reports of soil surveys, are a combined measure of runoff (which may be thought of as external drainage), internal drainage, and permeability. Runoff is closely related to soil slope. Internal soil drainage and permeability classifications overlap, since both are related to soil particle-size distribution and texture, structure, and cracking. Internal drainage classes, as used by the SCS, reflect the frequency and length of periods of water saturation. Therefore, internal drainage classes are also dependent upon precipitation patterns and the depth of the water table, which influences the hydraulic gradient.

As a condition of the soil, general soil drainage "refers to the frequency and duration of periods when the soil is free of saturation or partial saturation" (USDA, 1962, p. 165). In the context of geographic prediction of radon source strengths, general drainage therefore reflects the relative fraction of the time that bulk flow of soil gas is maximized, given that driving forces exist. Table 10, adapted from the USDA Soil Survey Manual (USDA, 1962), describes the general classes of drainage, and lists the causes for each state. Soil gas flow should be negligible in soils that are very poorly and poorly drained, of minor importance in imperfectly drained soils, and of increasing importance within the soils of the remaining classes, as listed.

d. Soil Taxonomy: The purpose of the taxonomy is to provide hierarchies of classes that allow us to understand the relationships between soils and also between the factors responsible for their character. Soil taxonomy is quite complex; we therefore provide a brief description, taken from USDA (1975), and refer the reader to that source for

additional information. Aspects of taxonomy that relate to geographic radon assessments are mentioned.

Six hierarchical taxonomic classes are used by the USDA. They are, from the most general (highest) to the most specific (lowest):

Order (10 in the world)

Suborder (47 in the world)

Great Group (approximately 225 in the world, 185 in the U.S.)

Subgroup (970 in the U.S.)

Family (approximately 4500 in the U.S.)

Series (approximately 10,500 in the U.S.)

Obviously, the degree of homogeneity increases from the highest to the lowest categories.

Orders are differentiated based upon the presence or absence of diagnostic horizons or features that are marks within the soil of the differences in the degree and kind of dominant sets of soil-forming processes. The criteria used to assign Suborders vary with the order, but generally include properties that influence or reflect soil genesis and that are extremely important to plant growth. The soil moisture regime is one criterion sometimes applied to assign Suborders that is of interest for radon migration. Great Groups, unlike Orders and Suborders, are differentiated on the basis of the entire soil profile and its most significant properties. Therefore, soils within the same Great Group are similar in the kind, arrangement, and degree of expression of soil horizons, in soil moisture and temperature regimes, and in base status. The importance of soil moisture as it influences radon production and migration is indicated in Figure 1. Table 11 describes soil moisture regimes, as used by the SCS.

The criteria described above for Orders, Suborders, and Great Groups focus on marks (marks are defined as visually-identifiable features) in the soil or causes of sets of processes that govern the course and degree of soil development. Many soils also have

subordinate marks that reflect important sets of soil-forming processes. Subgroups are differentiated on the basis of these subordinate marks. Some of these marks may be dominant in another Great Group, Suborder, or Order, but here only modify marks of primary sets of soil-forming processes. Other subordinate marks of processes are not used as criteria for higher taxonomic classes. Three types of Subgroups are recognized: typic, which reflect the central concept of the Great Group; intergrades, which are transitional to other Orders, Suborders, or Great Groups; and extragrades, which have some mark that is not representative of the Great Group, and is not transitional to any known kind of soil.

Families contain soils that are similar in profile, and in the chemical and physical properties that affect the movement and retention of water and soil aeration, namely: particle-size distribution, mineralogy, temperature regime, pH, and occasionally a few other properties. The criteria used to assign soil Series are the same as those used for Families and the higher taxonomic classes, except that the permissible range is restricted for one or more properties.

e. Interpretation of an SCS soil map: To clarify the information that may be derived from SCS soil surveys and its use, we include Figure 17, which is the general soil map for Spokane County, WA (USDA, 1968). Nine soil associations are shown on Figure 17. A soil association, on general soil maps at the county spatial scale, is a group of defined, named, and mapped soil series that are regularly geographically associated in a defined proportional pattern (USDA, 1962, p. 303). These associations typically consist of one or more major series and at least one minor series, and are named for the major series. The second column of Table 12 contains the additional descriptions of the soil associations that were a part of the legend of the original SCS map. The range of soil textures that occur in each association is given in each case. The general drainage classes, which were defined in Table 10, is sometimes given. The third column of Table 12 contains additional information

extracted from the textual descriptions of the soil associations shown on Figure 17 (USDA, 1968, pp 1 - 5).

For illustrative purposes, the Naff-Larkin-Freeman (number 1) and the Garrison-Marble-Springdale (number 2) associations, highlighted in Figure 17, will be discussed. From the legend of the general soil map (Table 12, column 2), we see differences in texture: the Naff-Larkin-Freeman association contains fine- to medium-textured soils, while the Garrison-Marble-Springdale association contains gravelly and sandy (or coarse-textured) soils. The Garrison-Marble-Springdale association contains soils that are somewhat excessively and excessively drained, implying that water is removed rapidly or very rapidly. Therefore these soils are effectively never close to complete saturation, and, because they are coarse-textured and therefore contain large pores, we deduce that these soils have high air-filled porosities. The textual description (Table 12, column 3) for the Naff-Larkin-Freeman association indicates that the soils of this association are moderately-well or well-drained, implying the following, in comparison with the Garrison-Marble-Springdale association: water is removed more slowly; the percent saturation is generally higher; and, because of a smaller mean pore-size and a higher percent saturation, the occurrence of large air-filled pores is less likely. The deduction based on the general drainage and texture classifications for the Naff-Larkin-Freeman association is confirmed in the textual description for this series, which indicates that during the fall, winter, and late spring, these soils contain as much hygroscopic and capillary water as they can hold. Air-filled porosities must be significantly reduced.

An important point indicated by the textual descriptions of the soil associations (Table 12, column 3) is the proportions of major and minor soils in each association. For example, only 77% of the area mapped on Figure 17 as the Naff-Larkin-Freeman association is actually occupied by these three series. In the case of the Garrison-Marble-Springdale association, only 80% of the corresponding mapped area is occupied by these three series. The fraction of the area of a soil association that is occupied by minor soils,

and the degree of similarity of physical properties between the major and minor soils will control the uncertainty associated with the assignment of estimates of physical properties to geographic areas based on general soil maps.

Table 13 contains additional data for each soil series, and is included for two purposes: to illustrate the ranges in soil texture, particle size, and permeability found in the associations shown on Figure 17, and to illustrate the deductions about the physical and environmental properties of soils that can be made on the basis of soil taxonomy. The particle-size classes, which were defined in Table 9, of the soil series are contained in the column labeled "Family," as the adjectival phrase preceding the first comma. All major soils (that is Naff, Larkin, and Freeman series) of the Naff-Larkin-Freeman association have a fine-silty particle-size classification; the minor soil Caldwell also is fine-silty, while the minor soil Dearyton is classified as fine. The major soils of the Garrison-Marble-Springdale association have particle-size classifications of loamy-skeletal, sandy, and sandy-skeletal, respectively; all three minor soils of this association (Bong, Clayton, and Phoebe) are classified as coarse loamy. Since the permeability associated with the particle-size class at the top of Table 9 is highest, and that associated with the class at the bottom of Table 9 is the lowest, we would expect the permeabilities of the Garrison-Marble-Springdale association to be significantly higher than that for the Naff-Larkin-Freeman association, based on particle-size class. Additional work is needed in order to quantify the correspondence between particle-size classes and permeability.

As mentioned earlier, SCS reports contain, in addition to the particle-size classes, soil textures (another indicator of permeability), and estimates of the saturated water permeability of soils. Particle-size classes, which are based on the entire soil profile, are more quickly obtained from the reports than are textures and permeabilities, which are presented for each soil series, by horizon, down to a depth of 1.5 meters. The soil horizon with the lowest permeability controls shallow vertical transport, and should limit the propagation times for pressure differences due to barometric pressure changes. In the

context of radon migration into basement or slab-on-grade houses, the permeability of the deepest soil horizon listed in detailed SCS reports is probably the most relevant value. A comparison of permeability, texture, and particle-size classes for the Naff-Larkin-Freeman and the Garrison-Marble-Springdale associations is now presented to illustrate how much additional information is obtained by looking at the more detailed texture and permeability data. When more than one entry occurs in the permeability or texture columns of Table 13, they are listed with increasing depth. The range of permeability classes for the major soils of the Naff-Larkin-Freeman association is very slow to moderate, corresponding to a range of intrinsic permeabilities of the order 10^{-14} to 10^{-12} m^2, while the range of permeability classes for the major soils of the Garrison-Marble-Springdale association is moderately rapid to very rapid, corresponding to a range of intrinsic permeabilities of the order 10^{-12} to 10^{-10} m^2. The textures of the major soils of the former association are silty clay loam and silt loam, while the textures of the major soils of the latter association are these: sand, gravel, and cobbles; gravelly coarse sand; gravelly sandy loam; very gravelly loam; coarse sand; loamy sand; and sandy loam (see Figure 2 for the fractions of clay-, silt-, and sand-sized grains in each textural class). As noted in equations (1) and (2), permeability varies roughly with the square of the mean grain diameter. Marshall developed the following equation for calculating permeability from porosity and specific surface area that does not include a tortuosity factor (Marshall, 1958):

$$k = \frac{\varepsilon^4}{2S^2} \tag{36}$$

If we assume the following values for the Garrison-Marble-Springdale and Naff-Larkin-Freeman associations, respectively: 200 and 20 μm for mean grain diameter, 0.4 and 0.5 for porosity, use equation (2) to calculate specific surface area (S), and insert that into equation (36), we compute permeabilities of 4×10^{-11} and 1×10^{-12} m^2, respectively, for the Garrison-Marble-Springdale and Naff-Larkin-Freeman associations. We see that the

deduced permeabilities for these two associations, whether based on permeability data, soil texture, or particle-size classes are similar.

Air permeability of soils was measured at several house sites in the Garrison-Marble-Springdale soil association as part of a study of remedial measures for radon (Turk et al., 1987). The eleven measurements were in the range (0.3 to 60) $\times 10^{-11}$ m^2 with a mean value of approximately 2×10^{-11} m^2. The agreement between the experimental data and the air permeability estimates based on SCS data and descriptions is good.

The taxonomy shown in Table 13 may also be used to obtain soil moisture and temperature regimes. Soil temperature regimes are listed as the last adjective under the column labeled "Family." Within Spokane County, all soils have a mesic temperature regime, with the exception of the Vassar series, which has a frigid temperature regime. The mesic regime implies a mean annual soil temperature that is greater than 8 but less than 15°C, and a difference between mean summer and winter temperatures that is more than 5°C at a depth of 50 cm. The frigid regime implies a mean annual soil temperature that is greater than 0 and less than 8°C, and mean summer soil temperatures that are greater than those of soils in the cryic (next colder) temperature regime (USDA, 1975, pp. 62-63). Moisture regimes, which were defined in Table 11, are given as formative elements in either the suborder or the great group name. The Garrison series, for example has a xeric moisture regime, as indicated by the "xer" in the middle of its subgroup name, shown in the second column of Table 13. The soil moisture regimes of the major soils of the Garrison-Marble-Springdale association are xeric (the regime for the Marble series is not indicated in its subgroup name). The moisture regimes of the major soils of the Naff-Larkin-Freeman association are xeric (Naff and Larkin series) and udic (Freeman series). The ustic (e.g., Athena series), and aquic (e.g., Caldwell series) soil moisture regimes also occur within Spokane County.

2. Radiological Factors

Radium content is one important parameter in estimating the radon source potential of soils. Data exist for surficial radium concentrations sampled from most of the United States. These data were acquired by the National Airborne Radiometric Reconnaissance (NARR) survey conducted by the U.S. Department of Energy as a part of the National Uranium Resource Evaluation program beginning in 1974 (Mitchell, 1981). Although the purposes of the survey were unrelated to the determination of radon concentrations in houses, the data on uranium content of soil is easily convertible to equivalent radium content and therefore provides the necessary foundation for the investigation of the relationship between radon concentrations in soils and houses.

The NARR survey employed aerial NaI(Tl)-based γ-spectrometry to measure the concentrations of ^{40}K, ^{238}U, and ^{232}Th in the near-surface soil. The determination of the uranium concentration in the soil is based on the intensity of the 1.76 MeV photopeak of ^{214}Bi, which is one of the short-lived progeny of ^{222}Rn, so the NARR ^{238}U data are actually a more direct measure of the ^{222}Rn and ^{226}Ra contents in the ground than of ^{238}U. Gamma rays generated within the soil to a depth of 0.3 m can be detected by airborne measurement systems.

Two factors may systematically bias these results, however. First, a fraction of the radon produced in the soil migrates into the atmosphere: hence, the bismuth activity near the surface of a uniform soil is lower than its radium activity. Second, soil bulk density varies with moisture content, and gamma attenuation is directly related to density. Consequently, aerial gamma measurements of a given soil are inversely related to its moisture content. The exposure rate above a soil containing 50% water by weight is 36% lower than that above the same soil when dry (Kirkegaard and Lovborg, 1980). Since the calibration pads for the aerial detectors contained 20-30% water, the measurements can be in error by up to 20% due to this effect.

The NARR survey measured γ-radiation from the earth along primary flight lines that were oriented east-west and generally separated by three miles in the western United States and by six miles in the eastern United States and along secondary flight lines that were oriented north-south and separated by 12 to 18 miles. In all, data have been acquired along more than 1.1 million miles of flight lines within the contiguous United States and Alaska. The unit of investigation for data acquisition, organization, and publication was the National Topographic Map Series of 1° (latitude) by 2° (longitude) quadrangles, each quadrangle representing an area of approximately 72 miles by approximately 90 to 125 miles, the latter distance being determined by the latitude of the quadrangle. The contiguous U.S. comprises 474 such quadrangles.

The data acquisition system aboard each aircraft recorded measurements of γ-radiation, total magnetic field intensity, temperature, and barometric pressure every second, averaged the terrain clearance every second, and triggered the position-tracking camera every three seconds. Gamma-spectrometric data were corrected for background, and for variations in atmospheric ^{214}Bi, temperature, barometric pressure, and terrain clearance. Base maps of flight lines and measurement sites were superimposed on geologic maps (1:250,000 scale) so that a geologic map unit, defined on the bases of lithology and geologic age, could be assigned to each measurement point.

The complete data set has been processed by LBL for the production of maps based on the radium data (Moed et al., 1984; Revzan, 1988; Revzan et al., 1988a). The first step was the reduction of the data to manageable size. For each file on tape, representing a quadrangle—or a portion of a quadrangle in those cases where closely spaced flight lines were flown—a computer program averaged the data for each east-west flight line over 0.0160° of longitude and that for each north-south flight line over 0.0125° of latitude, the averaging interval in both cases being somewhat less than 1 mile. These intervals were chosen for manageability in processing, and for suitability to our mapping capabilities. The

result was a set of 125 records for each east-west flight line and 80 records for each north-south flight line.

Several parameters from the tape were stored on disk: the flight line number, a code representing the flight line type, the coordinates of the central point of the averaging interval, the number of observations, the average values and standard deviations for radium, thorium, potassium-40, gross gamma radiation, and atmospheric ^{214}Bi correction, and the code of the predominant rock type in the interval, together with Federal Information Processing System (FIPS) codes representing the state and county of the point. The files of reduced data are designed to be compatible with the Socio-Economic-Environmental-Demographic Information System (SEEDIS), a public domain database supported principally by the U.S. Department of Labor and managed by the Computer Science Research Department of Lawrence Berkeley Laboratory (McCarthy et al., 1982).

From the averaged data, four types of maps can be generated; examples of two such maps are shown here for the San Jose (CA) quadrangle. The first, illustrated in Figure 18, is a scatter plot of the latitude and longitude of each reduced data point whose value lies between indicated limits. County boundaries are shown as dotted lines. The second example, reproduced as Figure 19, shows the data represented by a contour map, based on a least-squares approximation to the reduced data. While this figure provides the best immediate sense of the nature of the data, this technique has a significant disadvantage, as may be seen by comparing the contour map with the scatter plot for data having the highest radium concentration (> 150 Bq kg^{-1}). The contouring program smooths the data in such a manner that all of the points lying above 105 Bq kg^{-1} are effectively lost; it thus displays the general tendency of the data at a cost in resolution. Duval (1983) has developed a technique for producing composite color images from the NURE data that may prove to be a useful tool in geographical characterization of the radon source potential.

Examination of the scatter plots produced so far has revealed two possible problems that require further investigation before the data can be accepted as valid. First, a visual

comparison of the data from north-south and east-west flight lines for a region shows discrepancies that are statistically significant in some cases. While this is disconcerting when assessing data quality, these discrepancies may be real, resulting from differences in the precise area from which radiation was detected. Second, the data from certain quadrangles show a steep gradient between immediately adjacent flight lines that cannot be explained by differences in geology. The present working hypothesis is that both of these difficulties may be due to differences in atmospheric conditions at the time of flight. Analysis of the atmospheric ^{214}Bi data may permit resolution of the problems.

In general, given the inherent difficulties with large data sets obtained by different contractors, this approach to treating these data appears to provide a good basis for systematic analysis of the aerial radiometric data for the United States. We have compared ^{226}Ra maps generated at LBL for the ten quadrangles covering the state of Ohio with a similar statewide radiometric map generated by the U.S. Geological Survey (USDI, 1985). The contour maps for these quadrangles were visually compared with the USGS contour map of the state, and the results were in substantial agreement.

3. *Climatological Factors*

Climatic data are important for geographic characterization of radon source strengths in two general contexts: determining the availability of radon produced in the soil; and assessing the strength of driving forces (both climatic and those induced by house operation in response to weather) for radon migration, especially by convective transport of soil gas. Soil moisture is very important for radon availability, since it influences the radon emanation coefficient, diffusion coefficient, and air permeability of soil (see Figures 1, 5, 6, 8, and 9). Geographical and seasonal variations in indoor-outdoor temperature differences, indoor-soil temperature differences, wind speeds, the frequency, rate, and sign of barometric pressure changes (Clements and Wilkening, 1974), average frequency and

amount of precipitation, and depth to the water table may all influence the strength of the driving forces that promote convection of soil gas.

The primary source of climatic data for the United States is the Department of Commerce's National Oceanic and Atmospheric Administration, National Climatic Center. The spatial cells treated are states, state climatic divisions (SCDs, which are portions of states characterized by similar climates), counties, and weather stations. For initial geographical analyses of potential radon source strengths, SCDs (353 in the United States) or counties (3071 in the United States) seem to be the appropriate spatial cell. While county data are useful for regional studies, caution must be exercised because these data are computed, not measured, since there are fewer weather stations than counties. Primary climatic variables that are relevant to describing the driving forces for the flow of soil gas include, at least, the following: average temperature, average wind speed, and average total precipitation. Several secondary, or computed, climatic variables are also relevant for geographic characterization of radon source strengths, including these: heating-degree days, which are linearly related to fuel consumption, and should therefore indicate the importance of indoor-outdoor and indoor-soil temperature differences as driving forces; potential evapotranspiration, which is a computed estimate of water loss from soil (Thornthwaite, 1948); and moisture index, which is the ratio of precipitation to potential evapotranspiration, and is an indicator of the magnitude of the accumulation or depletion of soil water (Thornthwaite, 1948).

We have reviewed the climatic data contained in the Climatic Atlas of the United States (USDC, 1968), in the National Atlas of the United States (USDI, 1970), in Geoecology, a county-level environmental data base located at Oak Ridge National Laboratory (Olson et al., 1980), and in the Socio-Economic-Environmental-Demographic Information System (SEEDIS) (McCarthy et al., 1982). The data contained in the two atlases are predominantly presented as small-scale country-wide contour maps. The Climatic Atlas contains more climatic data than the National Atlas, and includes

precipitation data by SCDs. Monthly averages of temperature and precipitation by SCDs are contained in USDC (1973a). The above variables plus heating- and cooling-degree days may be found, by state, in USDC (1973b).

Geoecology, as a source of climatic data is attractive because the data are already digitized and on-line, and are available at the county and SCD spatial cell.. In addition, Geoecology includes evapotranspiration and moisture index data, which are not contained in the atlases. The only disadvantage to its use is that, for a number of variables of interest in assessing radon source strengths, the coverage is not national. Geoecology includes the following data for the entire United States by SCD: monthly average, maximum, and minimum temperature; monthly average, maximum, and minimum precipitation; and indices of SCD names, state area- and population-weighting factors, and the counties that comprise the SCD. Geoecology includes the following climatic data, by county, for the central and southern portions of the Eastern and Central United States: monthly and annual average temperatures, precipitation totals, potential evapotranspiration, and moisture indices (Olson et al., 1980). We are presently uncertain whether such county climatic data have been calculated for the remainder of the United States, or even whether it makes sense to do so, in light of the huge size of and large elevation ranges within counties in the western U.S.

SEEDIS contains temperature and precipitation data, by county, for the entire United States. These data could be used in equations (Thornthwaite, 1948) to calculate potential evapotranspiration and moisture indices for counties.

B. A Predictive Framework for Geographic Characterization of Radon Source Potential

Several studies have addressed the topic of geographic characterization. In Sweden, "GEO-radiation" maps have been produced from airborne radiometric surveys, ground measurements of gamma radiation and geological mapping (Åkerblom and Wilson,

1982; Wilson, 1984). The purpose of these maps is to document areas and geologic formations with gamma emission levels exceeding 30 $\mu R\ h^{-1}$ with the intention of identifying areas at risk for high indoor radon levels due to entry from soil. The geologic and soil characteristics used in Sweden to assign areas to high, potentially high, normal, and low radon risk categories included the following: uranium and radium contents of soil and bedrock, permeability, moisture content, and the volume of available soil gas (Wilson, 1984).

One approach to geographic characterization that has been proposed is the development of a Radon Index Number (RIN) that would combine the major factors determining radon entry into a single variable (Eaton and Scott, 1984; DSMA, 1983). The goal of work towards geographic radon assessments is to develop and validate a RIN formula that accounts for the diversity of climate, soils, and perhaps, geology that occurs within the United States. Figure 1 shows, in schematic form, the considerable number of relevant variables for such a formula. This formula could then be applied to assign areas to one of several relative radon risk categories.

In its most general form, such an index might be given by (after DSMA, 1983):

$$RIN = \log A_{Ra} + n \log k + \sum_i B_i + \sum_i C_i \qquad (45)$$

where A_{Ra} is the radium concentration in the soil, k is the air permeability, n is a weighting factor less than 1 and the parameters B_i and C_i incorporate building factors and climatic factors, respectively. Based on numerical modeling of radon entry, n has been estimated to be 0.45 (DSMA, 1985).

The first term in this formula corresponds to an estimate of the generation rate of emanating radon within the soil. The radium activity of the soil, estimated from NARR data, for example, could be modified by two additional factors: one which accounts for variations in radon emanation coefficient with grain size, and another which accounts for

variations in emanation coefficient with moisture saturation. The data in Table 4 show a variation in soil radium concentrations that spans a factor of 17. The emanation coefficient for radon release from soil, as shown in Table 6, varies over a similarly broad range. These modifying factors might be directly incorporated in the first term, or contained in one of the C_i terms.

The second term in this RIN formula embodies information on the characteristic radon migration distance for the area. Permeability, k, might be estimated, for a constant soil saturation, from USDA classifications of soil texture, particle-size, or saturated water permeabilities. However, the air permeability of a soil decreases with increasing moisture saturation; the percent saturation at which the rate of decrease in air permeability is greatest (that is, field capacity) increases with increasing median grain size of the soil. This percentage saturation should vary as permeability, since both are roughly proportional to grain-size distribution, only with a much smaller range. A factor of two reduction in air permeability as the soil moisture increases from wilting point to field capacity is not significant, given a potential range of ten orders of magnitude in permeability. However, moisture contents greater than field capacity reduce the air permeability by one to three orders of magnitude, which is significant if such moisture contents persist for significant periods. This might be the case, for example, in areas where precipitation is frequent, or in areas where the water table is shallow. Therefore, for geographic comparisons, a factor indicating average or seasonal moisture saturation should be incorporated into this term in the RIN equation, or included as a separate element in the C_i terms, since typical precipitation and resultant soil moisture patterns vary geographically within the United States. The USDA classifications of soil moisture regimes (Table 11), or soil drainage (Table 10) may be useful here. Alternatively, the moisture index, a computed climatic variable, may be useful for this purpose.

Geographic variations in climatic data that reflect differences in the relative strength and persistence of driving forces for convection of soil gas are also important for estimating

characteristic migration distances of diverse areas. Pressure differences that result from the stack effect are approximately proportional to the indoor-outdoor temperature difference. Either average temperatures (annual or seasonal) or heating-degree and cooling-degree days might be used to formulate a factor by which this second term would be modified to reflect the relative geographic importance of indoor-outdoor temperature differences as a cause of pressure-driven flow of soil gas. The square of average wind speeds may also be useful for indicating geographic variations in wind-induced pressure differences (see equation 31). Such factors could be explicitly included in the B_i terms in equation (45).

As noted in Section V.C, the dimensionless quantity $Pe_p = k\varepsilon P_o(\mu D_e)^{-1}$ permits the evaluation of the relative importance of diffusive and convective transport of radon. As noted earlier, assuming a small pressure difference, and typical values for ε, μ, and D_e, Pe_p equals one when k is of order 10^{-11} m^2. At this permeability, diffusion and convection are of equal importance. Therefore, convective transport dominates in coarse-textured soils (gravel and coarse sand on Figure 3, sand and loamy sand on Figure 2). For fine-textured soils (uniform silt, sandy and silty clay, and clay on Figure 3; clay loam, sandy and silty clay loam, sandy and silty clay, and clay on Figure 2) diffusion is the dominant migration process, and convection through bulk soil can be ignored. For medium-textured soils (medium sand, well-graded sand and gravel, fine sand, silty sand and gravel, and silty sand on Figure 3; sandy loam, loam, silt loam, and silt on Figure 2) both transport processes should be considered. It should be noted that the influence of soil saturation on Pe_p has not been accounted for here.

The diffusive flux of radon is proportional to I_∞ and $D_e^{1/2}$ (see equations 15 and 17). Since I_∞ is proportional to radium activity, so is the diffusive flux of radon. As seen in the curve fitted to the data of Figure 6, moisture saturation controls the order of magnitude of D_e.

Moisture saturation therefore influences the radon generation rate, and the diffusive and convective transport of radon. An equation for the computation of moisture saturation for the Western United States has been reported (Kalkwarf et al., 1984) as follows:

$$m = \left[0.124P^{0.5} - 0.0012E - 0.04 + 0.156f_{sc}\right] \times \left[1 - \left(\frac{0.7 + f_{sc}}{H}\right)^2\right] + \left[\frac{0.7 + f_{sc}}{H}\right]^2 \quad (46)$$

where m is the moisture saturation, P is the annual precipitation (in inches), E is the annual lake evaporation (in inches), f_{sc} is the fraction of soil with grains finer than 75 μm (i.e., silt plus clay), and H is the depth to the water table (in feet).

Such a climatological term may be explicitly included in the RIN formulation as one of the C_i terms.

C. Measuring the Indoor Radon Source Potential of a Building Site

The three components—soil structural factors, radiological factors, and climatological factors—used to assess radon source potential on a geographical basis may also be applied on a scale the size of a building site. A purpose for such an assessment is to determine, in advance of construction, the need to incorporate radon-resistant features into the building. If only a small fraction of buildings require radon-resistant measures, a large cost savings could be realized if a reliable method for predicting radon source potential were developed, particularly given that the cost of remedial action is much higher than the cost of preventive measures taken during construction. Site assessment could also be a useful tool in making decisions about real-estate purchases.

Several methods have been proposed that are potentially suitable for assessing radon source potential at a building site (DSMA Atcon, 1983; Tanner, 1988; Kunz et al., 1988; Nazaroff and Sextro, 1989; Yokel, 1989). These methods are substantially similar, but differ in detail. Each method is based on the recognition that the radon source potential

of soil depends on two key parameters: the rate of generation of mobile radon by the soil grains and the extent to which radon can migrate in the soil. Differences among the methods arise in the incorporation of subsidiary factors in the analysis, in the methods of sampling, and in the aggregation of the data into a source potential index.

In the pioneering work (DSMA Atcon, 1983), the radium content of the soil was determined by *in situ* gamma spectrometry, and the soil permeability was measured by a probe-based permeameter. The source potential was characterized as a radon index number, as given in equation (45), which incorporates building-related characteristics such as ventilation rate.

Tanner (1988) defined "radon availability" as the radon concentration in the soil pores multiplied by the mean one-dimensional migration distance of radon in a homogeneous soil. In his method, the radon concentration in the soil pores and the soil permeability are measured by extracting air from an augured hole using a specially designed probe. A distinguishing feature of Tanner's method is the explicit incorporation of radon migration by diffusion through soil pores.

Kunz et al. (1988) characterize source potential in terms of the radon index number, taken as the product of a source term, such as the soil-gas ^{222}Rn concentration, and the square root of the permeability. As is the case in Tanner's method, measurements are made by withdrawing air from a sampling probe installed in the soil. In contrast to Tanner's approach, the sampling probe is simply driven into the soil.

The sampling method used by Nazaroff and Sextro (1989) is similar to that of Kunz et al. The distinction in their approach is the interpretation method: radon source potential is determined as the maximum sustainable entry rate of radon into a building with specified characteristics considering transport by pressure-driven flow through a uniform soil. The numerical modeling work of Nazaroff (1988), described in Section VI.C, serves as a basis for the analysis.

A limitation of each of these methods is the possible variation of results with time. As was discussed in previous sections, radon emanation and permeability both vary with soil moisture content which itself varies with time. To overcome this problem, Yokel (1989) has proposed a method for characterizing the source potential based on invariant soil properties: radium activity concentration, dry density, porosity, and dry gas permeability.

Each of these methods, except that of Yokel (1989), has been validated in limited field tests. Further studies may reveal advantages to one or more of these approaches over the others, but at present they appear to have roughly equal potential.

VIII. SUMMARY AND CONCLUSIONS

In less than a decade the consensus concerning the nature and extent of the problem of radon in indoor air has been radically revised. Rather than simply a problem that arises due to molecular diffusion of radon from industrially contaminated building materials or fill materials, we now recognize that the vast majority of structures with elevated indoor concentrations are unexceptional in other regards. In most cases, radon enters predominantly via the substructure through convective flow augmented by molecular diffusion. The importance of soil as a source of indoor radon and the importance of the convective flow process for radon entry are seen in the considerable success of control measures directed at reversing the ordinary direction of flow of soil gas through pathways across the building substructure.

We have described and discussed mechanisms of radon generation in soil and entry into the soil pore space, the physics of radon migration through soil, and the driving forces that generate pressure gradients in the soil surrounding buildings which lead to convective migration of radon into buildings. A mathematical description of radon concentration in the soil pore space has been developed that accounts for production and removal by radioactive decay and for diffusive and convective flow through the soil. We have reviewed the important soil and climatic variables that influence these processes and have attempted to evaluate their effects.

Key factors that influence radon emanation in soil and its migration through soil and into buildings have been identified and a basic understanding of these factors has been developed. Soil grain-size distribution and moisture saturation are two important elements. In summary, the production of migratory radon is influenced by the grain-size and the percent moisture saturation of soil as follows: both the radium content and the radon emanation coefficient tend to increase with decreasing soil grain-size; the radon emanation coefficient tends to increase with increasing percent saturation.

Analysis based on the dimensionless form of the general transport equation for radon in soil indicates that the air permeability of the soil is the most important variable for determining the relative importance of diffusive and convective transport. The air permeability of soil is influenced by the percent moisture saturation, and by the pore-size distribution, which, in turn, is related to the grain-size distribution. More specifically, the air permeability tends to decrease as the volume percentage of large pores decreases, and as the percent saturation in the large pores increases. Therefore, moist, coarse-grained soils are expected to exhibit the highest availability of radon for entry into houses. The moisture saturation also strongly influences the effective diffusion coefficient of radon through soil pores, an important consideration for cases in which diffusive migration is significant.

We have examined data bases providing extensive national coverage and containing relevant information for assessing geographic variations of radon source potential, with a view toward developing a predictive capability. Among these are the Soil Conservation Service maps and associated data, published at the county scale. These data include taxonomic categories, soil texture classifications, and saturated water permeabilities, from which air permeability and soil moisture information may be extracted. Another potentially useful data set covering most of the United States is the aerial radiometric data obtained from the NURE program. These data can provide information on the surficial radium concentration in soils. Climatic data that affect driving forces for soil-gas entry are also available. The same framework used for geographic assessment of radon source potential can be applied at the scale of a building site to determine the potential for high concentrations in advance of construction.

Despite considerable progress achieved during the past decade, much work remains before we can first confidently assert that we understand all the factors influencing soil as a source of indoor radon and second fully exploit that understanding in reducing exposures. Key areas requiring further work include these: continued development (including validation) of numerical models for radon migration in soil; investigations of the multiple

roles of moisture in affecting radon emanation and transport; studies of the usefulness of various data bases and their key data elements, particularly those relating to soil permeability, in predicting radon entry rate potential; and development of the most appropriate mathematical form of the a radon source potential index for geographic predictions of potential radon entry rates.

In addition to developing these concepts further, experiments to verify some of the critical relationships are essential. Among these are investigations of the influence of moisture saturation on radon emanation in ordinary soils, further examination of the coupling between the building structure and the surrounding soil (and the effect of air permeability on this coupling), and an evaluation of the correspondence between water and air permeabilities in various soil types.

Pursuing these and other investigations of soil as a source of indoor radon will undoubtedly yield large benefits in improving the basis for controlling human exposures to the decay products of radon in buildings.

IX. REFERENCES

ACS (1969) *Symposium on Flow Through Porous Media*, American Chemical Society Publications, Washington, DC.

AECB (1980) *Proceedings of the Third Workshop on Radon and Radon Daughters Associated with Uranium Mining and Processing*, Atomic Energy Control Board, Ottawa, Canada.

Åkerblom, G., and Wilson, C.(1982) Radon—Geological aspects of an environmental problem, rapporter och meddalanden nr 30, Sveriges Geologiska Underskning, Luleå, Sweden.

Al-Jibury, F. K. (1961) Saturated water permeability of soils as related to air permeability at different water tensions, Ph.D. dissertation, Oregon State College, Corvallis, OR.

Andrews, J. N., and Wood, D. F.(1972) Mechanism of radon release in rock matrices and entry into groundwaters, *Trans. Inst. Min. Metall.*, **Sec. B, 81**, 198.

Austin, S. R., and Droullard, R. F. (1977) Radon emanation from domestic uranium ores determined by modifications of the closed-can gamma-only assay method, report BuMines RI 8264, Denver Mining Research Center, Denver, CO.

Baranov, V. I., and Novitskaya, A. P. (1949) Diffuziya radona v prirodnykh gryazyakh ("Diffusion of radon in natural muds"), *Akad. Nauk SSSR Biogeochim. Lab. Trudy*, **9**, 161-171, cited by Tanner (1964).

Barden, L., and Pavlakis, G. (1971) Air and water permeability of compacted unsaturated cohesive soil, *J. Soil Sci.*, **22**, 302.

Barretto, P. M. C. (1973) Emanation characteristics of terrestrial and lunar materials and the radon-222 loss effect on the uranium-lead system discordance, Ph.D. dissertation, Rice University, Houston.

Bates, R. C., and Edwards, J. C. (1981) The effectiveness of overpressure ventilation: a mathematical study, in *Radiation Hazards in Mining: Control, Measurement and Medical Aspects*, Gomez, M., Ed., Society of Mining Engineers, New York, p. 149.

Baver, L. D. (1938) Soil permeability in relation to non-capillary porosity, *Soil Sci. Soc. Am. Proc.*, **3**, 52.

Baver, L. D. (1940) *Soil Physics*, Wiley, New York.

Bedinger, M. S. (1961) Relation between median grain size and permeability in the Arkansas River Valley, Arkansas, U. S. Geol. Survey Prof. Paper 424-C, C31.

Bird, R. B., Stewart, W. E., and Lightfoot, E. N. (1960) *Transport Phenomena*, Wiley, New York.

Blomsterberg, A. K., Sherman, M. H., and Grimsrud, D. T. (1979) A model correlating air tightness and air infiltration in houses, report LBL-9625, Lawrence Berkeley Laboratory, Berkeley, California.

Bossus, D. A. W. (1984) Emanating power and specific surface area, *Radiat. Prot. Dosim.*, **7**, 73.

Botset, H. G. (1940) Flow of gas-liquid mixtures through consolidated sand, *Am. Inst. Mining Eng. Trans.*, **136**, 91.

Bowles, J. E. (1979) *Physical and Geotechnical Properties of Soils*, McGraw-Hill, New York, p. 213.

Boyle, R. W. (1911) The solubility of radium emanation. Application of Henry's law at low partial pressures, *Phil. Mag.*, **22**, 840.

Bruno, R. C. (1983) Sources of indoor radon in houses: A review, *J. Air Pollut. Control Assn.*, **33**, 105.

Buckingham, E. (1904) Contributions to our knowledge of the aeration of soils, Bulletin No. 25, U.S. Dept. of Agriculture, Bureau of Soils, Washington, DC.

Burdine, N. T., (1953) Relative permeability calculations from pore-size distribution data, *Am. Inst. Mining Eng. Petroleum Trans.*, **198**, 71.

Burmister, D. M. (1954) Principles of permeability testing of soils, in *Symp. on Permeability of Soils*, ASTM Special Technical Publication No. 163, American Society for Testing Materials, Philadelphia, p. 3.

Carslaw, H. S., and Jaeger, J. C. (1959) *Conduction of Heat in Solids*, 2nd edn., Oxford University Press, Cambridge.

Childs, E. C. (1969) *An Introduction to the Physical Basis of Soil Water Phenomena*, Wiley, London.

Clements, W. E., and Wilkening, M. H. (1974) Atmospheric pressure effects on ^{222}Rn transport across the earth-air interface, *J. Geophys. Res.*, **79**, 5025.

Cliff, K. D., Wrixon, A. D., Miles, J. C. H., and Lomas, P. R. (1987) Remedial measures to reduce radon concentrations in a house with high radon levels, in *Radon and Its Decay Products: Occurrence, Properties and Health Effects*, Hopke, P. K., Ed., ACS Symposium Series 331, American Chemical Society, Washington, DC, pp. 536-559.

Cohen, B. L. (1980) Health effects of radon from insulation of buildings, *Health Phys.*, **39**, 937.

Collé, R., Rubin, R. J., Knab, L. I., and Hutchinson, J. M. R. (1981) Radon transport through and exhalation from building materials: A review and assessment, NBS Technical Note 1139, U.S. Government Printing Office, Washington, DC.

Collins, R. E. (1961) *Flow of Fluids Through Porous Materials*, Reinhold, New York.

Corey, A. T. (1957) Measurement of water and air permeability in unsaturated soil, *Soil Sci Soc. Am. Proc.*, **21**, 7.

Crane, T. (1947) *Architectural Construction: The Choice of Membrane Materials*, Wiley, New York.

Crozier, W. D. (1969) Direct measurement of radon-220 (thoron) exhalation from the ground, *J. Geophys. Res.*, **74**, 4199.

Culot, M. V. J., Olson, H. G., and Schiager, K. J. (1976) Effective diffusion coefficient of radon in concrete, theory and method for field measurements, *Health Phys.*, **30**, 263.

Currie, J. A. (1960) Gaseous diffusion in porous media. Part 2—Dry granular materials, *Brit. J. Appl. Phys.*, **11**, 318.

Currie, J. A. (1961) Gaseous diffusion in porous media. Part 3—Wet granular materials, *Brit. J. Appl. Phys.*, **12**, 275.

D'Ottavio, T. W., and Dietz, R. N. (1986) Discussion of 'Radon transport into a detached one-story house with a basement', *Atmos. Environ.*, **20**, 1065.

Damkjær, A., and Korsbech, U. (1985) Measurement of the emanation of radon-222 from Danish soils, *The Science of the Total Environ.*, **45**, 343.

Desai, C. S., and Abel, J. F. (1972) *Introduction to the Finite Element Method: A Numerical Method for Engineering Analysis*, Van Nostrand Reinhold, New York.

DSMA Atcon (1983) Review of existing instrumentation and evaluation of possibilities for research and development of instrumentation to determine future levels of radon at a proposed building site, report INFO-0096, Atomic Energy Control Board, Ottawa.

DSMA Atcon (1985) A computer study of soil gas movement into buildings, report 1389/1333, Department of Health and Welfare, Ottawa.

Duval, J. S. (1983) Composite color images of aerial gamma-ray spectrometric data, *Geophysics*, **48**, 722.

Eaton, R. S., and Scott, A. G. (1984) Understanding radon transport into houses, *Radiat. Prot. Dosim.*, **7**, 251.

Ericson, S. O., and Schmied, H. (1984) Modified technology in new constructions, and cost effective remedial action in existing structures, to prevent infiltration of soil gas carrying radon, in *Indoor Air: Buildings, Ventilation and Thermal Climate*, vol. 5, Berglund, B., Lindvall, T., and Sundell, J., Eds., Swedish Council for Building Research, Stockholm, p. 153.

Ericson, S. O. and Schmied, H. (1987) Modified design in new construction prevents infiltration of soil gas that carries radon, in *Radon and Its Decay Products: Occurrence, Properties and Health Effects*, Hopke, P. K., Ed., ACS Symposium Series 331, American Chemical Society, Washington, DC, pp. 526-535.

Fisk, W. J., and Turiel, I. (1983) Residential air-to-air heat exchangers: performance, energy savings and economics, *Energy and Buildings*, **5**, 197.

Fleischer, R. L., and Mogro-Campero, A. (1980) Techniques and principles for mapping integrated radon emanation within the earth, in *Proc. Natural Radiation Environment III*, Gesell, T. F., and Lowder, W. M., Eds., Conf-780422, U.S. Dept. of Commerce, National Technical Information Service, Springfield, VA, p. 57.

Fraser, H. J. (1935) Experimental study of the porosity and permeability of clastic sediments, *J. Geology*, **43**, 910.

Freeze, A. R., and Cherry, J. A. (1979) *Groundwater*, Prentice-Hall, Englewood, NJ, p. 604.

Fukuda, H. (1955) Air and vapor movement in soil due to wind gustiness, *Soil Sci.*, **79**, 249.

Garcia-Bengochea, I., Lovell, C. W., and Altschaeffl, A. G. (1979) Pore distribution and permeability of silty clays, *Proc. ASCE*, **105**, 839.

George, A. C., and Breslin, A. J. (1980) The distribution of ambient radon and radon daughters in residential buildings in the New Jersey—New York area, in *Proc. Natural Radiation Environment III*, Gesell, T. F., and Lowder, W. M., Eds., Conf-780422, U.S. Dept. of Commerce, National Technical Information Service, Springfield, VA, p. 1272.

Gray, R. W., and Ramsay, W. (1909) Some physical properties of radium emanation, *J. Chem. Soc. (London) Trans.*, **95**, 1073.

Grimsrud, D. T., and Odenwalder, D. M. (1988) The impact of gas furnace operation on radon concentrations in residences: A literature survey, report LBL-25718, Lawrence Berkeley Laboratory, Berkeley, CA.

Hernandez, T. L., and Ring, J. W. (1982) Indoor radon source fluxes: experimental tests of a two-chamber model, *Environ. Int.*, **8**, 45.

Hernandez, T. L., Ring, J. W., and Sachs, H. (1984) The variation of basement radon concentration with barometric pressure, *Health Phys.*, **46**, 440.

Hirst, W., and Harrison, G. E. (1939) The diffusion of radon gas mixtures, *Proc. Roy. Soc. London (A)*, **169**, 573.

Hodgson, A. T., Garbesi, K., Sextro, R. G., and Daisey, J. M. (1988) Evaluation of soil-gas transport of organic chemicals into residential buildings: Final report, report LBL-25465, Lawrence Berkeley Laboratory, Berkeley, CA.

Holub, R. F., Droullard, R. F., Borak, T. B., Inkret, W. C., Morse, J. G., and Baxter, J. F. (1985) Radon-222 and ^{222}Rn progeny concentrations in an energy-efficient house equipped with a heat exchanger, *Health Phys.*, **49**, 267.

Hubbard, L. M., Bolker, B., Socolow, R. H., Dickerhoff, D., and Mosley, R. B. (1988) Radon dynamics in a house heated alternately by forced air and by electric resistance, paper #VI-1, EPA 1988 Symp. on Radon and Radon Reduction Technology, Denver, CO, 17-21 October.

Hurwitz, H., Jr. (1983) The indoor radiological problem in perspective, *Risk Analysis*, **3**, 63.

Ingersoll, J. G. (1983) A survey of radionuclide contents and radon emanation rates in building materials used in the U.S., *Health Phys.*, **45**, 363.

Ingersoll, J. G., Stitt, B. D., and Zapalac, G. H. (1983) A fast and accurate method for measuring radon exhalation rates from building materials, *Health Phys.*, **45**, 550.

Israelsson, S. (1980) Meteorological influences on atmospheric radioactivity and its effects on the electrical environment, in *Proc. Natural Radiation Environment III*, Gesell, T. F., and Lowder, W. M., Eds., Conf-780422, U.S. Dept. of Commerce, National Technical Information Service, Springfield, VA, p. 210.

Iyengar, M. A. R., and Markose, P. M. (1982) An investigation into the distribution of uranium and daughters in the environment of a uranium ore processing facility, cited in Raghavayya, M., Khan, A. H., Padmanabhan, N., and Srivastava, G. K., Exhalation of Rn-222 from soil: some aspects of variation, in *Natural Radiation Environment*, Vohra, K. G., Mishra, U. C., Pillai, K. C., and Sadasivan, S., Eds., Wiley Eastern, New Delhi, p. 584.

Jasinska, M., Niewiadomski, T., and Schwabenthan, J. (1982) Correlation between soil parameters and natural radioactivity, in *Natural Radiation Environment*, Vohra, K. G., Mishra, U. C., Pillai, K. C., and Sadasivan, S., Eds., Wiley Eastern, New Delhi, p. 206.

Kalin, M., and Sharma, H. D. (1981) Radium-226 and other group two elements in abandoned uranium mill tailings in two mining areas in south central Ontario, in *Radiation Hazards in Mining: Control, Measurement and Medical Aspects*, Gomez, M., Ed., Society of Mining Engineers, New York, p. 707.

Kalkwarf, D. R., Freeman, H. D., and Hartley, J. N. (1984) Validation of methods for evaluating radon-flux attenuation through earthen covers, report PNL-5092, Pacific Northwest Laboratory, Richland, WA.

King, C. Y., Ed. (1984/85) Earthquake hydrology and chemistry, special issue of *J. Appl. Geophys.*, **122**, 294.

Kirkegaard, P., and Lovborg, L. (1980) Transport of terrestrial gamma radiation in plane semi-infinite geometry, *J. Comp. Phys.*, **36**, 20.

Klinkenberg, L. J. (1941) The permeability of porous media to liquids and gases, *Am. Petrol. Inst. Drilling and Production Practice*, 200.

Kothari, B. K., and Han, Y. (1984) Association of indoor radon concentrations with airborne surveys of uranium in surficial material, *Northeastern Environ. Sci.*, **3**, 30.

Kraner, H. W., Schroeder, G. L., and Evans, R. D. (1964) Measurements of the effects of atmospheric variables on radon-222 flux and soil-gas concentrations, in *Natural Radiation Environment*, Adams, J. A. S., and Lowder, W. M., Eds., University of Chicago Press, Chicago, p. 191.

Kunz, C., Laymon, C. A., and Parker, C. (1988) Gravelly soils and indoor radon, paper #V-6, EPA 1988 Symp. on Radon and Radon Reduction Technology, Denver, CO, 17-21 October.

Landman, K. A. (1982) Diffusion of radon through cracks in a concrete slab, *Health Phys.*, **43**, 65.

Landman, K. A., and Cohen, D. S. (1983) Transport of radon through cracks in a concrete slab, *Health Phys.*, **44**, 249.

Liddament, M., and Allen, C. (1983) The validation and comparison of mathematical models of air infiltration, Technical Note AIC-11, Air Infiltration Centre, Berkshire, England.

Lorrain, P., and Corson, D. (1970) *Electromagnetic Fields and Waves*, 2nd edn., Freeman, San Francisco, Chapter 2.

Loureiro, C. O. (1987) Simulation of the steady-state transport of radon from soil into houses with basements under constant negative pressure, Ph. D. Dissertation, University of Michigan, Ann Arbor (also issued as report LBL-24378, Lawrence Berkeley Laboratory, Berkeley, CA).

Lucas, H. F. (1957) Improved low-level alpha scintillation counter for radon, *Rev. Sci. Instrum.*, **28**, 680.

Marshall, T. J. (1958) A relation between permeability and size distribution of pores, *J. Soil Science*, **9**, 1.

Marshall, T. J. and Holmes, J. W. (1979) *Soil Physics*, Cambridge University Press, London, p. 12.

Mason, D. D., Lutz, J. F., and Petersen, R. G. (1957) Hydraulic conductivity as related to certain soil properties in a number of great soil groups: Sampling errors involved, *Soil Sci. Soc. Am. Proc.*, **21**, 554.

McCarthy, J. L., Merrill, D. W., Marcus, A., et al. (1982) The SEEDIS project: A summary overview of the Social, Economic, Environmental, Demographic Information System, report PUB-424-250, Lawrence Berkeley Laboratory, Berkeley, CA.

McKeague, J. A., Wang, C., and Topp, G. C. (1982) Estimating saturated hydraulic conductivity from soil morphology, *Soil Sci. Soc. Am. J.*, **46**, 1239.

Megumi, K., and Mamuro, T. (1974) Emanation and exhalation of radon and thoron gases from soil particles, *J. Geophys. Res.*, **79**, 3357.

Mitchell, S. D. (1981) NURE geoscience data: Their nature and availability, Bendix Field Engineering Corp., Grand Junction, CO.

Mitchell, T. K., Hooper, D. R., and Campanella, R. G. (1965) Permeability of compacted clay, *Am. Soc. Civil Eng. Proc.*, **SM4**, 41.

Modera, M. P., and Sonderegger, R. C. (1980) Determination of the *in-situ* performance of fireplaces, report LBL-10701, Lawrence Berkeley Laboratory, Berkeley, CA.

Modera, M. P., Sherman, M. H., and Levin, P. A. (1983) A detailed examination of the LBL infiltration model using the Mobile Infiltration Test Unit, report LBL-15636, Lawrence Berkeley Laboratory, Berkeley, CA.

Moed, B. A., Nazaroff, W. W., Nero, A. V., Schwehr, M. B., and Van Heuvelen, A. (1984) Identifying areas with potential for high indoor radon levels: Analysis of the National Airborne Radiometric Reconnaissance for California and the Pacific Northwest, report LBL-16955, Lawrence Berkeley Laboratory, Berkeley, CA.

Morse, P. M., and Feshbach, H. (1953) *Methods of Theoretical Physics*, 2 vol., McGraw-Hill, New York, Chapter 10.

Mowris, R. J. (1986) Analytical and numerical models for estimating the effect of exhaust ventilation on radon entry in houses with basements or crawl spaces, M.S. Thesis, University of Colorado, (also issued as report LBL-22067, Lawrence Berkeley Laboratory, Berkeley, CA.)

Mowris, R. J. and Fisk, W. J. (1988) Modeling the effects of exhaust ventilation on ^{222}Rn entry rates and indoor ^{222}Rn concentrations, *Health Phys.*, **54**, 491-501.

Muskat, M. (1946) *The Flow of Homogeneous Fluids Through Porous Media*, J. W. Edwards, Ann Arbor.

Myrick, T. E., Berven, B. A., and Haywood, F. F. (1983) Determination of concentrations of selected radionuclides in surface soil in the U. S., *Health Phys.*, **45**, 631.

Nazaroff, W. W., Boegel, M. L., Hollowell, C. D., and Roseme, G. D. (1981) The use of mechanical ventilation with heat recovery for controlling radon and radon-daughter concentrations in houses, *Atmos. Environ.*, **15**, 263.

Nazaroff, W. W., and Doyle, S. M. (1985) Radon entry into houses having a crawl space, *Health Phys.*, **48**, 265.

Nazaroff, W. W., Feustel, H., Nero, A. V., Revzan, K. L., Grimsrud, D. T., Essling, M. A., and Toohey, R. E. (1985), Radon transport into a detached one-story house with a basement, *Atmos. Environ.*, **19**, 31.

Nazaroff, W. W., Lewis, S. R., Doyle, S. M., Moed, B. A., and Nero, A. V. (1987a) Experiments on pollutant transport from soil into residential buildings by pressure-driven air flow, *Environ. Sci. Technol.*, **21**, 459.

Nazaroff, W.W., Doyle, S.M., Nero, A.V., and Sextro, R.G. (1987b) Potable water as a source of airborne ^{222}Rn in U. S. dwellings: A review and assessment, *Health Phys.*, **52**, 281.

Nazaroff, W. W. (1988) Predicting the rate of ^{222}Rn entry from soil into the basement of a dwelling due to pressure-driven air flow, *Radiat. Prot. Dosim.*, **24**, 199-202.

Nazaroff, W. W., and Sextro, R. G. (1989) Technique for measuring the indoor ^{222}Rn source potential of soil, *Environ. Sci. Technol.*, **23**, 451-458.

Nero, A. V., and Nazaroff, W. W. (1984) Characterizing the source of radon indoors, *Radiat. Prot. Dosim.*, **7**, 23.

Nero, A. V., Schwehr, M. B., Nazaroff, W. W., and Revzan, K. L. (1986) Distribution of airborne radon-222 concentrations in U. S. homes, *Science*, **234**, 992.

Nitschke, I. A., Wadach, J. B., Clarke, W. A., Traynor, G. W., Adams, G. P., and Rizzuto, J. E. (1984) A detailed study of inexpensive radon control techniques in New York State houses, in *Indoor Air: Buildings, Ventilation and Thermal Climate*, vol. 5, Berglund, B., Lindvall, T., and Sundell, J., Eds., Swedish Council for Building Research, Stockholm, p. 111.

Olson, R. J., Emerson, C. J., and Nungesser, M. K. (1980) Geoecology: A county-level environmental data base for the conterminous United States, report ORNL/TM-7351, Oak Ridge National Laboratory, Oak Ridge.

Osaba, J. S., Richardson, J. G., Kerver, J. K., Hafford, J. A., and Blair, P. M. (1951) Laboratory determination of relative permeability, *Am. Inst. Mining Eng. Trans.*, **192**, 47.

Pall, R., and Mohsenin, N. N. (1980) Permeability of porous media as a function of porosity and particle-size distribution, *Trans. ASAE*, **23**, 742.

Paton, T. R. (1978) *The Formation of Soil Material*, George Allen & Unwin, London.

Pearson, J. E., and Jones, G. E. (1965) Emanation of radon 222 from soils and its use as a tracer, *J. Geophys. Res.*, **70**, 5279.

Penman, H. L. (1940) Gas and vapour movements in soil: the diffusion of vapours through porous solid, *J. Agr. Sci.*, **30**, 437.

Powers, R. P., Turnage, N. E., and Kanipe, L. G. (1980) Determination of radium-226 in environmental samples, in *Proc. Natural Radiation Environment III*, Gesell, T. F., and Lowder, W. M., Eds., Conf-780422, U.S. Dept. of Commerce, National Technical Information Service, Springfield, VA, p. 640.

Popretinskiy, I. F. (1961) Opredeleniye koeffitsiyentov diffuzii radona i emaniruyushchey sposobnosti gornykh porod po krivym emanatsionnogo zondirovaniya ("Determination of the coefficients of diffusion of radon and of the emanating power of rocks from enanation sounding curves") in *Voprosy Rudnoy Geofiziki ("Problems of Mining Geophysics")*, Moscow, Vses. Nauchno-Issled. Inst. Razved. Geofiziki, **2**, 105-114, cited by Tanner (1964).

Pruess, K. (1987) *TOUGH* user's guide, report LBL-20700, Lawrence Berkeley Laboratory, Berkeley, CA.

Rawls, W. J. (1983) Estimating soil bulk density from particle size analysis and organic matter content, *Soil Science*, **135**, 123.

Reeve, R. C. (1953) A method for determining the stability of soil structure based upon air and water permeability measurements, *Soil Sci. Soc. Am. Proc.*, 324.

Reeve, R. C. (1965) Air-to-water permeability ratio, in *Methods of Soil Analysis, Part 1: Physical and Mineralogical Properties, Including Statistics of Measurement and Sampling*, Black, C. A., Evans, D. D., Ensminger, L. E., White, J. L., and Clark, F. E., Eds., American Society of Agronomy, Madison, p. 520.

Revzan, K. L. (1988) Supplemental Information on the National Aerial Radiometric Reconnaissance (NARR) Database, report LBID-1453, Lawrence Berkeley Laboratory, Berkeley, CA.

Revzan, K. L., Nero, A. V., and Sextro, R. G. (1988a) Mapping surficial radium content as a partial indicator of radon concentrations in U. S. houses, *Radiat. Prot. Dosim.*, **24**, 179-183.

Revzan, K. L., Turk, B. H., Harrison, J., Nero, A. V., and Sextro, R. G. (1988b) Parametric modelling of temporal variations in radon concentrations in homes, report LBL-24179, Lawrence Berkeley Laboratory, Berkeley, CA.

Revzan, K. L. (1989) Radon entry, distribution, and removal in two New Jersey houses with basements, report LBL-26830, Lawrence Berkeley Laboratory, Berkeley, CA (submitted to *Atmos. Environ.*)

Rice, P. A., Fontugne, D. J., Latini, R. G., and Barduhn, A. J. (1969) Anisotropic permeability in porous media, in *Symp. on Flow Through Porous Media*, American Chemical Society Publications, Washington, DC, p. 48.

Rogers, V. C., Nielson, K. K., Merrell, G. B., Kalkwarf, D. R. (1983) The effects of advection on radon transport through earthen materials, report NUREG/CR-3409, PNL-4789, RAE-18-4, U.S. Nuclear Regulatory Commission, Washington, DC.

Rogers, V. C., Nielson, K. K., and Kalkwarf, D. R. (1984), Radon attenuation handbook for uranium mill tailings cover design, report NUREG/CR-3533, United States Nuclear Regulatory Commission, Washington, DC.

Rundo, J., Markun, F., and Plondke, N. J. (1979) Observation of high concentrations of radon in certain houses, *Health Phys.*, **36**, 729.

Rutherford, E., and Soddy, F. (1903) Condensation of radioactive emanations, *Phil. Mag. Ser. 6*, **5**, 561.

Sachs, P. (1972) *Wind Forces in Engineering*, Pergamon Press, Oxford.

Scheidegger, A. E. (1960) *The Physics of Flow Through Porous Media*, MacMillan, New York.

Schery, S. D., Gaeddert, D. H., and Wilkening, M. H. (1982) Transport of radon from fractured rock, *J. Geophys. Res.*, **87**, 2969.

Schery, S. D., Gaeddert, D. H., and Wilkening, M. H. (1984) Factors affecting exhalation of radon from a gravelly sandy loam, *J. Geophys. Res.*, **89**, 7299.

Schery, S. D., and Siegel, D. (1986) The role of channels in the transport of radon from the soil, *J. Geophys. Res.*, **91B**, 12366-12374.

Schery, S. D., Holford, D. J., Wilson, J. L., and Phillips, F. M. (1988) The flow and diffusion of radon isotopes in fractured porous media: Part 2, semi-infinite media, *Radiat. Prot. Dosim.*, **24**, 191-197.

Schlichting, H. (1979) *Boundary-Layer Theory*, seventh edn., McGraw-Hill, New York.

Scott, R. F. (1963) *Principles of Soil Mechanics*, Addison-Wesley, Reading.

Scott, A. G. (1983) Computer modeling of radon movement, in *EML Indoor Radon Workshop, 1982*, George, A. C., Lowder, W., Fisenne, I., Knutson, E. O., and Hinchcliffe, L., Eds., report EML-416, Environmental Measurements Laboratory, New York, p. 82.

Scott, A. G., and Findlay, W. O. (1983) Demonstration of remedial techniques against radon in houses on Florida phosphate lands, report EPA 520/5-83-009, U. S. Environmental Protection Agency, Eastern Environmental Radiation Facility, Montgomery, AL.

Scott, A. G. (1988) Preventing radon entry, in *Radon and Its Decay Products in Indoor Air*, Nazaroff, W. W. and Nero, A. V., Eds., Wiley, New York, pp. 407-433.

Sextro, R. G., Moed, B. A., Nazaroff, W. W., Revzan, K. L., and Nero, A. V. (1987) Investigations of soil as a source of indoor radon, in *Radon and Its Decay Products: Occurrence, Properties and Health Effects*, Hopke, P. K., Ed., ACS Symposium Series 331, American Chemical Society, Washington, DC, pp. 10-29.

Sherman, M. H. (1980) Air infiltration in buildings, Ph.D. dissertation, University of California, Berkeley, CA.

Silker, W. B., and Kalkwarf, D. R. (1983) Radon diffusion in candidate soils for covering uranium mill tailings, report NUREG/CR-2924, PNL-4434, Pacific Northwest Laboratory, Richland, WA.

Simiu, E., and Scanlan, R. H. (1978) *Wind Effects on Structures: An Introduction to Wind Engineering*, Wiley, New York.

Sisigina, T.I. (1974) Assessment of radon emanation from the surface of extensive territories, in *Nuclear Meteorology*, Israeli Program of Scientific Translations, Jerusalem, 239.

Stranden, E., Kolstad, A. K., and Lind, B. (1984) The influence of moisture and temperature on radon exhalation, *Radiat. Prot. Dosim.*, **7**, 55.

Strong, K. P., Levins, D. M., and Fane, A. G. (1981) Radon diffusion through uranium tailings and earth cover, in *Radiation Hazards in Mining: Control, Measurement and Medical Aspects*, Gomez, M., Ed., Society of Mining Engineers, New York, p. 713.

Strong, K. P., and Levins, D. M. (1982) Effect of moisture content on radon emanation from uranium ore and tailings, *Health Phys.*, **42**, 27.

Tanner, A. B. (1964) Radon migration in the ground: A review, in *Natural Radiation Environment*, Adams, J. A. S., and Lowder, W. M., Eds., University of Chicago Press, Chicago, p. 161.

Tanner, A. B. (1980) Radon migration in the ground: A supplementary review, in *Proc. Natural Radiation Environment III*, Gesell, T. F., and Lowder, W. M., Eds., Conf-780422, U. S. Dept. of Commerce, National Technical Information Service, Springfield, VA, p. 5.

Tanner, A. B. (1985) U. S. Geological Survey National Center, Reston, VA, personal communication.

Tanner, A. B. (1988) Measurement of radon availability from soil, in *Geologic Causes of Natural Radionuclide Anomalies: Proceedings of the GEORAD Conference*, Marikos, M. A., and Hansman, R. H., Eds., Special Publication No. 4, Division of Geology and Land Survey, Missouri Department of Natural Resources, Rolla, pp. 139-146.

Terzaghi, K., and Peck, R. B. (1967) *Soil Mechanics in Engineering Practice*, 2nd Edn, Wiley, New York.

Thamer, B. J., Nielson, K. K., and Felthauser, K. (1981) The effects of moisture on radon emanation including the effects on diffusion, report BuMines OFR 184-82, PB83-136358, U.S. Dept. of Commerce, National Technical Information Service, Springfield, VA.

Thornthwaite, C. W. (1948) An approach toward a national classification of climate, *Geogr. Rev.*, **38**, 55.

Topp, G. C, Zebcuk, W. D., and Dumanski, J. (1980) The variation of *in-situ* measured soil water properties within soil map units, *Can. J. Soil Sci.*, **60**, 497.

Tuma, J. J., and Abdel-Hady, M. (1973) *Engineering Soil Mechanics*, Prentice-Hall, Englewood Cliffs, NJ, p. 102.

Turk, B. H., Prill, R. J., Fisk, W. J., Grimsrud, D. T., Moed, B. A., and Sextro, R. G. (1987) Radon and remedial action in Spokane River Valley homes. Volume 1: Experimental design and data analysis, report LBL-23430, Lawrence Berkeley Laboratory, Berkeley, CA.

Uniform Building Code (1982) International Conference of Building Officials, Whittier, CA.

USDA (1962) *Soil Survey Manual*, U. S. Department of Agriculture Handbook No. 18, Soil Conservation Service, Washington, DC.

USDA (1968) *Soil Survey, Spokane County, Washington*, U. S. Department of Agriculture, Soil Conservation Service, Washington, DC.

USDA (1975) *Soil Taxonomy-A Basic System for Making and Interpreting Soil Surveys*, U. S. Department of Agriculture Handbook No. 436, U. S. Department of Agriculture, Washington, DC.

USDC (1968) *Climatic Atlas of the United States*, U. S. Department of Commerce, National Oceanic and Atmospheric Administration, Environmental Data Service, Asheville.

USDC (1973a) Monthly averages of temperature and precipitation for state climatic divisions, 1941-1970, *Climatography of the U. S.*, report no. 85, U. S. Department of Commerce, National Oceanic and Atmospheric Administration, Environmental Data Service, Asheville, NC.

USDC (1973b) Monthly normals of temperature, precipitation, and heating and cooling degree days, 1941-1970, *Climatography of the U. S.*, report no. 81, U. S. Department of Commerce, National Oceanic and Atmospheric Administration, Environmental Data Services, Asheville, NC.

USDI (1970) *The National Atlas of the United States*, U. S. Department of the Interior, U. S. Geological Survey, Washington, DC.

USDI (1985) *Aerial Radiometric Contour Maps of Ohio*, Geophysical Investigations Map GP-968, U.S. Geological Survey, Washington, DC.

Van der Hoven, I. (1957) Power spectrum of horizontal wind speed in the frequency range from 0.0007 to 900 cycles per hour, *J. Meteor.*, **14**, 160.

Weeks, E. D. (1978) Field determination of vertical permeability to air in the unsaturated zone, U.S. Geological Survey Professional Paper 1051, U. S. Government Printing Office, Washington, DC.

Whitaker, S. (1984) *Introduction to Fluid Mechanics*, reprint edition, R. E. Krieger, Malabar, FL.

Wilkening, M. H., Clements, W. E., and Stanley, D. (1972) Radon-222 flux measurements in widely separated regions, in *Proc. Natural Radiation Environment II*,

Adams, J. A. S., Lowder, W. M., and Gesell, T. F., Eds., Conf-720805, U. S. Dept. of Commerce, National Technical Information Service, Springfield, VA, p. 717.

Wilkening, M. H. (1974) Radon-222 from the island of Hawaii: Deep soils are more important than lava fields or volcanoes, *Science*, **183**, 413.

Williams, H., Turner, F. J., and Gilbert, C. M. (1954) *Petrography*, Freeman, San Francisco, CA.

Wilson, C. (1984) Mapping the radon risk of our environment, in *Indoor Air: Radon, Passive Smoking, Particulates and Housing Epidemiology*, vol. 2, Berglund, B., Lindvall, T., and Sundell, J., Eds., Swedish Council for Building Research, Stockholm, p. 85.

Wollenberg, H. A. and Smith, A. R. (1984) Naturally occurring radioelements and terrestrial gamma-ray exposure rates: An assessment based on recent geochemical data, report LBL-18714, Lawrence Berkeley Laboratory, Berkeley, CA.

Yokel, F. Y. (1989) Site characterization for radon source potential, report NSTIR 89-4106, National Institute of Standards and Technology, Gaithersburg, MD.

Youngquist, G. R. (1969) Diffusion and flow of gases in porous solids, in *Symp. on Flow Through Porous Media*, American Chemical Society Publications, Washington, DC, p. 58.

Table 1. Physical Characteristics of Soils: Representative Values[a]

Texture class	Grain Size (μm)	Soil bulk density (kg m^{-3})	Porosity	Field Capacity Saturation[b] (%)	Wilting Point Saturation[b] (%)
Sand	50-2000	1440-1580	0.40-0.46	15-20	5
Sandy loam		1180-1640	0.38-0.55	20-30	
Loam		1270-1490	0.44-0.52	30-45	
Silt	2-50		0.5	58	10
Silt loam		980-1450	0.45-0.63	30-50	
Clay loam		1270-1540	0.42-0.52	45-60	
Silty clay loam		1270-1490	0.44-0.52	45-60	
Silty clay				55-90	
Clay	< 2	1180-1540	0.42-0.56	55-90	33

[a] Sources: Marshall and Holmes, 1979, p 12;
Rawls, 1983;
Tuma and Abdel-Hady, 1973, p 28;
USDA, 1962, p 352.

[b] A saturation of 100% means that the entire pore volume is filled with water.

Table 2. Representative Permeabilities (k) Based on Kozeny Theory[a]

Soil type	d (μm)	ε	S (m^{-1})	k (m^2)
Clay	1	0.5	3×10^6	7×10^{-15}
Silt	20	0.5	2×10^5	1×10^{-12}
Sand	200	0.4	2×10^4	4×10^{-11}

[a] $c = 0.5$; $T = 1/\varepsilon$ (Marshall, 1958); d = particle diameter; ε = porosity; S = specific surface area.

Table 3. Effective Diffusion Coefficients for Radon in Soil

Soil Description	Reference	D_e (m^2 s^{-1})	Comments
Mill tailings (2 samples)	Strong *et al.*, 1981	$(5.4 - 7.2) \times 10^{-6}$	Moisture content = 0.7 - 1.5% dry wt.
Eluvial-detrital granodiorite	Tanner, 1964[a]	4.5×10^{-6}	Dry
Silty sandy clay	Strong *et al.*, 1981	2.7×10^{-6}	Moisture content = 1.5% dry weight
		2.5×10^{-7}	Moisture content = 10.5% dry weight
		6.0×10^{-8}	Moisture content = 17.3% dry weight
Compacted silty sands (12 samples)	Silker and Kalkwarf, 1983	$(3.0 \pm 1.3) \times 10^{-6}$	Porosity = 0.29 - 0.36; Saturation = 0.05 - 0.34
Compacted clayey sands (12 samples)	Silker and Kalkwarf, 1983	$(3.2 \pm 1.5) \times 10^{-6}$	Porosity = 0.32 - 0.39; Saturation = 0.09 - 0.55
Compacted inorganic clays (5 samples)	Silker and Kalkwarf, 1983	$(2.5 \pm 1.0) \times 10^{-6}$	Porosity = 0.32 - 0.43; Saturation = 0.06 - 0.34
Diluvium of metamorphic rocks	Tanner, 1964[a]	1.8×10^{-6}	Dry
Eluvial - detrital deposits of granite	Tanner, 1964[a]	1.5×10^{-6}	Dry
Loams	Tanner, 1964[a]	$8. \times 10^{-7}$	Dry
Varied clays	Tanner, 1964[a]	$7. \times 10^{-7}$	Dry
Mud	Tanner, 1964[b]	5.7×10^{-10}	Saturation = 0.37
Mud	Tanner, 1964[b]	2.2×10^{-10}	Saturation = 0.85

[a] Quoted Popretinskiy, 1961.

[b] Quoted Baranov and Noritskaya, 1949.

Table 4. ^{226}Ra and ^{232}Th Concentrations in Surface Soils[a]

State	N[b]	^{226}Ra (Bq kg^{-1})[c]	^{232}Th (Bq kg^{-1})[c]
Alabama	8	30 (17 - 52)	28 (13 - 56)
Alaska	6 (7)	24 (16 - 34)	32 (7 - 85)
Arizona	6	35 (9 - 74)	23 (7 - 48)
Arkansas	0 (1)		59
California	3	28 (9 - 48)	20 (11 - 28)
Colorado	32 (20)	52 (18 - 126)	48 (4 - 115)
Delaware	2	43 (41 - 44)	44
Florida	11 (10)	31 (9 - 85)	9 (4 - 14)
Georgia	9	33 (17 - 59)	41 (10 - 126)
Idaho	12 (13)	41 (24 - 59)	44 (16 - 70)
Illinois	7 (8)	36 (24 - 44)	36 (18 - 44)
Indiana	2	39 (37 - 41)	43 (41 - 44)
Kansas	6 (4)	36 (13 - 52)	48 (12 - 59)
Kentucky	13 (12)	56 (30 - 155)	44 (33 - 56)
Louisiana	2	26 (21 - 31)	24 (22 - 26)
Maryland	6	27 (18 - 44)	26 (18 - 32)
Michigan	10	41 (17 - 74)	21 (9 - 30)
Mississippi	3	44 (28 - 59)	41 (30 - 63)
Missouri	10	41 (11 - 52)	37 (12 - 48)
Nevada	6	56 (33 - 74)	56 (23 - 111)
New Jersey	24 (23)	32 (9 - 52)	33 (11 - 56)
New Mexico	13	56 (27 - 100)	35 (18 - 67)
New York	6	31 (18 - 44)	26 (15 - 41)
North Carolina	8	29 (18 - 44)	34 (16 - 56)
Ohio	12	56 (30 - 93)	37 (26 - 56)
Oregon	8 (9)	30 (9 - 78)	27 (16 - 56)
Pennsylvania	33	44 (17 - 89)	41 (14 - 63)
Tennessee	10 (11)	41 (24 - 52)	35 (24 - 56)
Texas	10	33 (20 - 52)	27 (15 - 41)
Utah	32 (28)	48 (20 - 70)	41 (7 - 85)
Virginia	13	31 (22 - 41)	32 (16 - 52)
West Virginia	11	48 (29 - 59)	52 (41 - 59)
Wyoming	13 (12)	37 (24 - 63)	41 (22 - 67)
All Samples	327 (331)	41 (9 - 155)	36 (4 - 126)

[a] Source: Myrick *et al.*, 1983.

[b] Where two numbers are given, the one in parentheses applies to ^{232}Th.

[c] Arithmetic mean (range of values).

Table 5. Radium Concentrations in Rocks[a]

Rock Class[c]	Example	^{226}Ra (Bq kg^{-1})			^{228}Ra (Bq kg^{-1})[b]		
		N	Mean[d]	Range	N	Mean[d]	Range
Acid Extrusives	rhyolite	131	71	10 - 285	131	91	4 - 470
Acid Intrusives	granite	569	78	1 - 372	573	111	0.4 - 1025
Intermediate Extrusives	andesite	71	26	2 - 64	71	27	2 - 113
Intermediate Intrusives	diorite	271	40	1 - 285	273	49	2 - 429
Basic Extrusives	basalt	77	11	0.4 - 41	77	10	0.2 - 36
Basic Intrusives	gabbro	119	10	0.1 - 71	110	9	0.1 - 61
Ultrabasic Rocks	dunite	31	4	0 - 20	30	6	0 - 30
Alkali Feldspathoidal Intermediate Extrusives[e]	phonolite	138	368	24 - 769	139	543	38 - 1073
Alkali Feldspathoidal Intermediate Intrusives[e]	syenite	75	692	4 - 8930	75	5	2 - 3560
Alkali Basic Extrusives	nephelinite	27	29	6 - 149	27	36	8 - 2670
Alkali Basic Intrusives	foidite	8	29	5 - 67	34	8	11 - 81
Chemical Sedimentary Rocks[f]	evaporites	243	45	0.4 - 335	239	60	0.1 - 535
Carbonates	limestone	141	25	0.4 - 223	131	7	0 - 45
Detrital Sedimentary Rocks[g]		412	60	1 - 992	411	50	0.8 - 1466
Clay		40	50	14 - 198	40	35	8 - 223
Shale		174	73	11 - 992	174	66	21 - 158
Sandstone and Conglomerate		198	51	1 - 770	198	39	3 - 919
Metamorphosed Igneous Rocks	gneiss	138	50	1 - 1835	138	60	0.4 - 421
Metamorphosed Sedimentary Rocks	schist	207	37	1 - 657	208	49	0.4 - 368

[a] Adapted from Wollenberg and Smith, 1984.

[b] Due to the relatively short half-lives of ^{228}Ac (6.1 h), ^{228}Th (1.9 y), and ^{224}Ra (3.7 d), one expects ^{224}Ra to be in equilibrium with ^{228}Ra.

[c] The classification used for the extrusive and intrusive igneous rocks is from Williams *et al.*, 1954. Rocks are classified on the bases of whole-rock silica content (acid > intermediate > basic > ultrabasic) and alkali and calcic feldspar mineralogy.

[d] Arithmetic mean.

[e] Although these rocks have elevated Ra contents, the alkali feldspathoidal rock class is thought to constitute less than 1 percent of all igneous rocks (Wollenberg and Smith, 1984).

[f] Includes carbonates.

[g] Includes clay, shale, sandstone, and conglomerates.

Table 6. Measurements of Radon Emanation Coefficients[a]

Material	N	Moisture Content	Emanation Coefficient[b]	Reference
Rock (crushed)	58	unknown	0.084 ± 0.086 (0.005 - 0.40)	Barretto, 1973
Soil	21	unknown	0.30 ± 0.16 (0.03 - 0.55)	Barretto, 1973
Soil[c]	1	dried-105 deg C, 24 h	0.25	Megumi and Mamuro, 1974
Soil	1[d]	33% of dry wt; dried-200 deg C, 90 h	0.68 0.09	Stranden *et al.*, 1984
Soil	1	air dry[e]	0.41	Nazaroff *et al.*, 1985
Soil	2	13 - 20% of dry wt	0.27 (0.22 - 0.32)	Nazaroff *et al.*, 1987a
Soil	1	4% of dry wt	0.38 ± 0.08	Schery *et al.*, 1982
Various soils (Hawaiian)				Wilkening, 1974
Lava fields		unknown	0.02	
Thin organic soils		unknown	0.55	
Deep agricultural soils		unknown	0.70	
Various soils (Danish)	70	0 - 70% of dry wt	0.22 ± 0.13 (0.02 - 0.7)	Damkjaer and Korsbech, 1985
Various soils				Sisigina, 1974
sand	7	unknown	0.14 (0.06 - 0.18)	
sandy loam	7	unknown	0.21 (0.10 - 0.36)	
silty loam	7	unknown	0.24 (0.18 - 0.40)	
[heavy] loam	12	unknown	0.20 (0.17 - 0.23)	
clay	5	unknown	0.28 (0.18 - 0.40)	
Sand	1	saturated	0.243	Andrews and Wood, 1972
Uranium ore	6	saturated; dried-110 deg C[f]	0.19 ± 0.10 (0.06 - 0.26) 0.05 ± 0.03 (0.014 - 0.07)	Strong and Levins, 1982

Table 6. (continued)

Material	N	Moisture Content	Emanation Coefficient[b]	Reference
Uranium ore (crushed)	17	moist-saturated;	0.28 ± 0.16 (0.055 - 0.55)	Thamer *et al.*, 1981
		vacuum dried	0.14 ± 0.11 (0.023 - 0.36)	
Uranium ore	950	unknown	0.26 ± 0.18 (<0.01 - 0.91)	Austin and Droullard, 1977
Tailings	2	saturated; dried-110 deg C[f]	0.29, 0.31 0.067, 0.072	Strong and Levins, 1982
Soil	2	dried-105 deg C, 24 h	0.09 - 0.10[g,h]; 0.12 - 0.15[g]	Megumi and Mamuro, 1974

[a] Except for the final entry (as noted) these coefficients are for ^{222}Rn

[b] Arithmetic mean ± one standard deviation (Range of values)

[c] Sample sieved through 20 μm mesh

[d] Only data for the soil sample with the highest exhalation rate were reported.

[e] Exposed to laboratory air for several days

[f] Dried to constant weight

[g] Emanation coefficient for ^{220}Rn

[h] This sample, when moist, had a ^{220}Rn emanation coefficient of 0.13

Table 7. Characteristic Times for Propagation of Pressure Disturbances in Soil[a]

Soil Type	Permeability (m^2)	τ_p (L_p = 1 m)	τ_p (L_p = 5 m)
Clay	10^{-16}	10 d	250 d
Sandy Clay	5×10^{-15}	5 h	5 d
Silt	5×10^{-14}	30 min	12 h
Sandy Silt and Gravel	5×10^{-13}	3 min	75 min
Fine Sand	5×10^{-12}	18 s	450 s
Medium Sand	10^{-10}	0.9 s	23 s
Gravel	10^{-8}	0.01 s	0.2 s

[a] $\tau_p = (L_p^2 \mu \varepsilon)\ (P_a k)^{-1}$;

$\mu = 17.5 \times 10^{-6}$ Pa s;

$\varepsilon = 0.5$;

$P_a = 1.01 \times 10^5$ Pa.

Table 8. Relationship Between Soil Conservation Service Permeability Classes, Saturated Hydraulic Conductivity, and Intrinsic Permeability

SCS Class Name	Saturated Hydraulic Conductivity, k_w (in. h^{-1})[a]	Intrinsic Permeability, k (m^2)[b]
very slow	<0.06	$<0.5 \times 10^{-13}$
slow	0.06 - 0.2	$(0.5 - 1.6) \times 10^{-13}$
moderately slow	0.2 - 0.6	$(1.6 - 4.9) \times 10^{-13}$
moderate	0.6 - 2.0	$(0.5 - 1.6) \times 10^{-12}$
moderately rapid	2.0 - 6.0	$(1.6 - 4.9) \times 10^{-12}$
rapid	6.0 - 20.	$(0.5 - 1.6) \times 10^{-11}$
very rapid	>20.	$>1.6 \times 10^{-11}$

[a] These units are used by the Soil Conservation Service, where 1 in. $h^{-1} = 7.1 \times 10^{-6}$ m s^{-1}.

[b] The kinematic viscosity of water (μ_w) = 0.001137 Pa s at 15° C and was used in the following conversion equation:

$$k = \frac{k_w \mu_w}{\rho_w g}$$

Table 9. Particle-Size Classification

Particle-size class	Definition
Fragmental	Stones, cobbles, gravel, and very coarse sand; too little fine earth to fill pores larger than 1 mm diameter (d).
Sandy-skeletal	Rock fragments 2 mm or larger ≥ 35% of volume; fine earth fills pores larger than 1 mm; fine earth is sandy, as defined for the sandy particle-size class.
Loamy-skeletal	Rock fragments ≥ 35% of volume; fine earth fills pores larger than 1 mm; fine earth is loamy, as defined for the loamy particle-size class.
Clayey-skeletal	Rock fragments ≥ 35% of volume; fine earth fills pores larger than 1 mm; fine earth is clayey, as defined for the clayey particle-size class.
Sandy	Rock fragments < 35% of volume. Texture of fine earth is sand or loamy sand, but not loamy very fine sand or very fine sand.
Loamy	Rock fragments < 35% of volume; texture of fine earth is loamy very fine sand, very fine sand, or finer, but clay < 35%.
Coarse-loamy	Fine sand (0.10 < d < 0.25 mm) or coarser particles, including fragments up to 7.5 cm d ≥ 15% by weight; clay ≤ 18% of fine earth.
Fine-loamy	Fine sand and coarser particles, including fragments up to 7.5 cm d ≥ 15% by weight; clay is 18 - 34% of the fine earth.
Coarse-silty	Fine sand and coarser particles, including fragments up to 7.5 cm d < 15% by weight; clay is < 18% of the fine earth.
Fine-silty	Fine sand and coarser particles, including fragments up to 7.5 cm d < 15% by weight; clay is 18 - 34% of the fine earth.
Clayey	Clay is ≥ 35% by weight of fine fraction; Rock fragments are < 35% by volume.
Fine	Clay is 35 - 59% by weight of the fine earth.
Very fine	Clay is ≥ 60% by weight of the fine earth.

Table 10. USDA General Classes of Soil Drainage

Class	Description	Causes and Comments
Very poorly drained	Water is removed so slowly that the water table remains at or near the surface most of the time. These soils are frequently ponded.	
Poorly drained	Water is removed so slowly that the soil remains wet for a large part of the time. The water table is commonly at or near the surface during a considerable part of the time.	High water table; a slowly permeable layer within the soil profile; additions of water through seepage; or a combination of the aforementioned causes.
Imperfectly or somewhat poorly drained	Water is removed slowly enough to keep it wet for significant periods, but not all of the time.	A slowly permeable layer within the profile; a high water table; additions of water through seepage; or a combination of the aforementioned causes.
Moderately well drained	Water is removed from the soil somewhat slowly, so that the profile is wet for a small but significant part of the time.	A slowly permeable layer within or immediately beneath the soil profile; relatively high water table; additions of water through seepage; or a combination of the aforementioned causes.
Well-drained	Water is removed from the soil readily but not rapidly.	These soils are usually intermediate in texture.
Somewhat excessively drained	Water is removed from the soil rapidly.	These soils usually have minor horizontal differentiation and are sandy and very porous.
Excessively drained	Water is removed from the soil very rapidly.	Soils may be steep, very porous, or both; may be a shallow soil on a slope.

Table 11. USDA Soil Moisture Regimes

Name	Description	Taxonomic Comments
Aquic	Soil is saturated either by ground water or by capillary fringe water. Reducing environment.	Aqu used as formative element in names of suborders connotes this regime.
Aridic or Torric	Moisture control section[a] is dry in all parts more than half the time that soil T at 50 cm depth is > 5 °C, and never moist in some or all parts for as long as 90 consecutive days when soil T at 50 cm is > 8 °C.	Torr used as formative element in names of great groups connotes this regime.
Udic	In most years, the soil moisture control section is not dry anywhere for as long as 90 cumulative days. Both gas and water must be present in part of the soil when soil T > 5 °C.	Ud as a formative element in names of suborders and great groups connotes this regime.
Ustic	This regime is intermediate between the aridic and udic regimes. The concept is one of limited moisture, but moisture must be present during the growing season. The precise definition varies with mean annual soil T.	Ust as a formative element in names of suborders or great groups connotes this regime.
Xeric	The soil moisture control section is dry everywhere for at least 45 consecutive days, within the 4 months following the summer solstice, and is moist everywhere for at least 45 consecutive days within the 4 months following the winter solstice. This is the classic Mediterranean climate, with cool moist winters and hot dry summers.	Xer as a formative element in names of suborders or great groups connotes this regime.

[a] The depth of soil moisture control sections varies with particle-size class as follows: between 10 and 30 cm for fine-loamy, coarse-silty, fine-silty, and clayey classes; between 20 and 60 cm for the coarse-loamy class; and between 30 and 90 cm for the sandy class.

Table 12. Legend for Spokane County General Soil Map

Soil association	Legend description	Description in text
Naff-Larkin-Freeman	Medium-textured to fine-textured soils on rolling loessal uplands, glacial plains, and mountain foot slopes.	58% Naff, 10% Freeman, 9% Larkin, 8% Caldwell, and 8% Dearyton soils. Naff and Larkin soils are deep, well-drained, and silty. Freeman and Dearyton soils are deep and moderately well-drained, with silt loam above either silty clay loam or silty clay. Fall and winter precipitation provide as much water as the soil can hold, and the supply is replenished in late spring.
Garrison-Marble-Springdale	Somewhat excessively drained and excessively drained sandy and gravelly soils formed in glacial outwash.	35% Garrison, 30% Marble, 15% Springdale, and 5% each Bong, Clayton, and Phoebe soils. Garrison soils are gravelly and medium-textured, and somewhat excessively drained. Marble soils are coarse-textured, excessively drained, and very deep. Springdale soils are gravelly, moderately coarse textured, somewhat excessively drained, and deep or moderately deep. Bong, Clayton, and Phoebe soils are moderately coarse textured and somewhat excessively drained.
Spokane-Dragoon	Shallow to deep, medium textured soils that formed in material that weathered from acid igneous rock on mountain foot slopes.	90% Spokane, 5% Dragoon soils. Both soils have granite, gneiss, or schist parent materials, and are well drained. Spokane soils re moderately coarse textured, and grade, at depths of 1 - 5 ft., into disintegrating rock. Dragoon soils are medium textured, and grade, at depths of 20 - 40 in., to disintegrating rock.
Bernhill	Deep, well drained and moderately well drained soils that formed chiefly in glacial lake deposits and glacial till on uplands.	60% Bernhill, 12% Uhlig, 8% Glenrose, and 7% Green Bluff soils. All of these soils are deep and medium-textured. Bernhill, Uhlig, and Glenrose soils are well drained. The Green Bluff soils are moderately well drained. Fall and winter precipitation provide as much water as the soil can hold, and the supply is replenished in late spring.
Hesseltine-Cheney-Uhlig	Dominantly moderately deep to shallow, gravelly or rocky soils of the channeled scablands.	53% Hesseltine, 16% Cheney, and 12% Uhlig soils. These soils are well drained, medium textured, and are underlain by gravel, cobblestones, or basalt.
Moscow-Vassar	Moderately deep and deep, medium textured soils of the hilly and mountainous areas.	80% Moscow, 18% Vassar soils. Vassar soils are at elevations > 4000 ft; Moscow soils are at lower elevations. Both soils are well drained. Growing season is short.
Athena-Reardan	Medium textured and moderately fine textured soils formed chiefly in loess.	71% Athena and 11% Reardan soils. These soils occupy the rolling hills. All soils in this association are well drained. Athena soils are medium textured throughout, while Reardan soils are medium textured at the surface and have a moderately fine or fine textured subsoil.

Table 12. (continued)

Soil association	Legend description	Description in text
Clayton-Laketon	Very deep, medium textured and moderately coarse textured soils on terraces.	85% Clayton, 5% Laketon soils. Both of these soils are well drained. Growing season is only about 100 days.
Bonner-Eloika-Hagen	Gravelly and sandy soils that formed in glacial materials.	40% Bonner, 35% Eloika, and 9% Hagen soils. Bonner soils are somewhat excessively drained, and are underlain, at 20 - 30 in. depth, by coarse sand and gravel. Eloika soils are well drained, more than 30 in. deep, and underlain by coarse sand and gravel. Hagen soils are somewhat excessively drained, coarse textured, and underlain, at a depth of 30 in., by coarse sand and gravel. Most of the soils are too droughty for crops.

Table 13. Taxonomy and Physical Characteristics for selected soils of Spokane County[a]

Series	Family; Subgroup	Permeability	Texture
Athena	Fine silty, mixed, mesic; Andic Haplustoll	moderate	silt loam
Bernhill	Coarse loamy, mixed, mesic; Andic Dystric Eutrochrept	moderate	silt loam
Bong	Coarse loamy, mixed, mesic; Typic Haplustoll	mod. rapid; very rapid	sandy loam; sand
Bonner	Coarse loamy over sandy and sandy-skeletal, mixed, mesic; Typic Normorthod	moderate; mod. rapid; rapid	silt loam; gravelly sandy loam; gravelly sand
Caldwell	fine silty, mixed, noncalcareous, mesic; Andic Cumulic Haplaquoll	mod. slow	silt loam
Cheney	Coarse loamy over sand and sandy skeletal, mixed, mesic; Andic Haplustoll	moderate; rapid; very rapid	gravelly silt and sandy loam; gravel and cobbles
Clayton	Coarse loamy, mixed, mesic; Typic Normorthod	moderate; mod. rapid	Sandy loam; loamy sand, sand
Dearyton	fine, mixed, mesic; Glossoboric Mollandeptic Normudalf	moderate; mod. slow; slow	silt loam; clay; gravelly clay loam
Dragoon	Fine loamy, mixed, mesic; Andic Argiustoll	moderate; mod. rapid	silt loam; sandy loam
Eloika	Coarse loamy, mixed, mesic; Typic Normorthod	moderate; rapid	silt loam; gravelly sandy loam, gravel
Freeman	Fine silty, mixed, mesic; Glossoboric Mollandeptic Normudalf	mod. slow; very slow	silt loam; silty clay loam
Garrison	Loamy skeletal, mixed, mesic; Andic Haploxeroll	mod. rapid; very rapid	Very gravelly loam; sand, gravel, and cobbles
Glenrose	Fine loamy, mixed, mesic; Typic Argixeroll	moderate	silt loam
Green Bluff	Coarse silty, mixed, mesic; Andic Dystrochrept	moderate	silt loam, sandy loam, gravelly silt loam
Hagen	Sandy, mixed, mesic; Typic Normorthod	mod. rapid; rapid	sandy loam; loamy sand, sand

Table 13. (continued)

Series	Family; Subgroup	Permeability	Texture
Hesseltine	Coarse loamy over sandy and sandy-skeletal, mixed, mesic; Andic Argixeroll	moderate; rapid	silt loam, gravelly loam; gravel, cobbles, and stones
Laketon	Coarse silty, mixed, mesic; Andic Dystric Eutrochrept	moderate; mod. slow	silt loam, sandy loam; silty clay loam
Larkin	Fine silty, mixed, mesic; Andic Argixeroll	moderate	silt loam
Marble	Sandy, siliceous, nonacid, mesic; Alfic Normipsamment	mod. rapid; rapid; very rapid	sandy loam; loamy sand; coarse sand
Moscow	Coarse loamy, mixed, mesic; Typic Normorthod	moderate; mod. rapid	silt loam; loam
Naff	Fine silty, mixed, mesic; Typic Argixeroll	moderate; mod. slow	silt loam; silty clay loam
Phoebe	Coarse loamy, mixed, mesic; Typic Haploxeroll	mod. rapid; rapid; very rapid	sandy loam; loamy sand; sand
Reardan	Fine, montmorillonitic, mesic; Andic Argiustoll	slow; moderate	silty clay; silt loam
Spokane	Coarse loamy, mixed, mesic; Typic Haploxeroll	moderate; rapid	loam to gravelly sandy loam; gravelly coarse loamy sand
Springdale	Sandy skeletal, mixed, mesic; Andic Entic Haploxeroll	very rapid	gravelly loamy sand; gravelly and very gravelly coarse sand
Uhlig	Coarse loamy, mixed, mesic; Andic Haploxeroll	moderate	silt loam to fine sandy loam
Vassar	Coarse loamy, mixed, frigid; Typic Normorthod	moderate; mod. rapid	silt loam; gravelly loam

[a] Adapted from USDA, 1968.

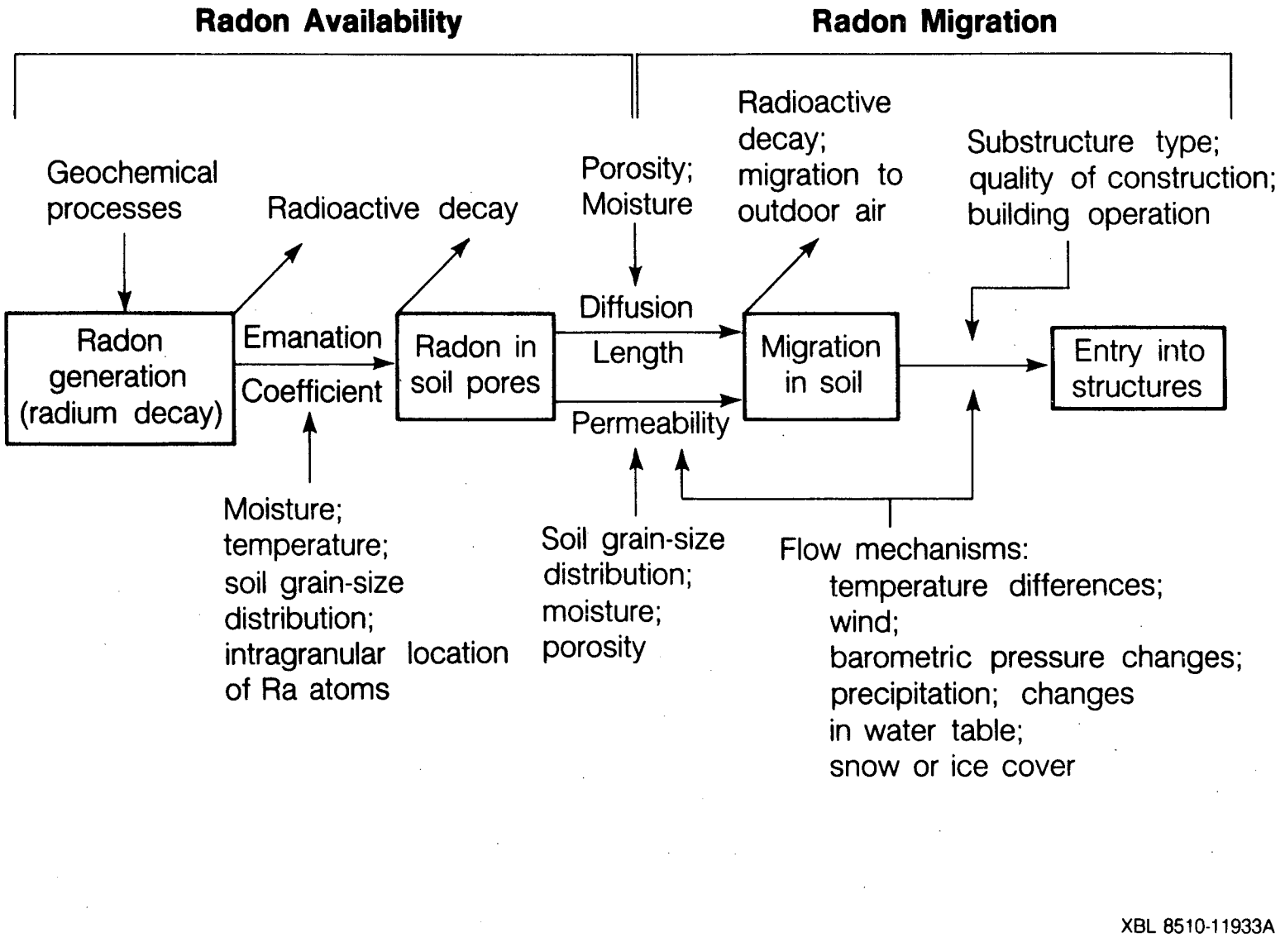

Figure 1. Schematic representation of radon production and migration in soil and its entry into buildings.

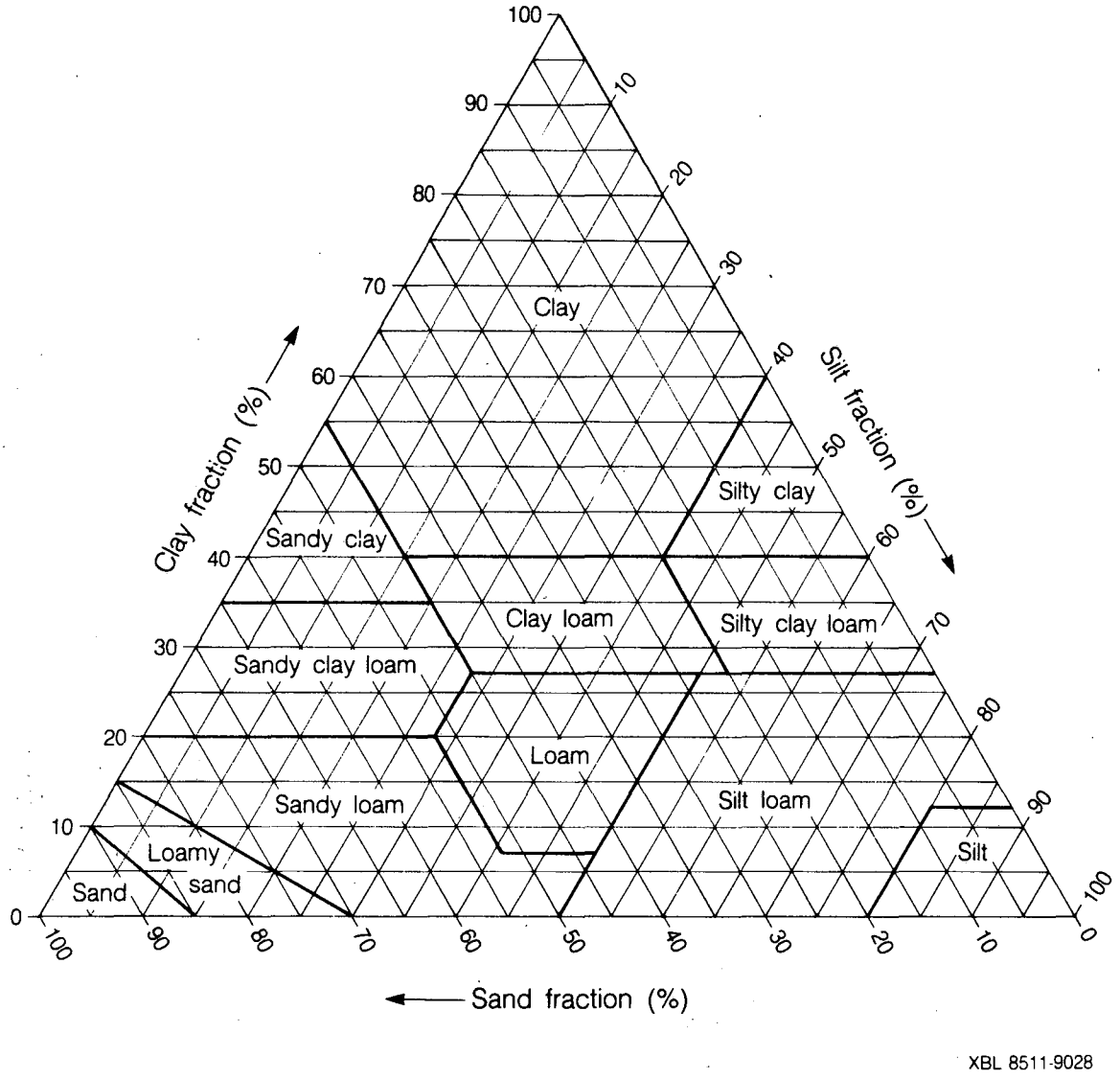

Figure 2. Soil texture categories used by the USDA. The chart shows the fraction of each of the three main grain-size classes—clay (<2 μm), silt (2-50 μm), and sand (50-2000 μm)—for each texture class.

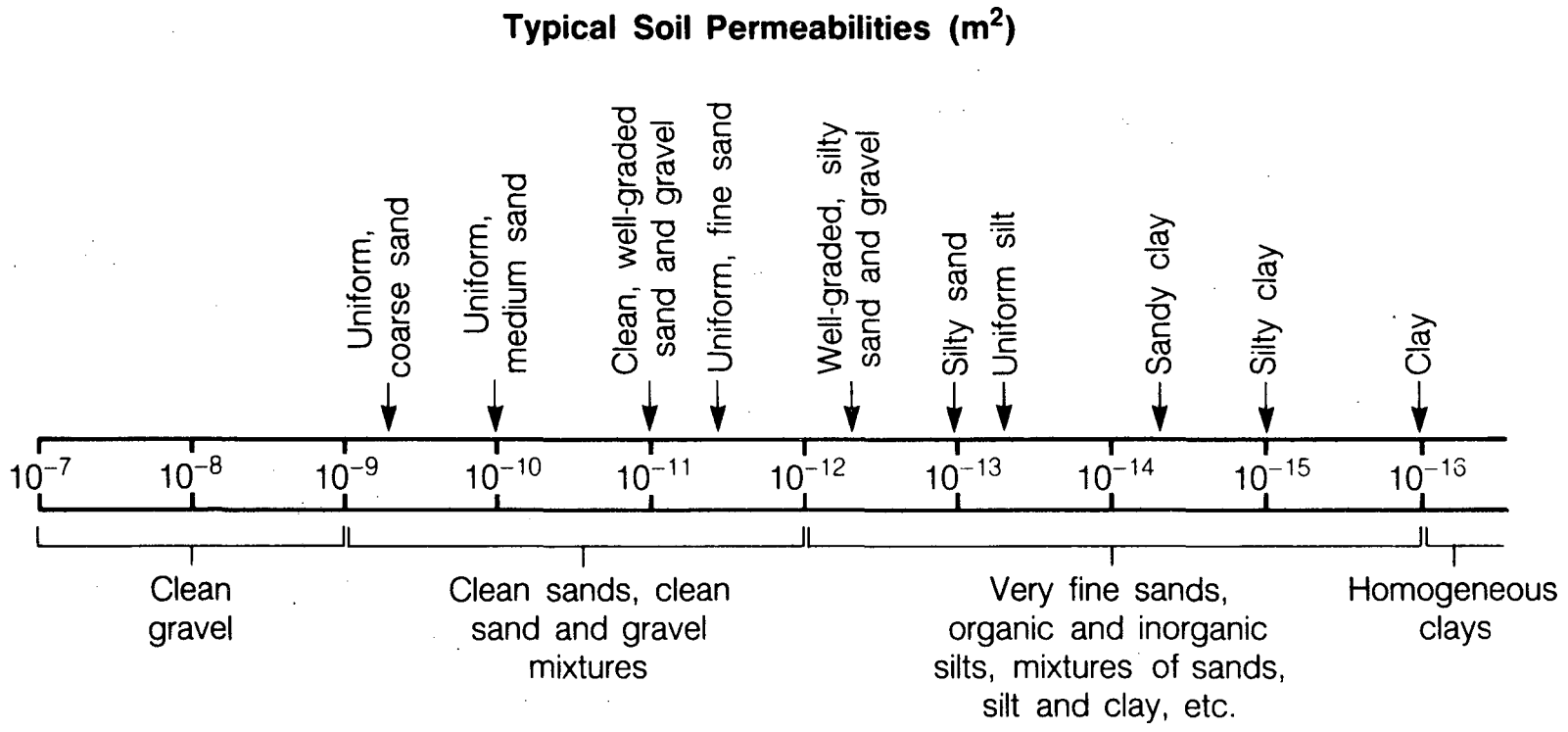

Figure 3. Permeability (m2) of representative soil types. Data from Terzaghi and Peck (1967); and Tuma and Abdel-Hady (1973).

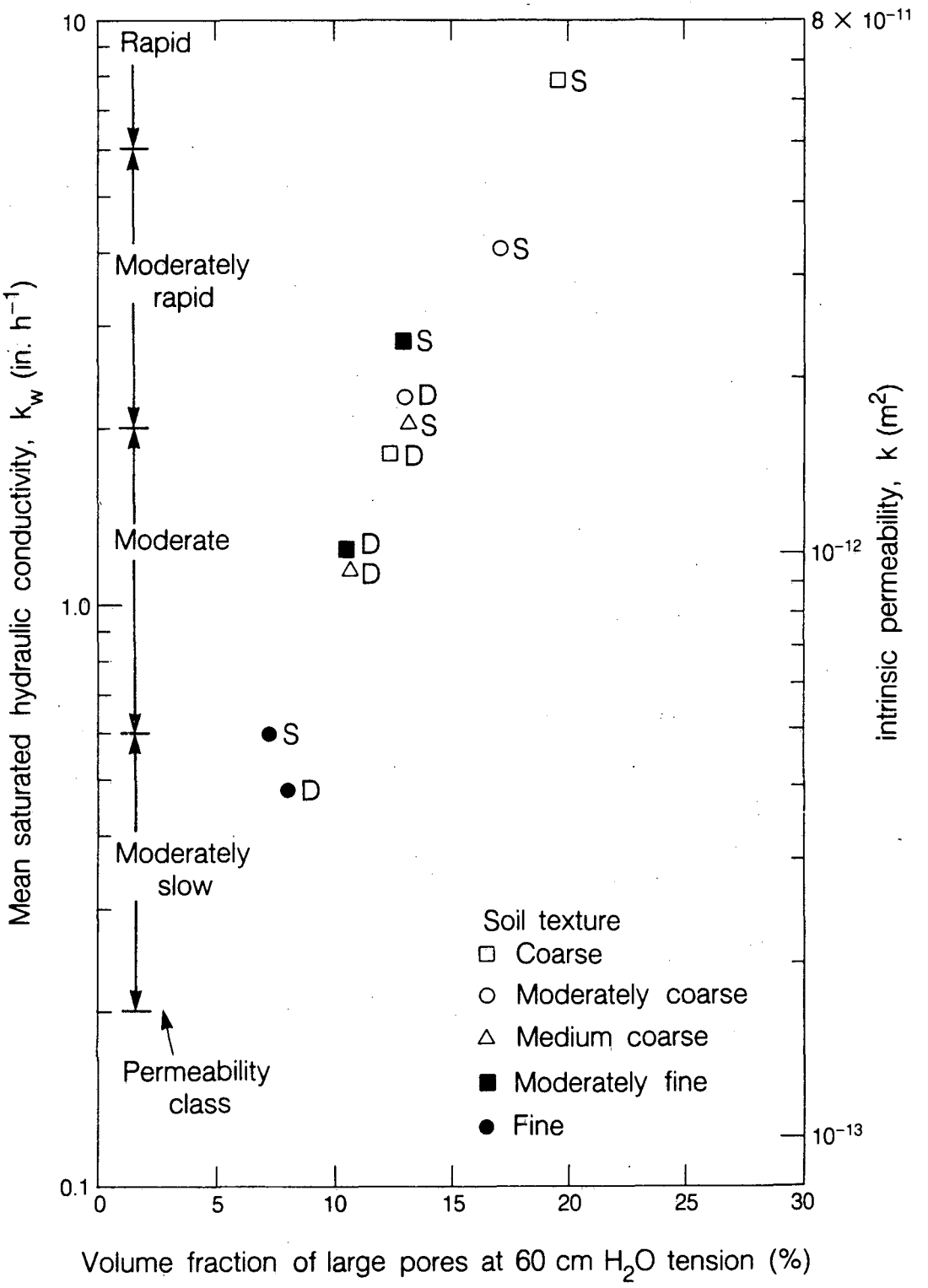

XBL 8511-9029A

Figure 4. Geometric mean hydraulic conductivity under saturated conditions, k_w plotted vs. the volume fraction of large pores for five soil texture classifications and for shallow (S) and deep (D) soil horizons. Data are from Mason et al. (1957).

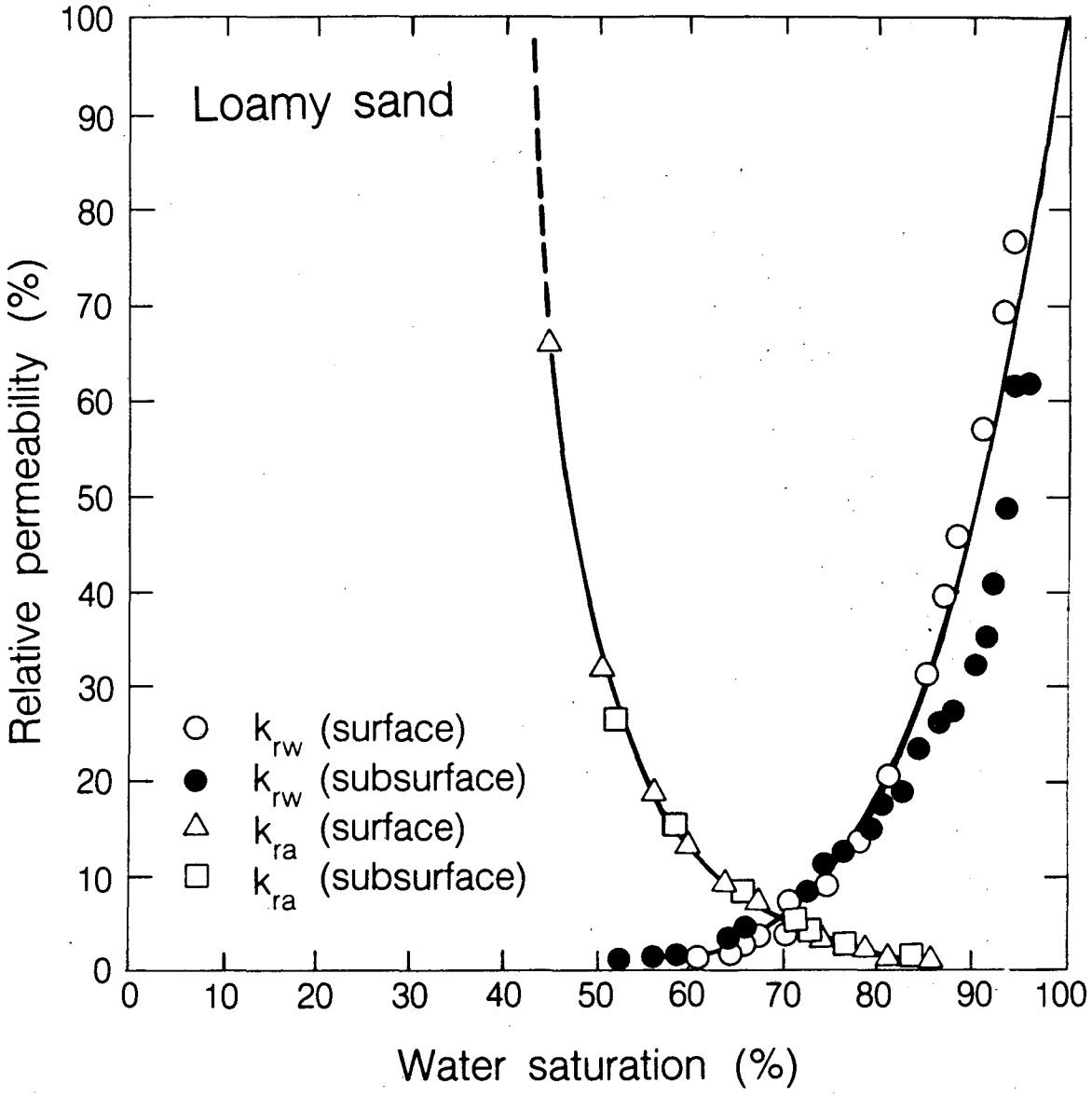

Figure 5. Relative permeability of loamy sand for air (k_{ra}) and water (k_{rw}) as a function of water saturation. Reproduced from Corey (1957).

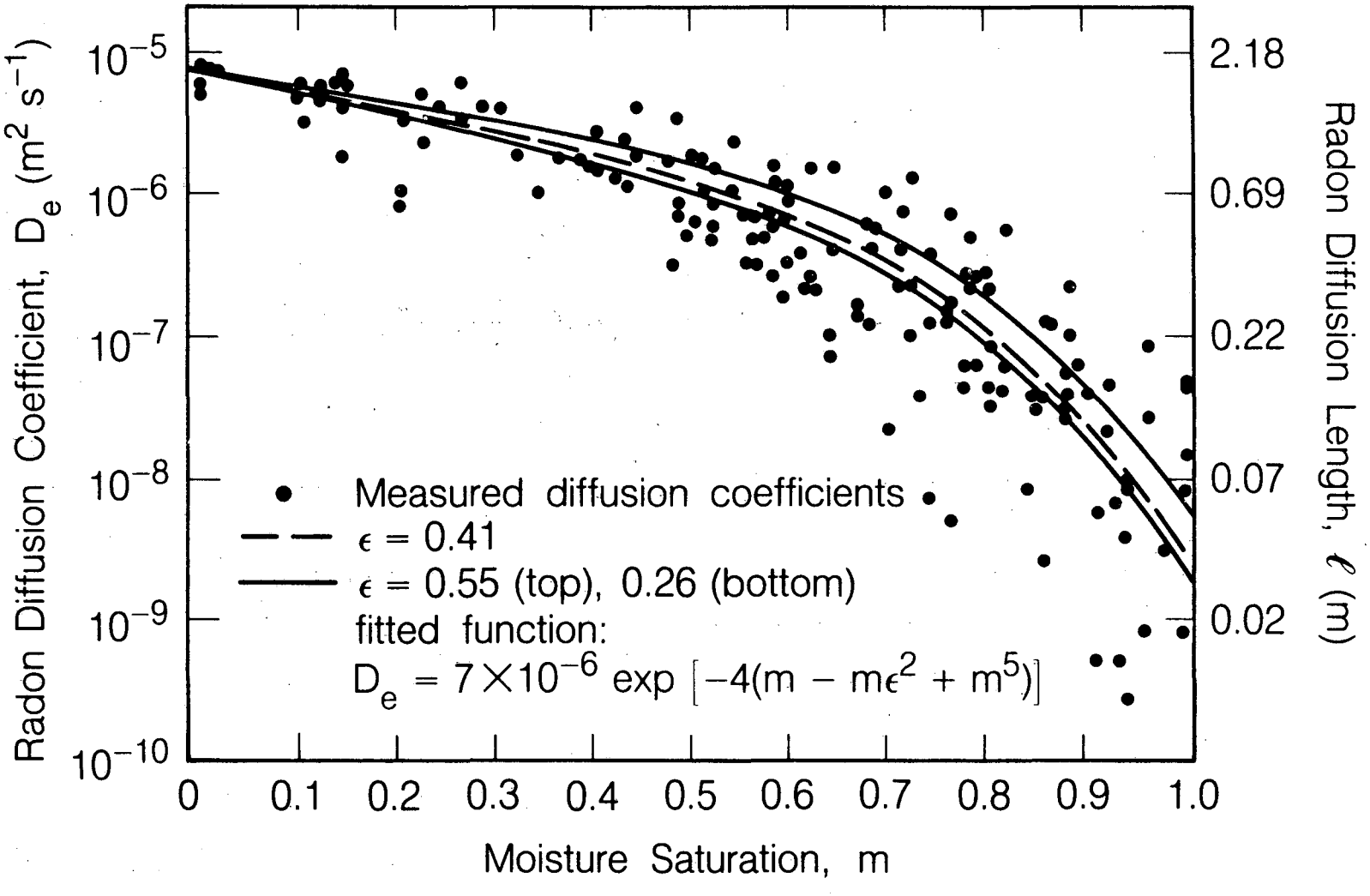

XBL8510-11935

Figure 6. Effect of soil moisture content on radon diffusivity. Moisture saturation (m) is the fraction of pore volume filled with water. The porosity is indicated by ε. Reproduced from Rogers et al. (1984).

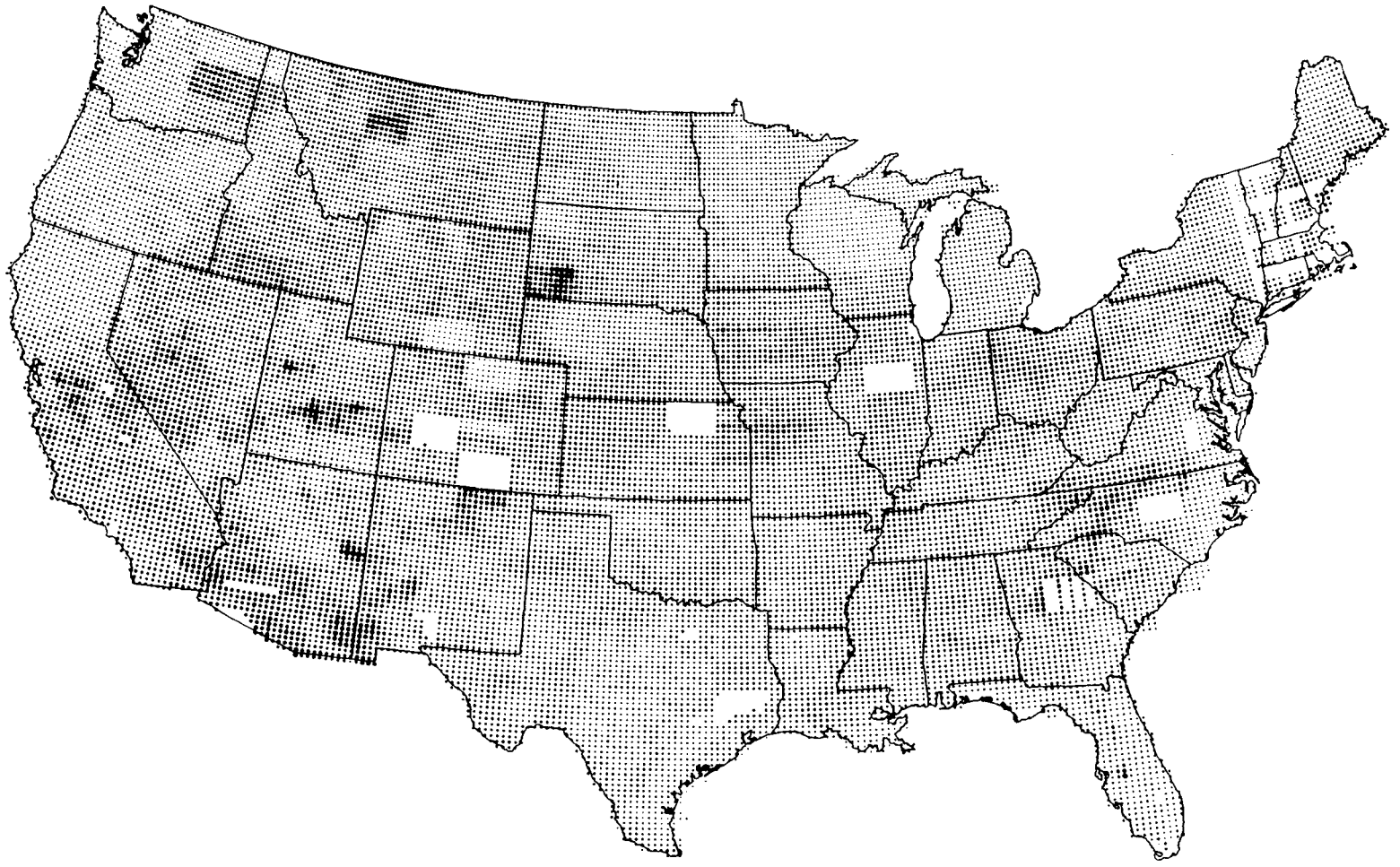

XBL 889-3350

Figure 7. Mean ^{226}Ra content in soil for 20 × 20 km areas of the contiguous 48 states. From the smallest to the largest, the 6 circle sizes represent concentrations of 0-20, 20-40, 40-60, 60-80, 80-100, and >100 Bq kg^{-1}. Figure reproduced from Revzan et al. (1988a).

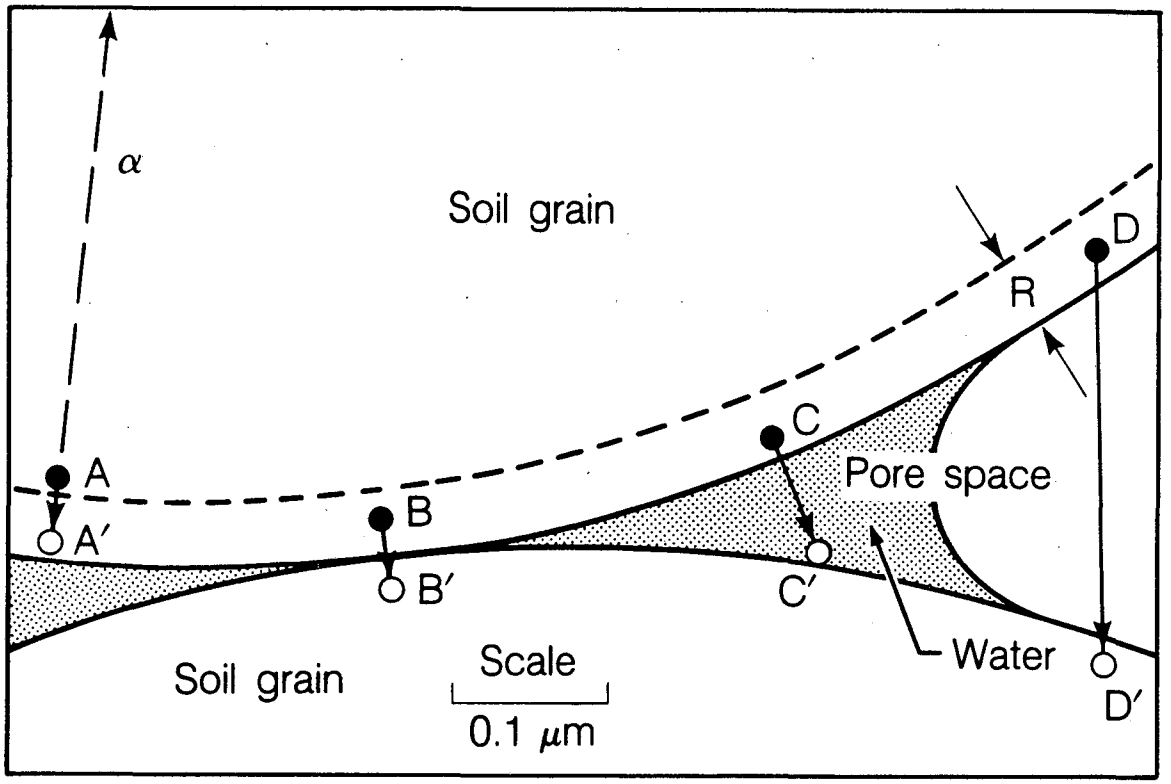

Figure 8. Schematic illustration of radon recoil trajectories in and between soil grains. Two spherical grains of 2 μm diameter (clay/silt) are in contact at point B. The stippled portion of the pore is water-filled. The recoil range, R, of the radon atoms is indicated by the dashed line. Radium-226 atoms, indicated by solid circles, decay, producing an alpha particle and a radon-222 atom which may end its recoil at the point indicated by the open circle. At A the radium atom is too deeply embedded within the grain for the radon atom to escape. At B and D the recoiling radon atom possesses sufficient energy after escaping the host grain to penetrate an adjacent grain. At C the radon atom terminates its recoil in the pore water. Illustration reproduced from Tanner (1980).

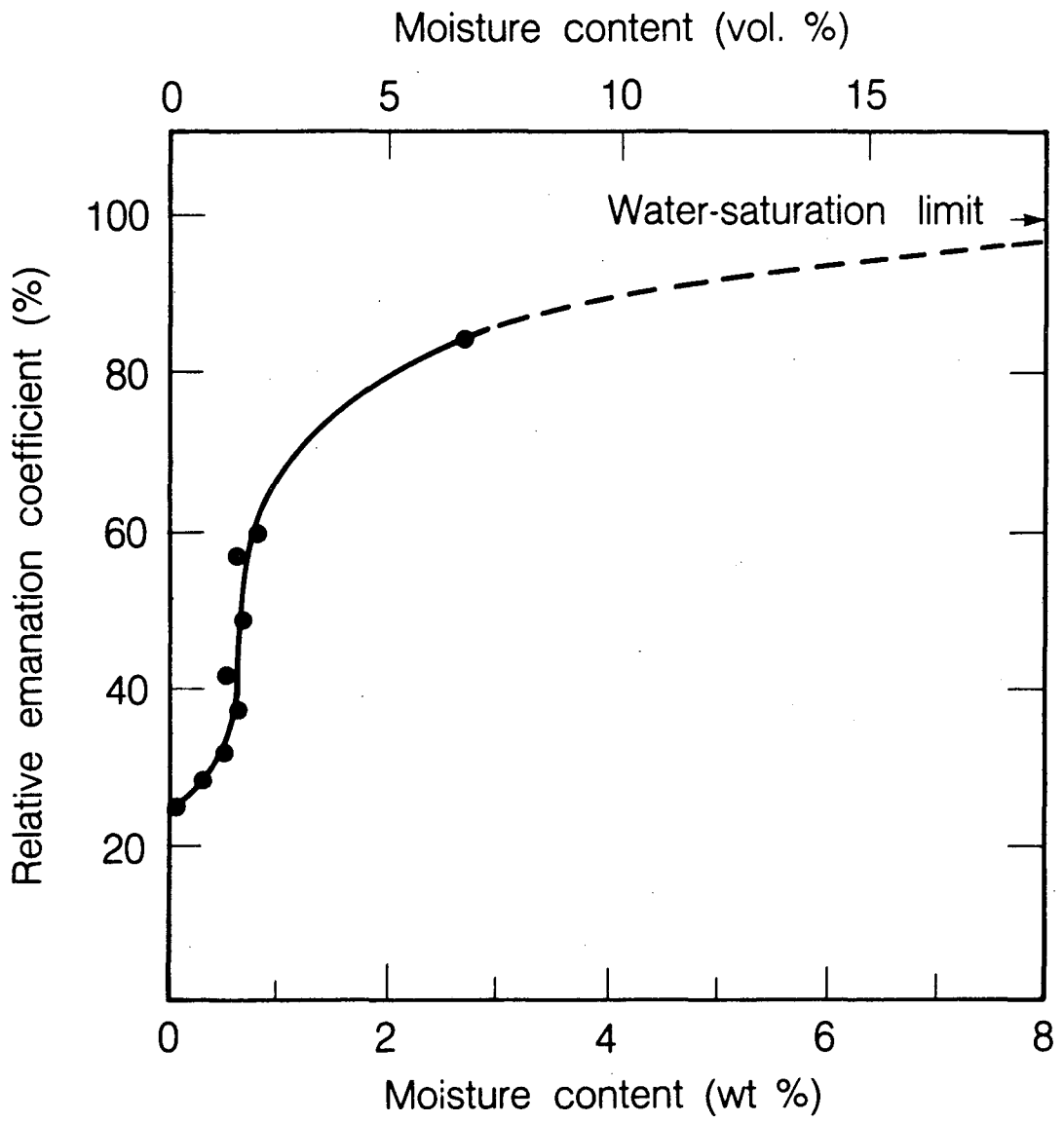

Figure 9. Effect of moisture content on the relative radon-222 emanation coefficient for a sample of uranium mill tailings. Reproduced from Strong and Levins (1982).

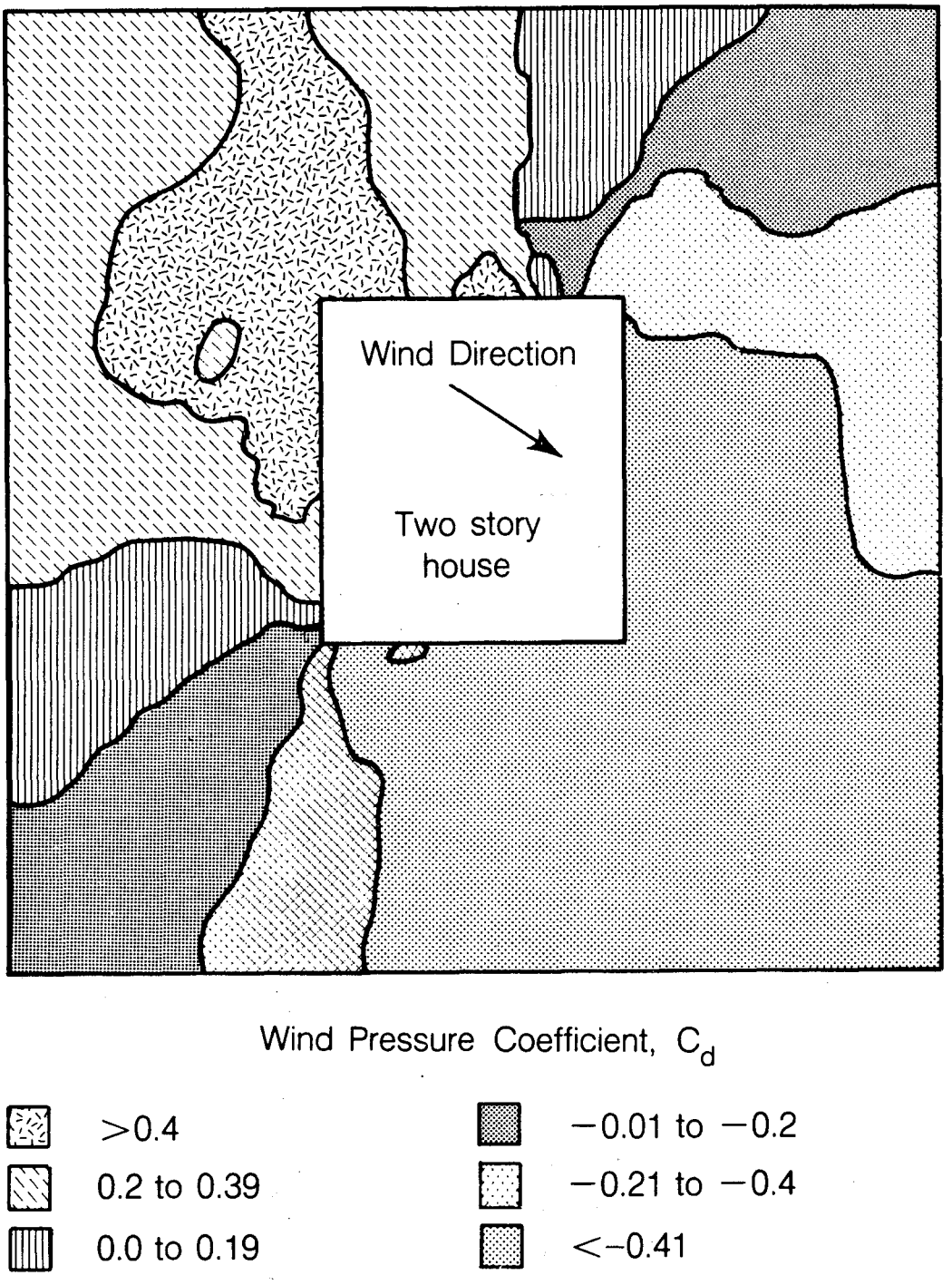

Figure 10. Wind pressure coefficient, C_d, at ground surface in vicinity of a model two-story house. Measurements were conducted in a wind tunnel. Illustration adapted from DSMA Atcon (1985).

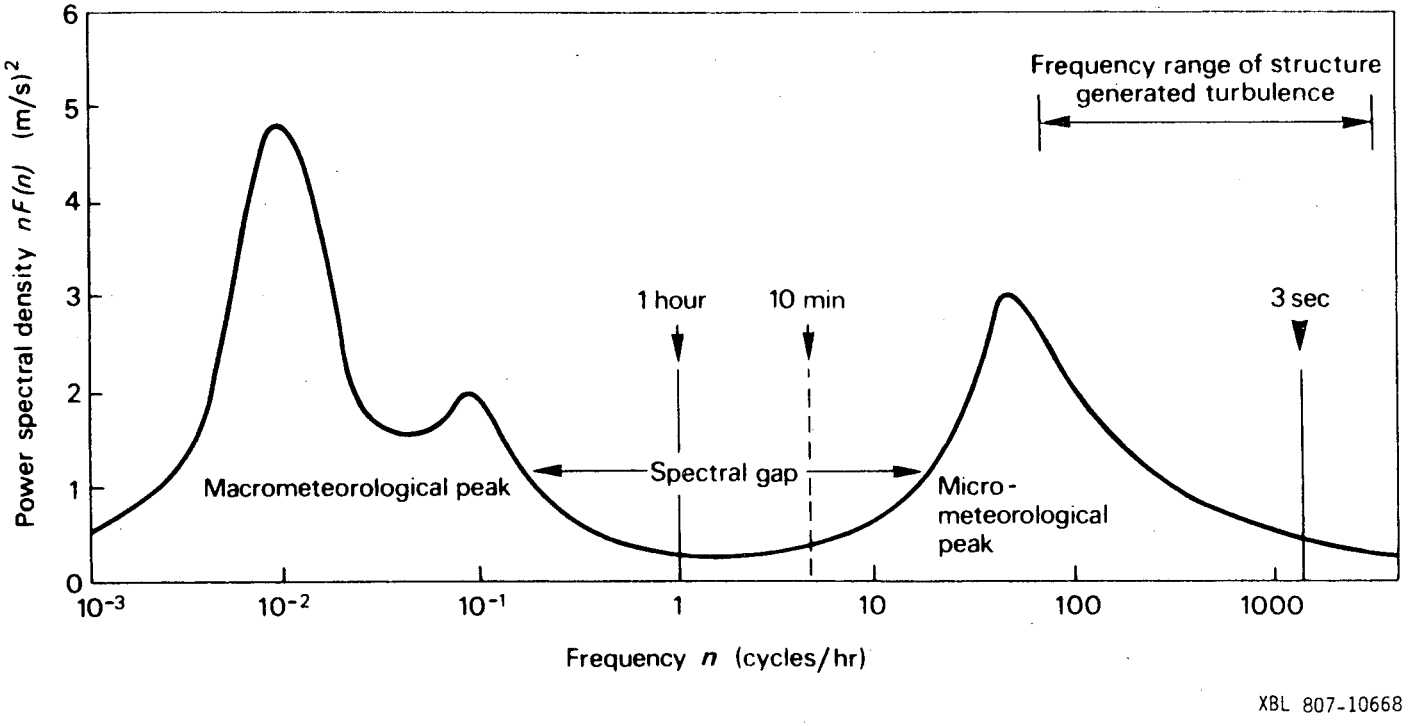

Figure 11. Horizontal wind-speed frequency spectrum measured at approximately 100 m height at Brookhaven, NY. Reproduced from Van der Hoven (1957).

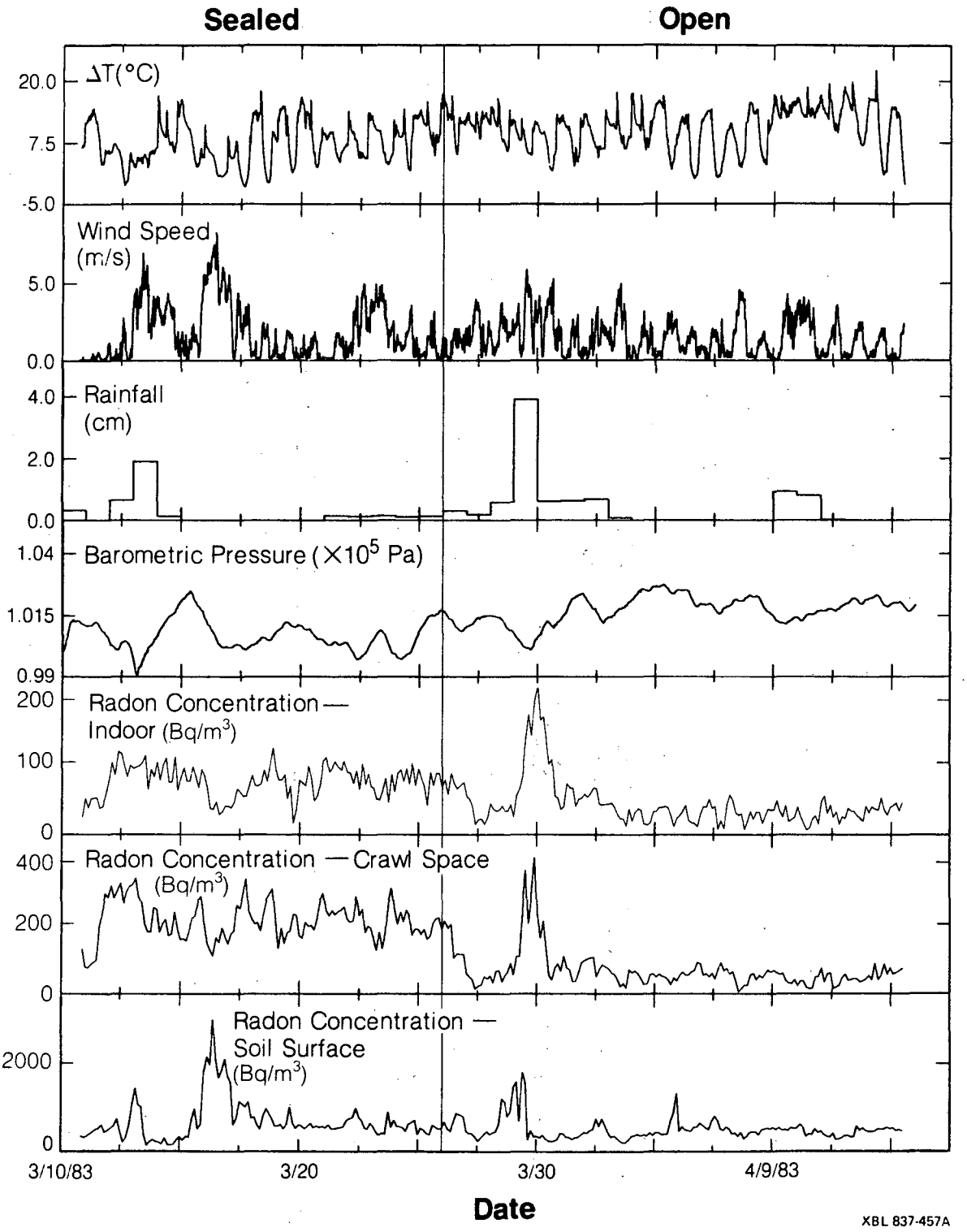

Figure 12. Radon-222 and meteorological measurements made over a five-week period at a house with a crawl space in Portland, Oregon. The crawl-space vents were sealed during the first two weeks and open during the final three. An episode of enhanced radon flux into the crawl space and house on March 29-30 corresponds to a period of heavy rainfall coupled with a modest drop in barometric pressure. ΔT represents the indoor-outdoor temperature difference. Figure reproduced from Nazaroff and Doyle (1985).

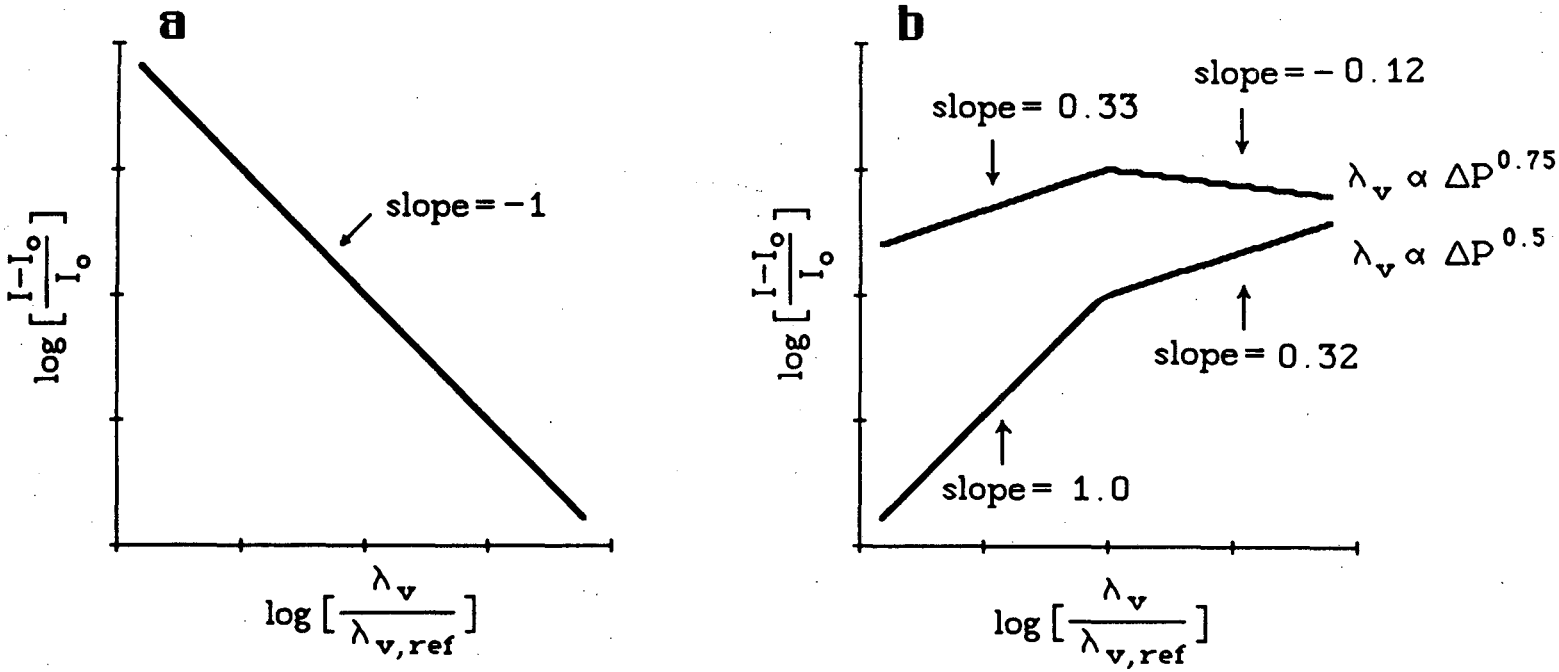

Figure 13. Relationship between radon concentration and air-exchange rate for a single structure. In case (a) it is assumed that either the ventilation system is entirely balanced or the radon entry mode is entirely passive. Case (b) represents the other extreme: the entry mode is active and the ventilation mode is unbalanced. In addition, the relative contributions of temperature difference, wind and mechanical ventilation to the pressure difference are assumed to remain constant for case (b). $\lambda_{v,ref}$ is an arbitrary, constant air-exchange rate.

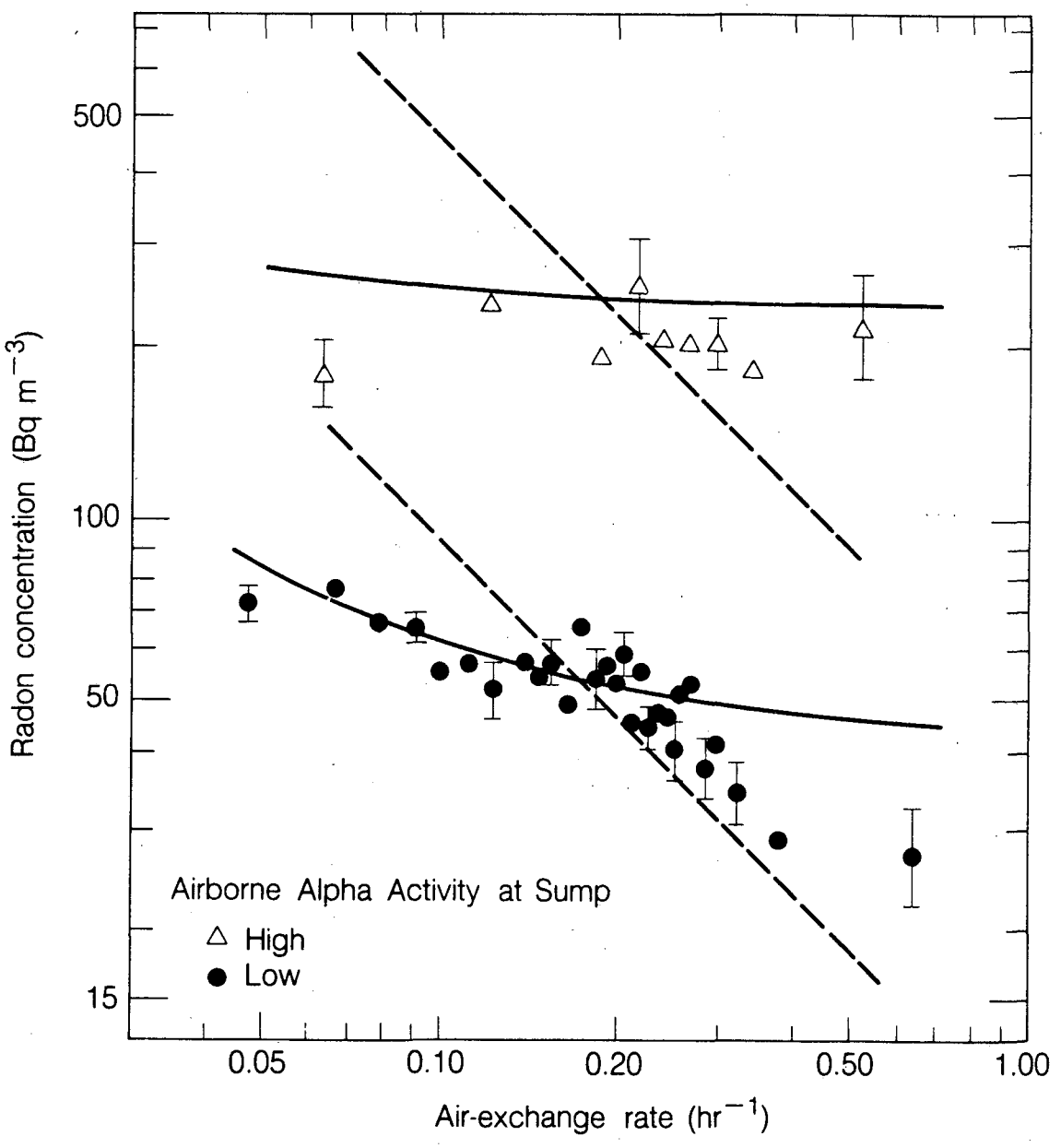

XBL836-2680A

Figure 14. Scatter plot of radon-222 concentration vs. air-exchange rate averaged over three-hour periods. Measurements were made continuously at a house with a basement in Chicago, Illinois over a five-month period. Data were sorted into two groups according to radon concentration above a sump in the basement: the concentration at this point during the "high" periods averaged greater than 10,000 Bq m-3; for "low" periods the average was less than 500 Bq m-3. Each point gives the geometric mean radon concentration of 19-21 measurements, grouped according to air-exchange rate. Error bars represent one geometric standard deviation of the mean. The dashed lines represent the expected relationship if the radon entry rate is independent of air-exchange rate. The solid lines reflect a model in which radon entry is presumed to have two components—one (diffusive) being constant, the other (convective) being proportional to air-exchange rate. Figure reproduced from Nazaroff, et al. (1985).

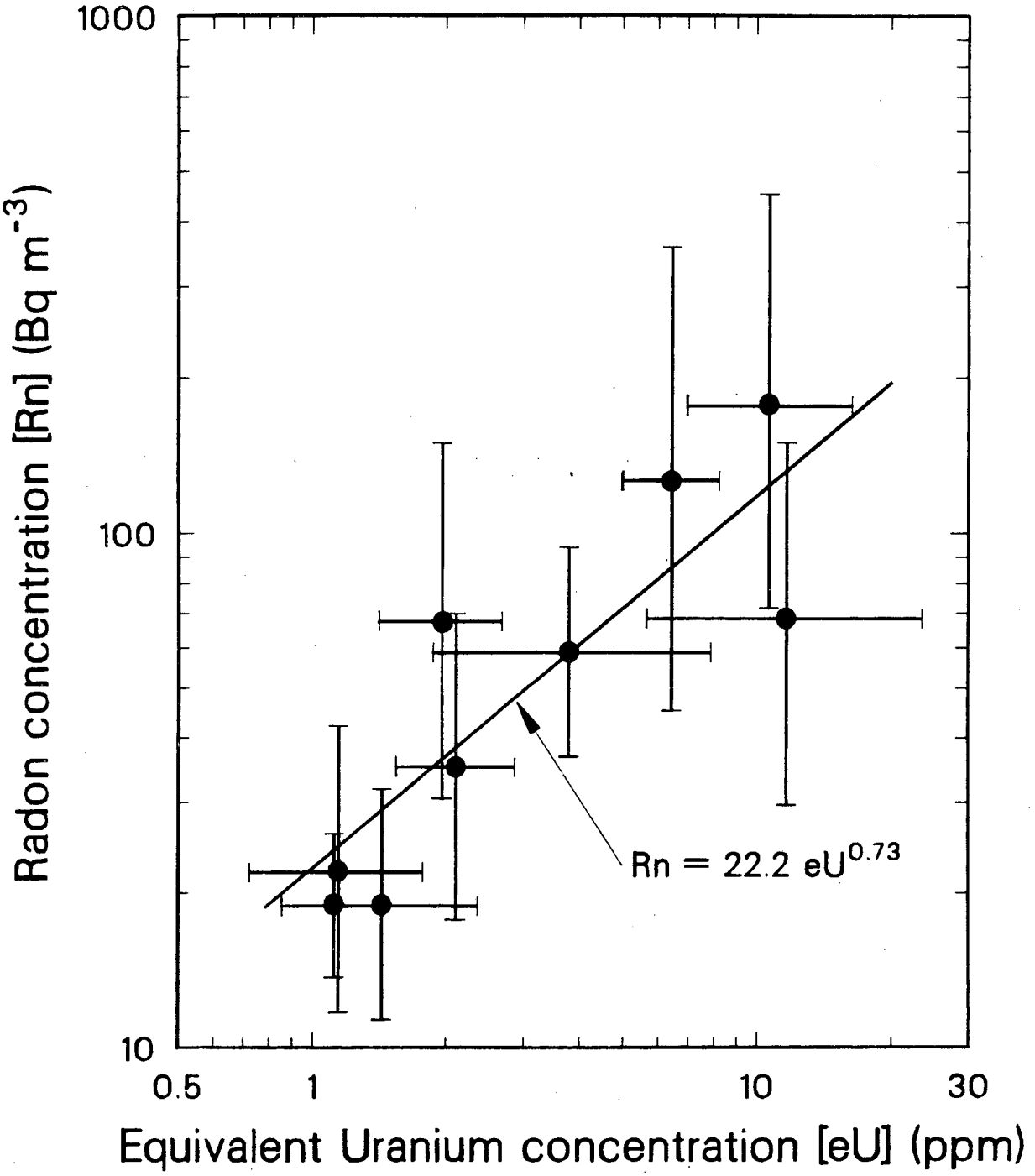

Figure 15. Scatter plot of geometric mean indoor radon-222 concentration and soil equivalent uranium concentration for nine U.S. communities. Error bars indicate one geometric standard deviation. Each point represents radon measurements in 8-69 houses. Equivalent uranium concentration was determined from an analysis of airborne radiometric (NARR) data. Data from Kothari and Han (1984).

XCG 8510-471

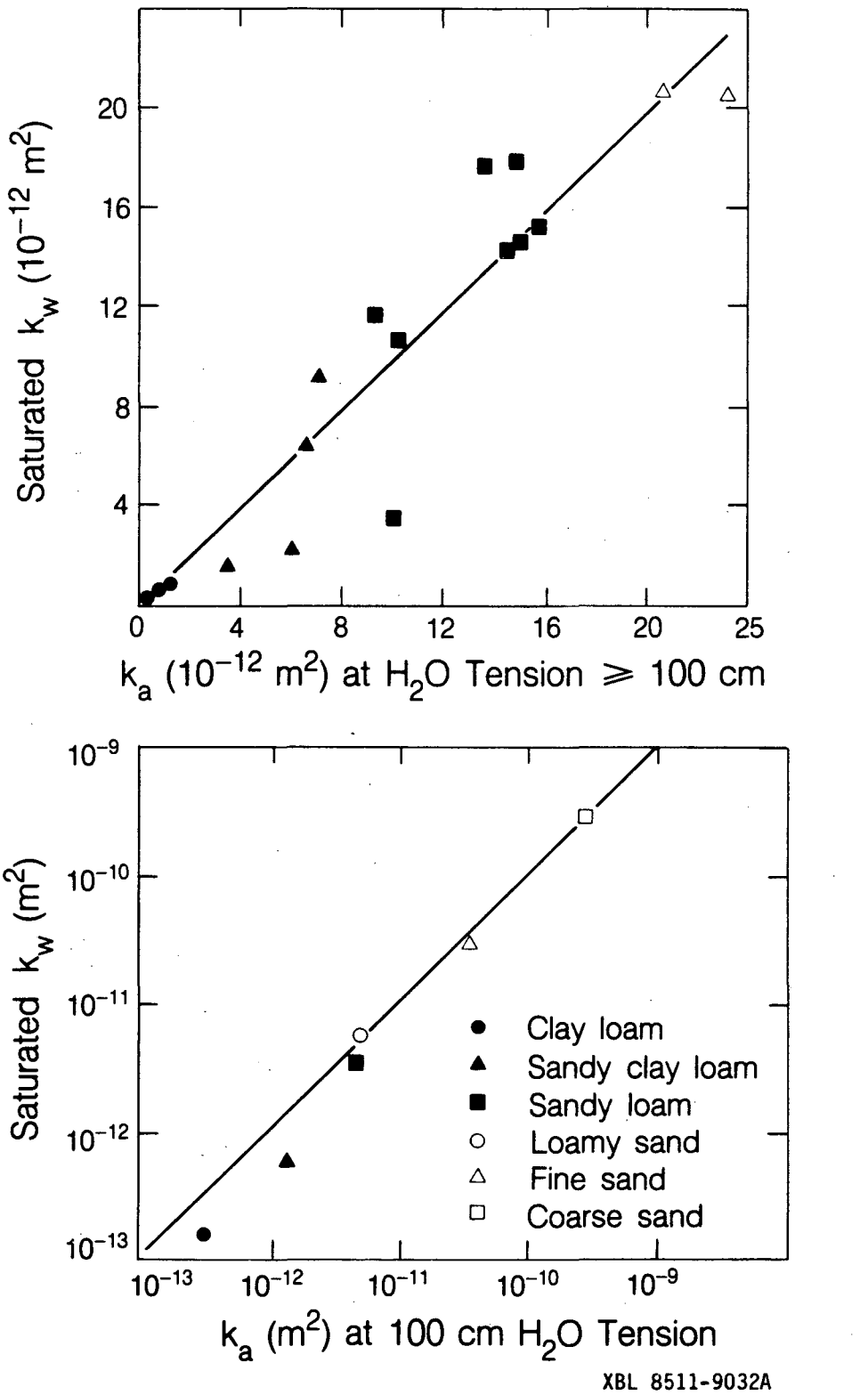

Figure 16. Saturated water permeability, k_w, vs. air permeability at a water tension of 100 cm (or greater), k_a, for six soil texture classes. Results for undisturbed soil cores are presented in the upper frame, and results for systematically packed, disturbed soil samples are shown in the lower frame. Figure adapted from Al-Jibury (1961).

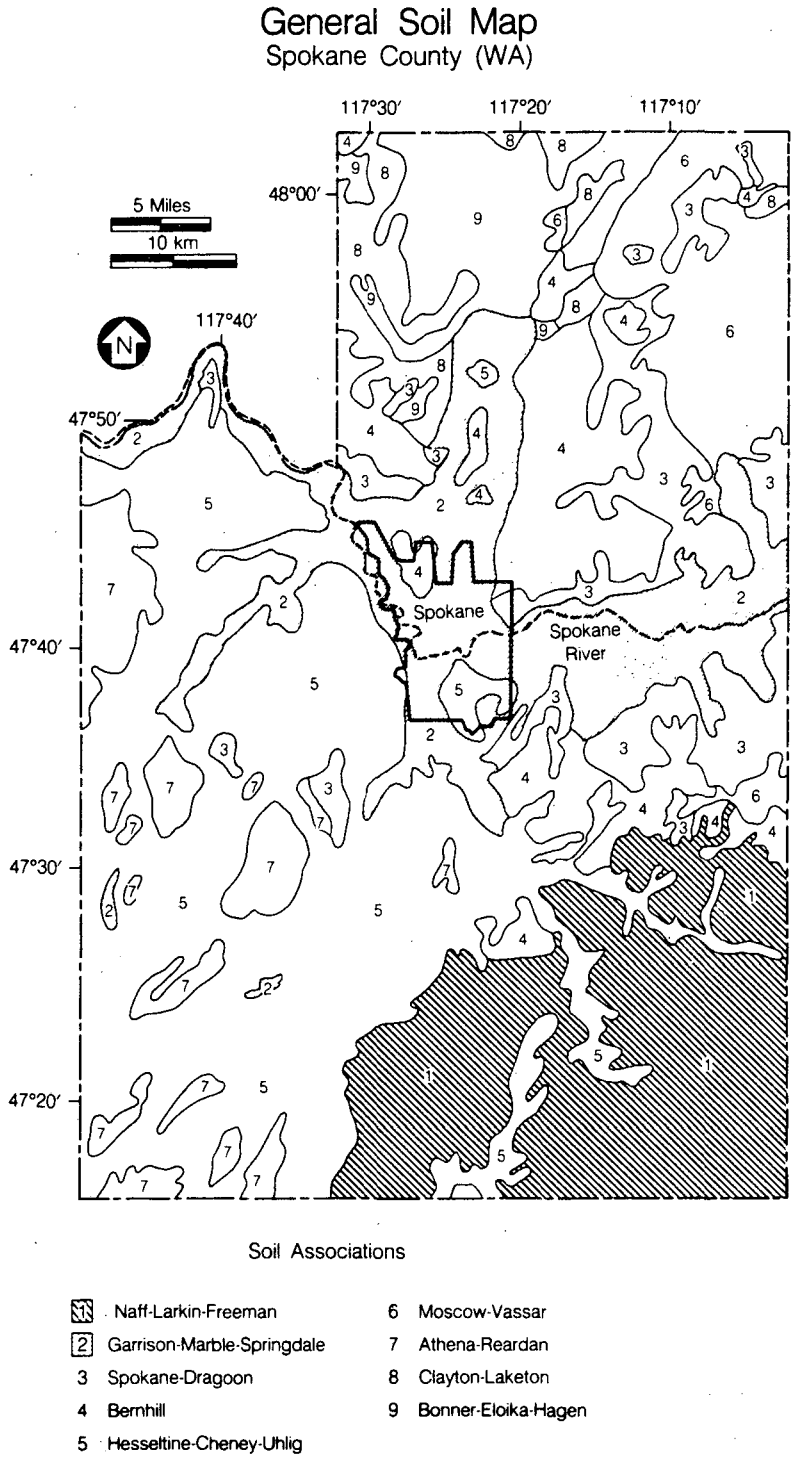

Figure 17. A general soil map for Spokane County, WA, showing the nine soil associations covering the county. Each soil association comprises two or three major soil series and one or more minor soil series. Two soil associations discussed in the text are shaded. The Spokane River is indicated by a dashed line and the approximate boundary for the city of Spokane is shown by a heavy border. Figure adapted from USDA (1968).

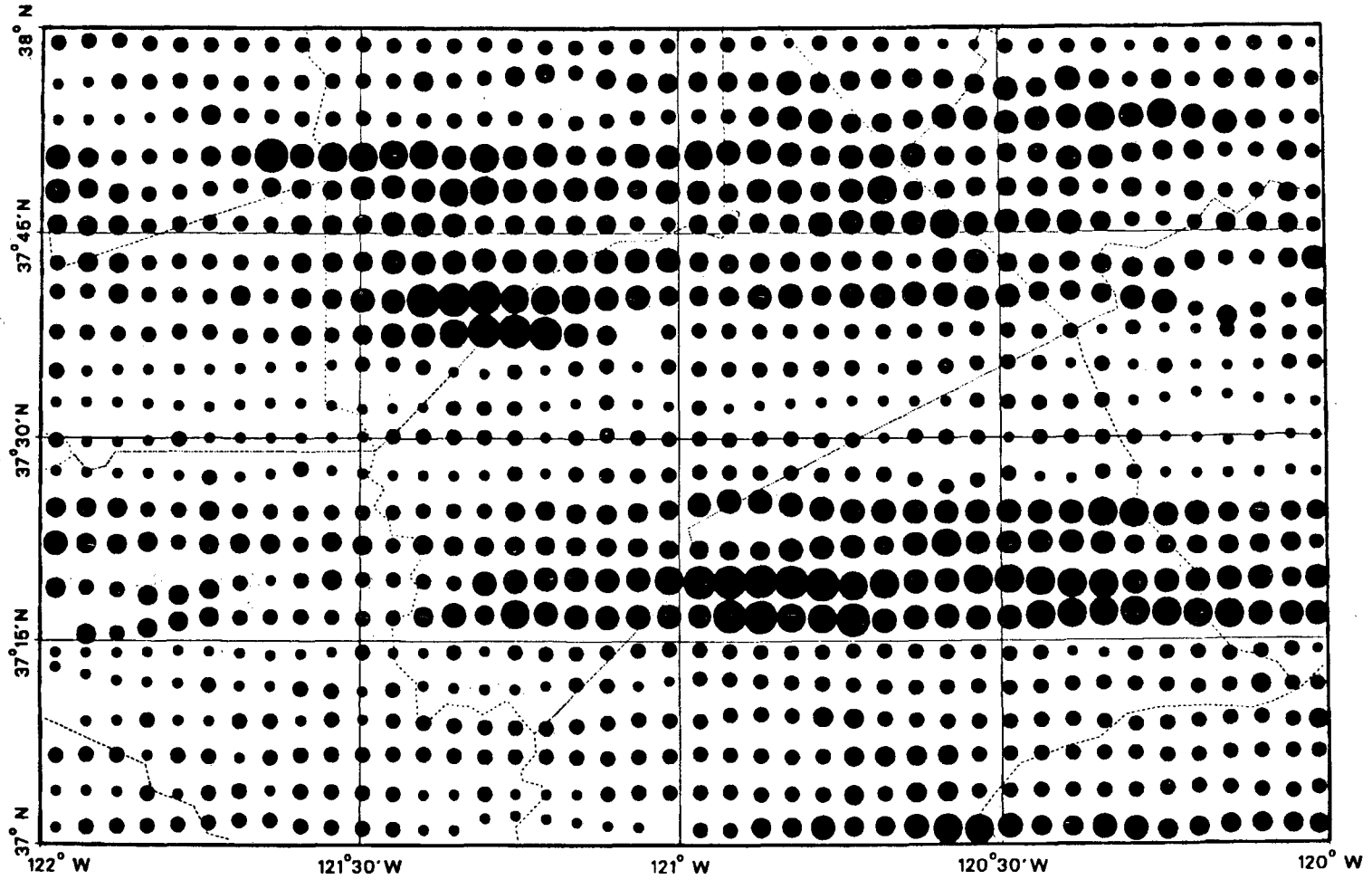

Figure 18. Mean ^{226}Ra concentration in soil for 5 km distances along primary flight lines of the San Jose (CA) quadrangle. From the smallest to the largest, the six circle sizes represent concentrations of 0-30, 30-60, 60-90, 90-120, 120-150, and >150 Bq kg^{-1}. Dotted lines represent county boundaries. Figure reproduced from Revzan et al. (1988a).

XBL 8711-4928

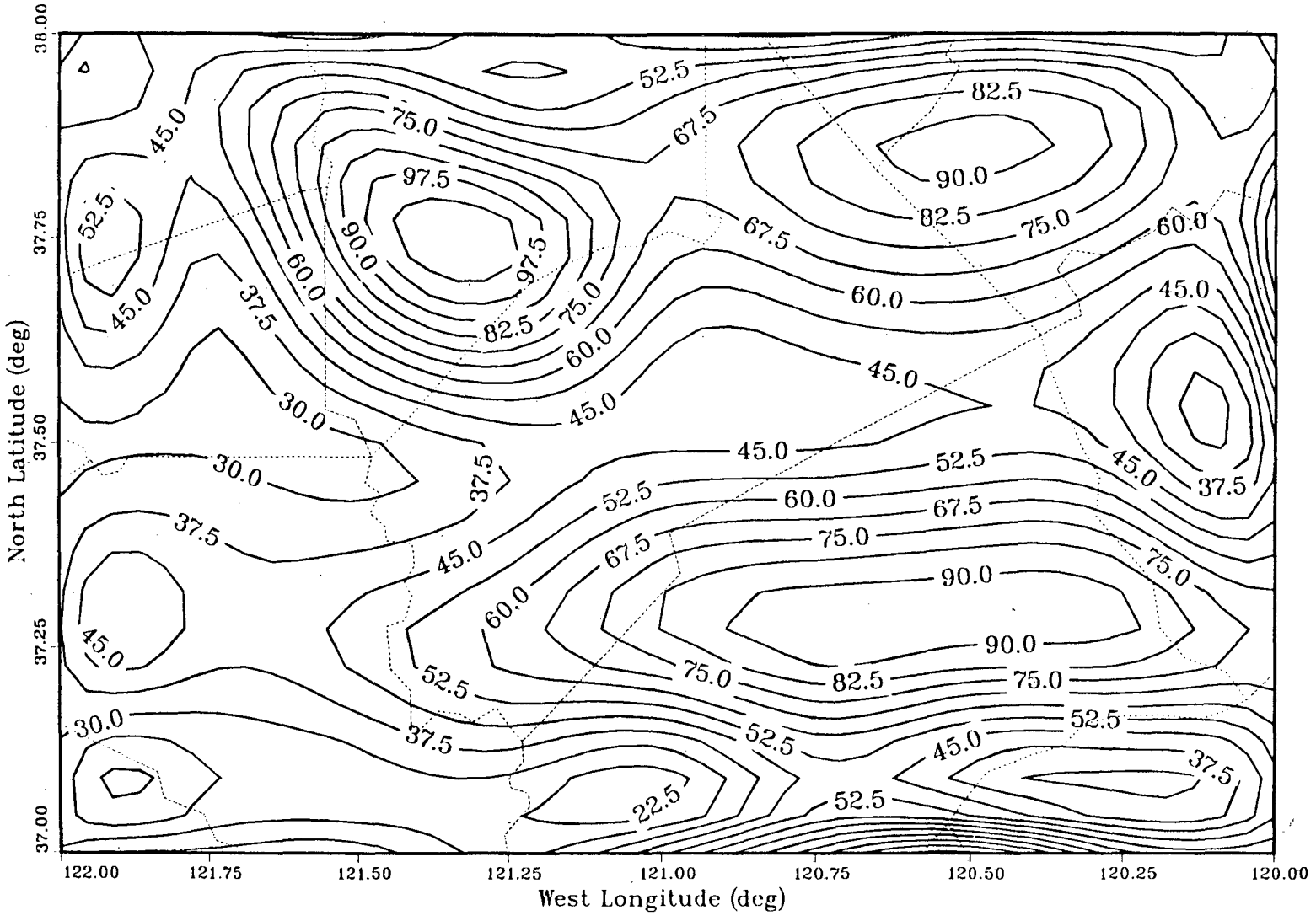

XBL 8711-4929

Figure 19. Contour map of ^{226}Ra concentration in soil for the San Jose (CA) quadrangle. The contour interval is 7.5 Bq kg^{-1}. Dotted lines represent county boundaries. Figure reproduced from Revzan et al. (1988a).

LAWRENCE BERKELEY LABORATORY
TECHNICAL INFORMATION DEPARTMENT
1 CYCLOTRON ROAD
BERKELEY, CALIFORNIA 94720